DISSERTATION

Characterization of a new endophytic astin producer, *Pelliciarosea asterica*, from *Aster tataricus*

to graduate as

Doctor rerum naturalium
(Dr. rer. nat.)

by Dipl.-Biol. Linda Jahn

born on 4 February 1987 in Dresden

submitted to the TU Dresden on 29 May 2015,
accepted on 26 October 2015

supervised by Prof. Dr. Jutta Ludwig-Müller (TU Dresden, Institute of Botany)
and Prof. Dr. Karl-Heinz van Pée (TU Dresden, Chair of Biochemistry)

Für Mama und Papa.

Contents

1 Abstract

Aster tataricus (Asteraceae) is a plant native to Northern Asia and known for its use in the Traditional Chinese and Japanese Medicine. Beside many other secondary metabolites, it contains pentapeptides called astins from which some show an antitumor activity against different human cell lines. Astins are chlorinated, cyclic pentapeptides consisting of proteinogenic and non-proteinogenic amino acids. The astin structure indicates the involvement of non ribosomal peptide synthetases as well as flavin-dependent halogenases. Both enzymes are currently only known from bacteria and fungi.

A new endophytic fungus *Pelliciarosea asterica* was isolated from *A. tataricus* which produces some of the astins found in the different plant organs. The nearest neighbors of *P. asterica* are ostropalean fungi from the Stictidaceae lineage (Stictidaceae, Ostropales, Lecanoromycetes, Pezizomycetes, Ascomycota).

P. asterica is located in all plant organs of *A. tataricus* but the highest accumulation of the fungus is found in rhizomes and above-ground organs like leaves or inflorescences. In contrast, the highest astin concentration was found in the roots where nearly no fungus was detectable. *P. asterica* produces only one of the dichlorinated astins (astin C) in liquid culture, but in *A. tataricus* all three forms of the dichlorinated astins (A/B and C) were found. This indicates that either the plant is "using" the fungal astin C and metabolize it into one of the other astins or that the fungus, once living inside the plant, is itself producing the other astins.

It was also searched for a candidate gene of a halogenase which is essential for the dichlorination of the astins with an antitumor activity. No halogenase could be found by PCR or Southern as well as colony blot, neither in *A. tataricus* nor in *P. asterica*. Even the genome sequencing of *P. asterica* revealed no candidate gene for a halogenase.

Endophytes support the plant by suppressing pathogens (antibiosis) or by providing additional nutrients like phosphates or iron to the plant. *P. asterica* can solubilize different phosphate sources on agar plates. Different fungi are inhibited in growth by *P. asterica* on agar plates.

The endophyte *P. asterica* from *A. tataricus* supports its host in different ways and

produces secondary metabolites. These secondary metabolites seem to be fungal metabolites either used or degraded by the plant. *P. asterica* is therefore a good alternative for a possible large-scale production of such antitumor acting astins.

Aster tataricus ist eine Pflanze aus der Familie der Korbblütengewächse (Asteraceae), heimisch im Norden von Asien. Sie ist schon lange in der Traditionellen Chinesischen und Japanischen Medizin bekannt. Neben anderen medizinisch wirksamen Sekundärmetaboliten enthält diese Pflanze Astine, von denen einige eine anti-kanzerogene Wirkung gegen humane Krebszelllinien zeigen. Astine sind chlorierte, zyklische Pentapeptide und bestehen aus proteinogenen und nicht-proteinogenen Aminosäuren. Ihre Struktur deutet darauf hin, dass nicht-ribosomale Peptidsynthetasen und Flavin-abhängige Halogenasen in der Biosynthese eine Rolle spielen. Beide Enzyme sind aber bis heute nur aus Bakterien und Pilzen bekannt.

Ein neuer, unbekannter, endophytisch lebender Pilz, *Pelliciarosea asterica*, konnte aus *A. tataricus* isoliert werden. *P. asterica* synthetisiert selbst einige Astine, die bis dahin nur von *A. tataricus* bekannt waren. *P. asterica* ist ein filamentöser Ascomycet und gehört zur Familie der Stictidaceae (Stictidaceae, Ostropales, Lecanoromycetes, Pezizomycetes, Ascomycota).

P. asterica wurde in allen Pflanzenorganen wie Wurzel, Rhizom, Blatt und Blütenstand nachgewiesen. Am stärksten war *P. asterica* in den Rhizomen und oberirdischen Pflanzenorganen vertreten. Im Gegensatz dazu wurde die höchste Astinkonzentration in den Wurzeln von *A. tataricus* gefunden. In den Wurzeln konnte jedoch so gut wie kein Pilz nachgewiesen werden. Als einziges dichloriertes Astin synthetisiert *P. asterica* in in vitro-Kulturen Astin C, in der Pflanze *A. tataricus* wurden aber drei verschiedene dichlorierte Astine (A bis C) gefunden. Dies deutet darauf hin, dass entweder die Pflanze *A. tataricus* die pilzlichen Astine in die anderen Astine umwandelt oder das der Pilz *P. asterica*, wenn er sich in der Pflanze befindet, die anderen Astine ebenfalls synthetisiert.

Wie bereits erwähnt, ist eine Flavin-abhängige Halogenase essentiell für die Biosynthese der Astine. Verschiedene Versuche wurden unternommen, um ein Kandidatengen zu finden. PCR, Southern- und Kolonie-Blot ergaben keine positiven Treffer. Selbst im Genom von *P. asterica* konnte kein Gen für eine Halogenase gefunden werden.

Endophyten unterstützen ihre Wirtspflanze auf unterschiedliche Art und Weise wie z.B. durch Hemmung von Phytopathogenen (Antibiose) oder durch Bereitstellung von zusätzlichen Nährstoffen aus dem Boden wie Phosphate oder Eisen. *P. asterica* ist in der

Lage, *in vitro* verschiedene Phosphatquellen aus dem Medium abzubauen. Außerdem hemmt *P. asterica* das Wachstum verschiedener Pilze, unter ihnen andere Endophyten und phytopathogene Pilze.

Der endophytische Pilz *P. asterica* aus *A. tataricus* unterstützt seine Wirtspflanze auf unterschiedlichen Weise und synthetisiert einige der in *A. tataricus* gefunden Astine. Damit stellt *P. asterica* eine mögliche Alternative für die biotechnologische Produktion dieser anti-kanzerogenen Stoffe dar.

2 Introduction

2.1 Astins as natural compounds of *Aster tataricus*

The first astins were isolated from *Aster tataricus* L.f. by Morita et al. in the nineties (Morita et al., 1993a,b, 1994; Itokawa et al., 1994; Morita et al., 1995a). Unfortunately, the concentration of astins is very low in roots. Morita et al. (1995b) isolated only milligrams of astins from 10 kg dried roots.

2.1.1 The plant *A. tataricus*

A. tataricus L.f., belonging to the Compositae (Asteraceae), is native to Siberia, China, Mongolia, Korea and Japan (Flann, 2009; Czerepanov, 1995; Gubanov, 1996). The perennial plant grows with a ground rosette from where the inflorescence is occurring. The inflorescence with branched stems holds many flower heads composed of yellow disk flowers surrounded by purple petals (Figure 2.1).

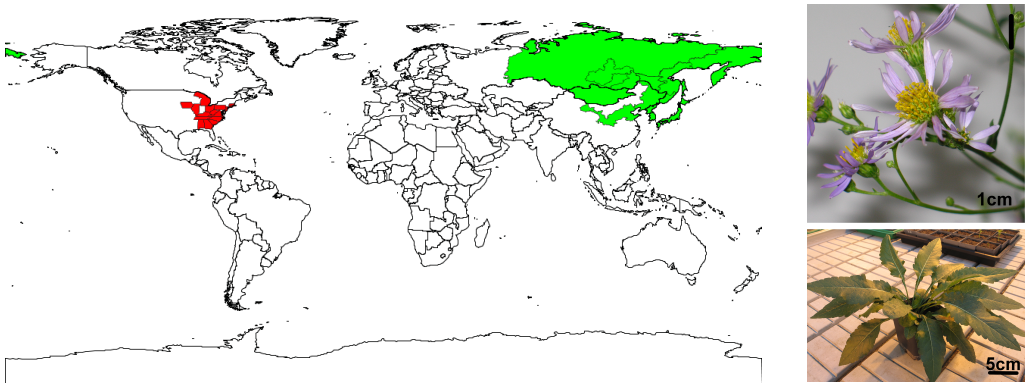

Figure 2.1: Distribution of *A. tataricus* (Flann, 2009). Indigenous areas are marked green (Siberia, Mongolia, China, Korea and Japan), whereas exotic areas are red (USA). *A. tataricus* is a perennial with a ground rosette and violet flowers.

The roots and rhizomes of *A. tataricus* are used in the Traditional Chinese and Japanese Medicine as herbal tea, known as "zi wan" and "shion". The root extract possesses

diuretic, antibacterial, antiviral and anti-ulcer activities caused by the compounds present in these root systems (Shao et al., 1997a,b; Shirota et al., 1997). Amongst these isolated secondary metabolites, there are astins and astin derivatives (Morita et al., 1993b,a, 1994, 1995a; Itokawa et al., 1994) with antitumor activity (Morita et al., 1996).

2.1.2 Chemical structure of astins

The astins and astin derivatives are characterized by a 16-membered ring system containing proteinogenic (proline and serine) and non-proteinogenic (β-amino phenylalanine, α-aminobutyric acid and *allo*threonine) amino acids (Morita et al., 1993b; Xu et al., 2013). The first nine astins reported (A to I) were described by Morita and colleagues in 1993 and 1994 and the astins K to P by Xu et al. in 2013 (Figure 2.2).

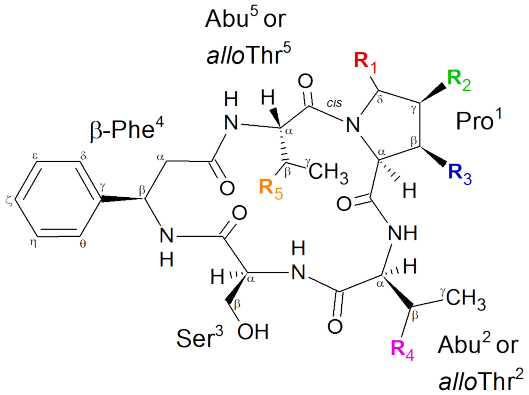

astin	R_1	R_2	R_3	R_4	R_5	γ to δ
A	H	Cl	Cl	H	OH	CH-CH
B	H	Cl	Cl	OH	H	CH-CH
C	H	Cl	Cl	H	H	CH-CH
D	Cl	H	H	H	H	C=C
E	Cl	H	H	OH	H	C=C
F	H	H	Cl	H	H	CH-CH
G	H	H	H	H	H	CH-CH
H	Cl	H	H	H	OH	C=C
I	H	Cl	OH	H	H	CH-CH
K	H	Cl	Cl	OH	OH	CH-CH
L	Cl	H	H	OH	OH	C=C
M	H	Cl	H	H	H	CH-CH
N	H	Cl	H	H	H	C=C

Figure 2.2: Structure of astins A to I (Morita et al., 1996) **and astins K to N** (Xu et al., 2013). Astins are composed of proteinogenic (proline, serine) and non-proteinogenic (α-aminobutyric acid, β-phenylalanine and *allo*threonine) amino acids. The kind of C-C bonding between the γ and δ position is indicated as well. For detailed explanation see text below.

All astins contain the amino acids proline, serine and β-phenylalanine. The two other amino acids are either α-aminobutyric acid or *allo*threonine dependent on the hydroxylation at the β-C atom. Besides the cyclic pentapeptide, astins are also characterized through their chlorination at the proline. The proline can be chlorinated at the β-, γ- or δ-C atom. Astins A, B, C and K show a dichlorination in position β and γ. A monochlorination of the proline at the δ-C atom were found in astins D, E, H and L. Only astin G shows no chlorination at the proline. Some astins show a double bond in the proline

between γ- and δ-C atom instead of a single bond. Additionally, the α-aminobutyric acid or *allo*threonine is connected with the proline in *cis* conformation. All other peptide bondings are in *trans*.

There are two other astins which do not fit into this scheme (Xu et al., 2013). Astin O is an astin C derivative containing an acetyl group at the β-C atom of serine. Astin P looks similar to astin K with the exception that the fifth amino acid *allo*threonine is replaced with the non-proteinogenic α-amino acid norvaline (also known as α-aminovaleric acid).

2.1.3 Astins function as antitumor compounds

Only those astins with the cyclic backbone and the *cis*-dichlorinated proline show an antineoplastic activity (Morita et al., 1996; Itokawa et al., 2000; Rossi et al., 2004; Saviano et al., 2004). This antitumor activity was first shown by Morita et al. (1996), when they tested different dichlorinated astins *in vivo* on sarcoma 180A in mice. The monochlorinated and non-chlorinated forms of the astins A to C as well as the other astins D to I did not inhibit the the tumor growth of sarcoma 180A. Only the dichlorinated forms, astins A, B and C, showed an antitumor activity against these tumors. This was confirmed by Itokawa et al. (2000) *in vitro* on nasopharynx carcinoma cells and *in vivo* on sarcoma 180A and P388 lymphocytic leukemia (Itokawa et al., 2000). Saviano et al. (2004), Rossi et al. (2004) and Cozzolino et al. (2005) tested newly synthesized astin analogues on different malignant human cell lines. One of the synthesized astins, a cyclopeptide related to astin G, showed similar activity against cell lines of human thyroid (NPA and ARO), ovary (SK-OV-3), breast (SK-BR-3) as well as epidermoid (A-431) carcinoma as found for astins A and B.

Furthermore, astin C shows an anti-inflammatory effect against activated T-cells (Shen et al., 2011) and astin B induces cell death and autophagy in human hepatic cell lines (Wang et al., 2014).

2.1.4 Cyclochlorotine - another dichlorinated cyclic pentapeptide

Another chlorinated cyclic pentapeptide, called cyclochlorotine, was found in *Talaromyces islandicus* (Sopp) Samson, Yilmaz, Frisvad & Seifert (Tatsuno et al., 1955; Samson et al., 2011). *T. islandicus* is a worldwide occurring mold of food like rice and wheat (Saito et al., 1971). Cyclochlorotine and hydroxycyclochlorotine (Mizutani et al., 2008) consists both of nearly the same amino acids as the astins. However, in contrast to the astins, cyclochlorotine induces liver injuries (Terao et al., 1984)

2.1.5 Astins - from structure to biosynthetic enzymes

The astin structure tells us much about potentially biosynthetic enzymes. Non-ribosomal peptide synthetases, monooxygenases or flavin-dependent halogenases are enzymes which may be involved in the astin biosynthesis.

2.1.5.1 Non-ribosomal peptide synthetases

The cyclic structure and the presence of non-proteinogenic amino acids indicate the involvement of a non-ribosomal peptide synthetase (NRPS) (Finking and Marahiel, 2004; Walsh, 2007). NRPS are large multifunctional enzyme complexes which assemble ribosome-independent structurally diverse peptides. These peptides are usually medicinal important secondary metabolites: antibiotics (daptomycin), antitumor (bleomycin) or antifungal drugs as well as immunosuppressants (cyclosporin) (Strieker et al., 2010). Beside proteinogenic and non-proteinogenic amino acids, fatty acids and α-hydroxy acids can be incorporated by the NRPS (Caboche et al., 2008). Until now, they are only known from the secondary metabolism of bacteria and fungi (Finking and Marahiel, 2004; Walsh, 2007).

2.1.5.2 Monooxygenases

In many cases only a hydroxyl group makes the difference between two or more astin variants: astins A, B, C and K are all dichlorinated at the proline in position β and γ, but they differ in the hydroxylation grade in the second and fifth amino acid (α-aminobutyric acid/*allo*threonine). Astins D, E, I and L are all monochlorinated at position δ of the proline and differ again in the second and fifth amino acid (Figure 2.2). Monooxygenases - a member of the large oxidoreductase family - are able to introduce one oxygen atom into their substrate to hydroxylate for example amino acids. The other oxygen atom is reduced to water (Apweiler et al., 2004). Different monooxygenases are known like flavin-dependent monooxygenases (reviewed in Huijbers et al. (2014)) or the heme-containing cytochrome P450 monooxygenases (reviewed in Urlacher and Girhard (2012)). Monooxygenases are involved in detoxification (Naumann et al., 2002), auxin biosynthesis (Hull et al., 2000; Zhao et al., 2001; Cheng et al., 2006), glucosinolate biosynthesis (Hansen et al., 2007; Li et al., 2008), plant development (Cheng et al., 2006), pathogen defense (Mishina and Zeier, 2006; Koch et al., 2006; Bartsch et al., 2006), drug biosynthesis (Chau and Croteau, 2004; Chau et al., 2004) and many other pathways.

2.1.5.3 Flavin-dependent halogenases

The astins can be divided according their chlorination at the proline into non- (astin G), mono- (astins D, E, F, I, L, M and N) or dichlorinated (astins A, B, C, K and O) astins. Not only the grade of chlorination but also the chlorinated C atom of the proline is different, involving a flavin-dependent halogenase.

Almost all astins contain a chlorinated proline indicating the presence of a halogenating enzyme during the biosynthesis. Three different groups of halogenating enzymes are known: Haloperoxidases, perhydrolases and flavin-dependent halogenases (reviewed in van Pée (2001)). Haloperoxidases and perhydrolases are enzymes which are not substrate specific and not regioselective. They cannot specifically halogenate a certain atom in a secondary metabolite. On the contrary, flavin-dependent halogenases are regioselective and substrate-specific (reviewed in van Pée and Patallo (2006)) so they are able to halogenate compounds such as astins and other secondary metabolites.

Flavin-dependent halogenases are enzymes requiring $FADH_2$for the reaction. A flavin reductase is essential to reduce FAD to $FADH_2$ (Keller et al. (2000), Figure 2.3). Only $FADH_2$ is accepted by the halogenase resulting from a highly conserved flavin binding domain (GXGXXG) close to the N-terminus of the protein (van Pée and Zehner, 2003). There is a second conserved sequence close to the middle of the enzyme: the tryptophan motif (WXWXIP). This motif may play a role in blocking of substrates binding near the flavin and inhibits thereby the monooxygenase activity of the halogenase(Dong et al., 2005).

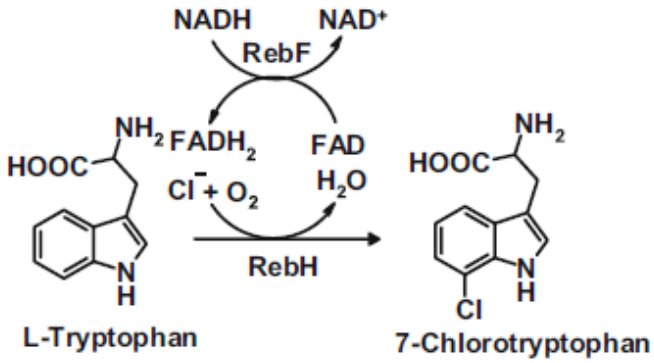

Figure 2.3: Halogenation of L-tryptophan to 7-chlorotryptophan in the rebeccamycin synthesis (van Pée and Patallo, 2006). The flavin reductase RebF reduces FAD to $FADH_2$ using NADH. The reduced $FADH_2$ is now used by the flavin-dependent halogenase RebH to introduce a chlorine atom into L-tryptophan. This reaction is oxygen dependent and produces water.

Tryptophan is chlorinated to 7-chlorotryptophan during the rebeccamycin synthesis. The reaction of $FADH_2$ and O_2 creates an FAD(C4a)-OOH intermediate in the active site of the 7-tryptophan-halogenase RebH (Yeh et al., 2006). In the presence of chlorine, the hypochlorous acid HOCl is formed (Dong et al., 2005; Yeh et al., 2006). The HOCl reacts now with the lysine residue in the active site of the halogenase and the substrate halogenation is completed (Yeh et al. (2007), Figure 2.4).

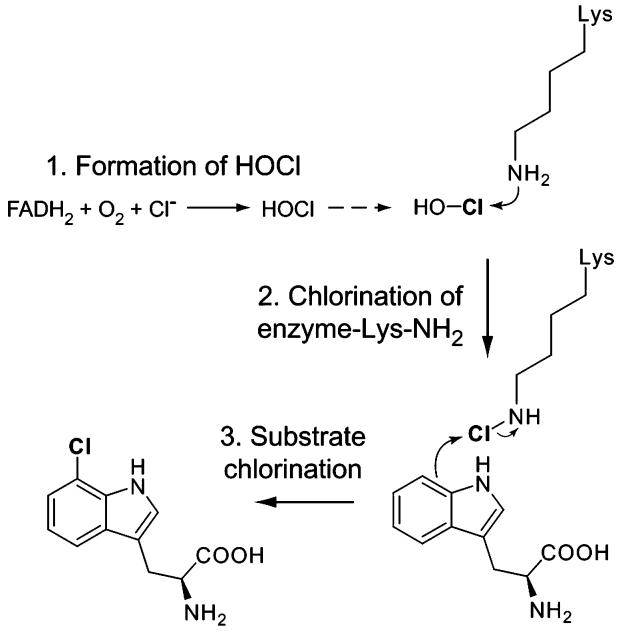

Figure 2.4: Proposed model of halogenation through the RebH halogenase (Yeh et al., 2007). In the presence of chloride, $FADH_2$ and oxygen reacts to the reactive intermediate HOCl. HOCl reacts with the lysine residue in the active site and the amino terminus is chlorinated. The chloride ion in the active site is now transferred to L-tryptophan.

2.2 Endophytes - inhabitants of (medicinal) plants

Every known plant harbors microorganisms like viruses, bacteria or eukaryotes. These inhabitants can interact with plants in different ways. Parasites benefits from the plant by harming the host plant like the rust fungi. The opposite of parasitism is symbiosis where symbionts and host plant live mutualistically together like in lichens. Commensalism means that one organism benefits from the host plant without affecting it.

Endophytes are typically bacteria or fungi which live inside a plant - either inter- or intracellular - and cause no negative effect to the growth and development of the host plant (Wilson, 1995). They can be isolated after surface sterilization from their host.

Several endophytes are sequenced, but have so far not been isolated from their host plant because they are unculturable (Hurek et al., 2002).

2.2.1 Endophytes as silent producers of secondary metabolites

Secondary metabolites as natural products play an important role in our drug industry and are isolated from different plants. Many of these plants harbor endophytic fungi which are able to synthesize these natural products. Several endophytes are known to produce important natural products from plants. These are paclitaxel from *Taxus* species (Wani et al., 1971), hypericin from *Hypericum perforatum* (Kusari et al., 2008), camptothecine from *Camptotheca acuminata* or *Nothapodytes nimmoniana* (Wall et al., 1966), vinblastine from *Catharanthus roseus* (Guo et al., 1998a) as well as other compounds of plants (Figure 2.5).

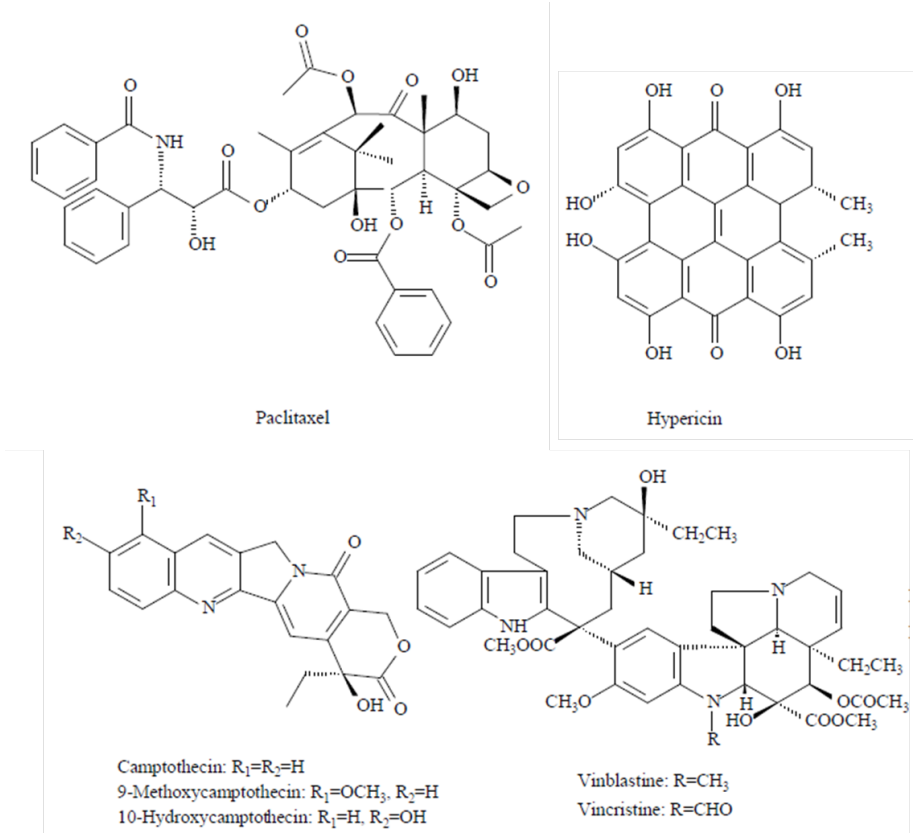

Figure 2.5: Important bioactive compounds from plants (Zhao et al., 2010).

Paclitaxel, also known as taxol, was originally found in *Taxus brevifolia* (Wani et al., 1971)

and isolated for drug production from wild *Taxus* plants. Paclitaxel can be found in *Taxus* only in extremely low amounts. In 1993, a paclitaxel producing endophytic fungus, *Taxomyces andreanae*, was discovered (Stierle et al., 1993). Up to now, over 19 genera of paclitaxel producing endophytes are known (reviewed in Zhao et al. (2010)). These endophytic fungi are a good alternative for paclitaxel production instead of the plant.

Hypericin is a well known drug for wound-healing and against depression (Tammaro and Xepapadakis, 1986). In addition, hypericin shows anti-inflammatory, antimicrobial and antioxidant activities (Zaichikova et al., 1985; Radulovic et al., 2007). Hypericin was isolated from *Hypericum perforatum* (Brockmann et al., 1939; Nahrstedt and Butterweck, 1997) harboring an hypericin producing endophyte (Kusari et al., 2008), similar to *Chaetomium globosum*. This endophyte produces hypericin in culture without the host plant (Kusari et al., 2008). Arbuscular mycorrhizas enhance the hypericin concentration in *Hypericum perforatum* (Wang and Qiu, 2006; Zubek and Blaszkowski, 2009).

Camptothecine and vinblastine are examples for anticancer drugs which are believed to be plant-derived. *Entrophospora infrequens* is the first endophytic fungus isolated from *Nothapodytes foetida* which produces camptothecin (Puri et al., 2005). The first isolated fungus producing vinblastine is an *Alternaria* sp. from the phloem of *Catharanthus roseus* (Guo et al., 1998b). Several other endophytic fungi were found to produce camptothecine or vinblastine, all isolated from their hosts (reviewed in Zhao et al. (2010)).

These examples show that endophytic fungi from plants become more and more important. They can be used as alternative producers of bioactive compounds and can therefore preserve the nature from extinction of medicinal important plants.

2.2.2 Plant growth promotion by endophytes

Plant growth promotion by endophyte - fungi or bacteria - contains many different aspects. The growth can be enhanced by providing additional nutrients like nitrogen or phosphate (biofertilisation). Endophytes can also inhibit the growth of competing microorganisms or of plant pathogens to protect the plant (biocontrol). They can also interfere with the plant hormone system or produce itself phytohormones to regulate the plant development (phytostimulation) (reviewed in Richardson et al. (2009); Gaiero et al. (2013), Figure 2.6).

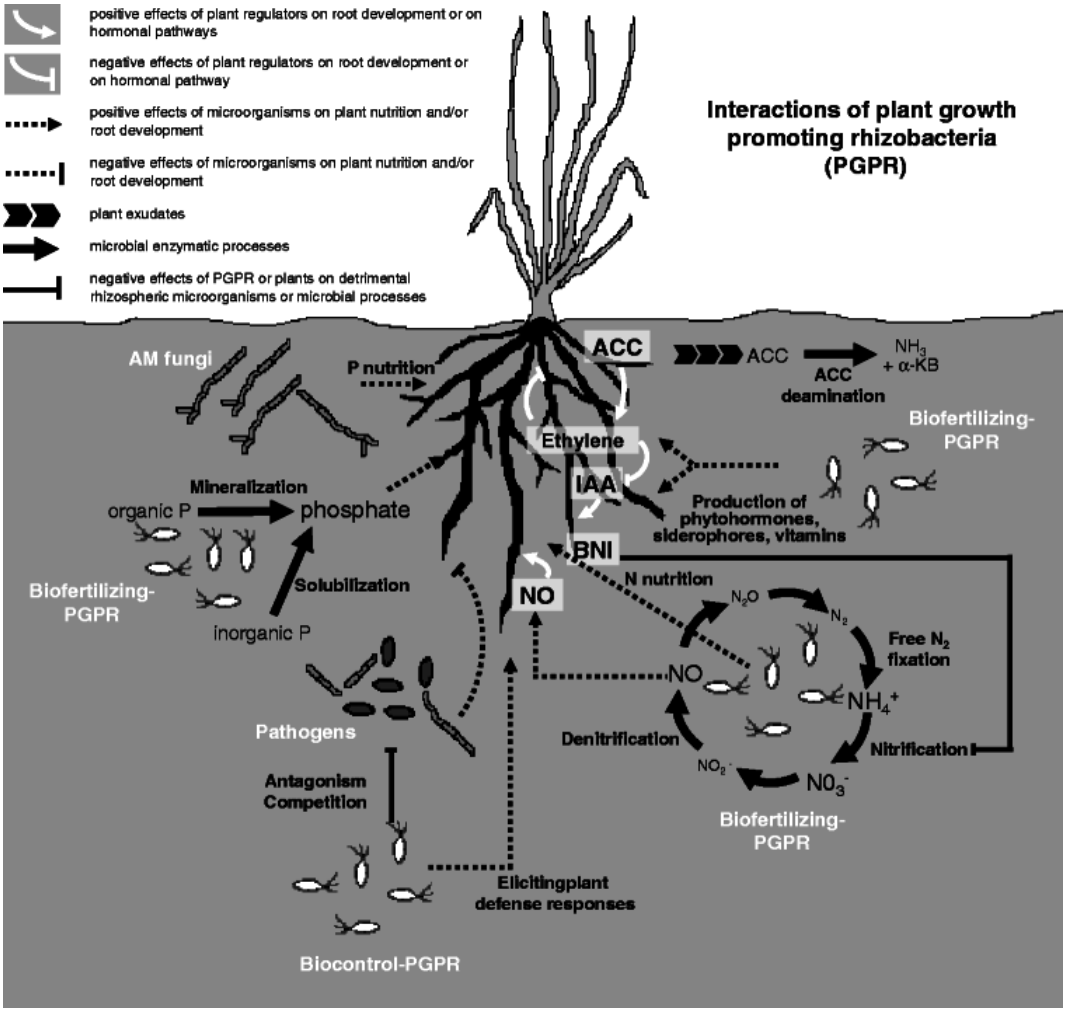

Figure 2.6: Major aspects of plant growth promotion through bacteria and fungi in soil (Richardson et al., 2009). Plant growth promoting rhizobacteria (PGPR) and arbuscular mycorrhiza fungi stimulate the growth of plants by supplying macronutrients (biofertilisation of phosphate and nitrogen), by controlling competitive microorganisms (pathogens) and by regulating phytohormones like indole-3-acetic acid (IAA) or ethylene. A detailed explanation is given in Richardson et al. (2009).

2.2.2.1 Biofertilisation of insoluble substances

Endophytes are able to make nutrients like phosphate or sulfate as well as iron(III) available for plants or supply plants with these nutrients (Bashan, 1998).

The best studied example for biofertilisation is the nitrogen uptake through the nitrogen-fixing bacteria (rhizobacteria). Rhizobacteria like *Rhizobium*, *Sinorhizobium* or *Mesorhizobium* form a symbiosis with their host plant (legumes) visible as nodules at

the roots of the plants. The nodules contain bacteroids which produce a nitrogenase complex. This complex needs a low oxygen environment created by the plant to convert air nitrogen into ammonia. This ammonia is used by the plant and the bacteroids get in exchange carbon moieties from the plant (reviewed in Wang et al., 2012).

Another example for biofertilisation is the phosphate uptake by soil microorganisms. Phosphate is essential for all organisms. Soluble phosphate which is applied to the soil is in the most cases bound to soil particles, therefore unavailable for plants. Even if soils have a high total phosphate concentration, only 0.1% of this reserve is available for plants (Zou et al., 1992). There are so called low-molecular weight organic acids (LMWOA) in the soil to increase the phosphate solubility like oxalic, succinic, tartaric, fumaric and other acids (Kaurichev et al., 1963, reviewed in Rodríguez and Fraga, 1999). These LMWOA are usually very low concentrated in soil, only increasing during plant residue decomposition (Stevenson, 1967). The LMWOAs solubilize the insoluble phosphates either by acidification or by chelation. Some bacteria and fungi are able to make the soil phosphate available for the plant with the help of organic acids like *Aspergillus* (Li et al., 2015) and *Penicillium* species (Whitelaw et al., 1999). *Aspergillus niger* An2, isolated from soil by Li et al. (2015), is able to solubilize phosphates of different types in the soil. An2 secretes mainly oxalic acid to solubilize calcium, magnesium, aluminum and iron(III) phosphates. Rock phosphates are solubilized through the release of tataric acid (Li et al., 2015).

Iron(III) is as well a rare bioavailable nutrient in soil. Under the biological pH, the ferric concentration in solution is not higher than 10^{-8}M (Neilands et al., 1987). But around 1µM iron is needed for growth (Neilands, 1995). The importance of iron lies in its ideal redox potential (used in electron transport and other metabolic pathways) and its ability as part of different enzymes to coordinate and activate oxygen. Microorganisms like bacteria and fungi are able to synthesize siderophores to cover their demand on iron. Siderophores are low molecular weight substances building a chelate complex with iron(III) which can then be transported into the cell or root via a specific transport system (see for details Hider and Kong (2010)).

All three examples show that microorganisms, either bacteria or fungi, can enhance plant growth by providing additional nutrients to the plant.

2.2.2.2 Biological control of competing microorganisms

Endophytes are not only able to "control" the plant but also to control other microorganisms through different mechanisms (biocontrol): antibiosis with their own secondary

metabolites, induced systemic resistance in the host plant or competition for niches which are just examples. The known antimicrobial acting substances belong to a variety of different chemical classes: alkaloids, peptides, steroids, terpenoids, quinones, flavonoids, alipathic compounds and phenols (Yu et al., 2010a).

Chaetomium globosum, for example, produces chloride-containing metabolites (chaetomugilin A and D as well as chaetoglobosin A and C) which inhibit the growth of *Mucor miehei* and brine shrimp (Qin et al., 2009). *Chaetomium globosum* lives in different plants like *Gingko biloba* (Qin et al., 2009) or pepper (Khan et al., 2012) as endophyte but also as decomposer of cellulose (Longoni et al., 2012).

The bacterium *Burkholderia* sp. produces antifungal and other substances suppressing many soil-borne phytopathogens (Holmes et al., 1998). *Burkholderia cepacia* has long been studied for its biocontrol activity (Leisinger and Margraff, 1979) of different plant diseases like *Pythium*, *Botrytis*, *Fusarium* and *Rhizoctonia* (Sijam and Dikin, 2005; Quan et al., 2006). One of the biocontrol agents in *Burkholderia cepacia* is pyrrolnitrin (Homma et al., 1989), a dichlorinated substance effective against yeasts and other fungi as well as gram-positive bacteria. Pyrrolnitrin is not only produced by *Burkholderia* (*Pseudomonas*) *cepacia* but also by other *Pseudomonas* species like *Pseudomonas fluorescens* (Arima et al., 1964).

Bacillus subtilis is a gram-positive bacterium living in the rhizosphere of plants. Beside its broad host range *Bacillus subtilis* produces a wide spectrum of antibiotics. Over two dozen antibiotics are known from *Bacillus subtilis* but not every strain produces all of these compounds (Stein, 2005). *Bacillus subtilis* is widely used in the agriculture. The first biological product of *Bacillus subtilis* was marketed as "Alinit" by Farbenfarbriken vorm. Friedrich Bayer & Co, Elberfeld, Germany (now known as Bayer AG) in 1897 (Killian et al., 2000). Today, many biopesticides are known and especially in the US marketed (US Environmental Protection Agency, http://www.epa.gov/pesticides/biopesticides/, accessed: 07-04-2015). Examples for the so called biopesticides are coming from *Agrobacterium*, *Bacillus* and *Pseudomonas* as well as from *Candida*, *Trichoderma* or *Ampelomyces*.

Not only antimicrobial secondary metabolites of endophytes can influence the growth of plant pathogens and other microbes. The endophyte can also use secreted lytic enzymes to interfere with pathogen growth.

2.2.3 Exoenzymes of fungi

Many microorganisms produce specific extracellular enzymes such as chitinase, cellulase, hemicellulase or protease. These enzymes usually decompose plant residues and non-living organic matter to obtain carbon nutrition.

Endophytic fungi produce different extracellular enzymes to use the nutrients available in the plant and for resistance mechanism against phytopathogens. Several enzyme activities could be detected in endophytic fungi: cellulase activities in *Talaromyces emersonii* or *Discosia* sp. and protease activities in *Aspergillus* sp. or *Cladosporium* amongst others (Sunitha et al., 2013).

Chitinases degrade fungal cell walls by breaking down the glycosidic bonds between the N-acetylglucosamine units of chitin. They can be found in all divisions: bacteria, fungi, protozoa, invertebrata, vertebrata and plants. In plants and invertebrata, chitinases play a role in the defense (Gooday, 1995), whereas in fungi, protozoa and invertebrata the morphogenesis is more important. Even in human serum, chitinase activity was detected, possible as a defense mechanism against fungal pathogens (Escott et al., 1996; Aerts et al., 1996). Chitinases in fungi have different functions: fungal growth, autolysis of the fungal cell wall as well as providing nutrition and mycoparasitism (Hartl et al., 2012). Mycoparasitism, for example, induces chitinase gene expression in *Trichoderma atroviride* (Gruber et al., 2011).

Cellulases break down the 1,4-β-D-glycosidic linkages in cellulose into shorter polysaccharides or monosaccharides. The cellulase complex consists of three different single enzymes: endo-1,4-β-D-glucanases (like carboxymethyl cellulase), exo-1,4-β-D-glucanase and β-glucosidase (Schomburg et al., 2004). The main natural agents for cellulose degradation are fungi and bacteria (Lederberg, 1992). Fungi with a high cellulase activity are the brown-rot and white-rot fungi. Brown-rot fungi (e.g. *Gloeophyllum sepiarium*, *Serpula incrassata*, *Postia placenta*) cleave cellulose and hemicellulose of wood almost completely, so that only modified lignin is found in brown-rotted wood (Eriksson et al., 1990). Contrary, white-rot fungi (e.g. *Bjerkandera adusta*, *Schizophyllum commune*) degrade crystalline cellulose with a complex of endoglucanases and cellobiohydrolases (Eriksson et al., 1990).

Proteins are the main nitrogen source in wood, therefore playing an important role for wood decaying fungi. Proteolytic enzymes are therefore important in xylotrophic basidiomycetes like the brown rot and white rot fungi. Extracellular proteases of filamentous fungi have different roles: processing of post-secreted proteins (Eneyskaya et al., 1999), formation of aerial mycelium (Wösten et al., 1996), nutrition (Archer and

Peberdy, 1997), adaptation to the environment (Leger et al., 1997) as well as building of fructification structures (Small and Bidochka, 2005). Secreted proteolytic enzymes are regulated by nutrition (Paoletti et al., 1998) and other environmental factors (Tibbett et al., 1999; Denison, 2000).

In some cases, extracellular enzymes can also act as biocontrol agents. *Serratia marcescens* seems to use chitinases to control *Sclerotium rolfsii* (Ordentlich et al., 1988). The β-1,3-glucanase of one *Burkholderia cepacia* strain is induced by different fungal cell walls (Fridlender et al., 1993). A β-1,3-glucanase from *Lysobacter enzymogenes* strain C3 is also supporting the biocontrol activities (Palumbo et al., 2005). The excretion of extracellular enzymes like chitinases or glucanases lyse the cell wall of living fungal phytopathogens and therefore influence their pathogenic properties.

2.3 Aim of work

Astins as antitumor compounds could so far only isolated in very low amounts from *A. tataricus* (Morita et al., 1996). We were therefore interested in identifying astin biosynthesis genes to express them heterologous in organ cultures.

Since the new endophytic astin producer *P. asterica* came across the investigations we decided to focus more on the endophyte. Beside the astin biosynthesis genes of *P. asterica* also the optimization of the fungal growth were analyzed to enhance the astin production in *P. asterica*. Furthermore, the interaction between *P. asterica* and *A. tataricus* should be analyzed to understand how the plant and/or the fungus might regulate the astin production and benefit from each other, e.g. by solubilization of additional nutrients or by controlling other microorganisms.

3 Material and methods

3.1 Organisms

Different plant cultivars were used for the analysis (Table 3.1). The Dresden cultivar of *A. tataricus* was cultivated from seeds obtained from the Botanical Garden in Dresden. The plants from the Botanical Garden Dresden originate from the botanical garden in Vladivostok, Russia. These seeds were germinated in the dark (covered with ca. 0.5 mm soil) and cultivated in soil. The Austrian cultivar was obtained from a plant selling company in Austria. Both cultivars were grown on the one hand in the greenhouse and on the other hand in a climate chamber under long day conditions (16 hours light with 23 °C and 8 hours dark with 18 °C). The light intensity in the greenhouse and in the climate chamber was 40 to 60 µmol/m^2s.

Table 3.1: Plants used in this work.

organism	cultivar	origin
A. tataricus	Dresden	Botanical Garden TU Dresden, Germany accession number: 013557-21
A. tatariucs	Austria	Sarastro Stauden, Austria

The *T. islandicus* WF-38-12 strain was obtained from LGC Standards GmbH, Wesel, Germany. The other fungi are from the collection of the laboratory of Plant Physiology (Table 3.2). All fungi were cultivated on typical fungal media like potato dextrose or malt extract.

Table 3.2: Fungi analyzed in this work.

Ascomycota	Basidiomycota
Acremonium alternatum	*Bjerkandera adusta*
Cladosporium sp.	*Daedalea quercina*
Fusarium avenaceum	*Gloeophyllum sepiarum*
Fusarium graminearum	*Piriformospora indica*
Fusarium culmorum	*Postia placenta*
Macrophomina phaseolina	*Schizophyllum commune*
Metarhizium anisopliae	
Trichoderma sp.	

3.2 Primers

Reference primers for *A. tataricus*

Sawai and colleagues found a shionone synthase in *A. tataricus* (Sawai et al., 2011). Their primers were used to assess the quality of nucleic acids from *A. tataricus* (Table 3.3). Beside this, a bachelor student of the laboratories of Plant Physiology, Cornelia Dolle, designed actin primers for *Helianthus annuus* which also amplify the actin gene in *A. tataricus* (Dolle, 2011).

Table 3.3: Primers binding to *A. tataricus* DNA.

name	target	sequence	T_a in °C	size in bp	reference
AstSHSf2	CDS of shionone synthase	CAA GTA TCG GCA TAC AAG CTC TGC	61	226	Sawai et al. (2011)
AstSHSr2		AGG CAG CAC GTT AAC CCT ATA GTC			
AstSHS3Uf1	3′ UTR of shionone synthase	CCA CCA GTC AAA CGT AAA ACT CTC	66	~200	
AstSHS3Ur1		CCA CAA CCT TTT GGT TGA TGA CTC			
CD-Ha-ACT2-fw	actin	CAG GGA GAA GAT GAC CCA GA	60		Cornelia Dolle
CD-Ha-ACT2-rv		ATC CTC CGA TCC AGA CAC TG			

Primers to identify and verify different fungi

Primers binding to the rDNA repeat unit were used to verify the different fungi (Tables 3.2 and 3.4). Vilgalys and Hester (1990) and White et al. (1990) designed these primers for phylogenetic analysis in fungi. The primer pairs ITS1F/ITS4, LR0R/LR7 and NS3/NS8 were used to identify and describe the new endophytic fungus (see subsection 3.6).

Table 3.4: Primers for identification of fungi.

name	sequence	T_a in °C	reference
ITS1	TCC GTA GGT GAA CCT GCG G	60	White et al. (1990)
ITS3	GCA TCG ATG AAG AAC GCA GC	60	
ITS1F	CTT GGT CAT TTA GAG GAA GTA A	47	
ITS4	TCC TCC GCT TAT TGA TAT GC		
LR0R	ACC CGC TGA ACT TAA GC	47	Vilgalys and Hester (1990)
LR7	TAC TAC CAC CAA GAT CT		
NS3	GCA AGT CTG GTG CCA GCA GCC	51	White et al. (1990)
NS8	TCC GCA GGT TCA CCT ACG GA		

The following primers (Table 3.5) were used to confirm the identity of the fungal species used in this thesis. The fragment size was calculated for genomic DNA. The reverse primer for *Gloeophyllum sepiarum* was ITS1.

The specific primers for *P. asterica* were designed for non-conserved regions of the SSU-ITS sequence. The primers were confirmed with a primer BLAST search (Ye et al., 2012) against fungi (taxid: 4751) resulting in no matching sequence. Additionally, the primer were tested in a PCR against the fungi from the collection of the laboratories of Plant Physiology. No PCR product was found at these high annealing temperatures.

Primers to identify possible halogenase genes

Different sequences of known and putative halogenases were used to design primers to identify a halogenase gene either in *A. tataricus* or *P. asterica* (Table 3.7). All forward primers lie in the FAD binding motif (GXGXXG) and the reverse primers amplify the nucleic acid sequence of the tryptophan motif (WXWXIP).

The bacterial halogenase primers were designed by Liane Flor (TU Dresden, Institute of Biochemistry, Germany). Halogenases from five different bacteria (Table 3.6) were aligned and the consensus sequence of the conserved motifs was used for the primer design (primers named LFHAL).

Table 3.5: Species-specific primers for identification of fungi.

name	organism	sequence	T_a in °C	size in bp	reference
AsnNIG1f	*Aspergillus niger*	GAT TTC GAC AGC ATT TTC CAG AA	60	245	Susca et al. (2007)
AsnNIG2r		AAA GTC AAT CAC AAT CCA GCC C			
FualTSf	*Fusarium graminearum*	CCA GAG GAC CCA AAC TCT AA	59	272	Schilling et al. (1996)
FualTSr		ACC GCA GAA GCA GAG CCA AT			
FucOPT18f	*Fusarium culmorum*	GAT GCC AGA CCA AGA CGA AG	55	472	Schilling et al. (1996)
FucOPT18r		GAT GCC AGA CGC ACT AAG AT			
FugUBC85f	*Fusarium graminearum*	GCA GGG TTT GAA TCC GAG AC	61	332	Schilling et al. (1996)
FugUBC85r		AGA ATG GAG CTA CCA ACG GC			
SCOM1	*Schizophyllum commune*	GTT GAC TAC GTC TAC CTC AC	58	305	Buzina and Lang-Loidolt (2001)
SCOM2r		GTT AGG CTC CAG CAG ACC TC			
GlsR	*Gloeophyllum sepiarum*	GTT AAT AAA AAC CGG GTG AG	55	398	Moreth and Schmidt (2000)
BjaF3	*Bjerkandera adusta*	ACC TTG CGC TCC TTG GTA T	60	188	Yamaura et al. (2013)
BjaB3		CTC CAC AGC AAC GCA GA			
NS8for2	*Pelliciarosea asterica*	GTC ACT ATT GAC GGC GAC ACT GA	68 to 72	752	own design
ITSrev2		GCG AGG TTG AGT TAC TAC GCT			

Table 3.6: **Bacterial halogenases** used for primer design.

species	halogenase	biosynthetic pathway
Pseudomonas fluorescens Pf-5	PltA and PltM	pyoluteorin
Pseudomonas aeruginosa	PltA and PltM	pyoluteorin
Streptomyces griseoflavus W-384	HrmQ	hormaemycin
Streptomyces vitaminophilus	Pyr 16 and Pyr29	pyrrolomycin
Actinoplanes sp. ATCC 33002	HalA and HalB	pentachloropseudilin

Beside the known halogenases especially in bacteria, there are putative halogenases in other organisms as well. The halogenase primers of *Penicillium marneffei* ATCC 18224 (PemHAL) were designed based on a hypothetical protein (protein ID XP_002151004.1). The halogenase sequence of *T. islandicus* (PeiHAL) was derived from its genome which was sequenced by the CeBiTec in Bielefeld, Germany.

The search for halogenases in EMBL-EBI InterPro (Mitchell et al., 2014) revealed eight candidate genes for tryptophan halogenases in two plants (*Ricinus communis* and *Mangifera indica*). The sequences showed that only the protein from *Ricinus communis* was closer related to bacterial halogenases (*Caulobacter* sp., *Asticcacaulis excentricus*, γ-proteobacteria and others). Only one out of eight candidates contained both conserved motifs (EMBL-EBI ID: B9THG3). Therefore, the sequence of this protein was used to build the RicHAL primer.

Table 3.7: Different primers used to amplify (putative) halogenases.

primer	sequence	T_a in °C	size in bp	
			CDS	DNA
LFHAL1for	ATC ATC GCY GGC GGC CCG GCC GG	58		
LFHAL3rev	GAT CGG GAT CTG CCA VAC CCA			
PemHALfor1	GGA GGT GGA CCT GCA GGA	45-70	696	
PemHALrev1	AGG AAT GTA CCA CGT CCA GCC			
PeiHALfor1	GGA GGT GGC CCT GGG GGG	68	687	949
PeiHALrev1	GGG GAT AGC CCA TGC CCA			
PeiHALBfor2	AGT GGT CGT GTA GGC TTG CT	60		268
PeiHALBrev1	CTG GAG AGC CAG ATT GAA CC			
RicHALfor1	GGT TTC GGC GAC TTC GGT	57	537	
RicHALrev1	CGG GAT GCG CCA CAG CCA			

Primers for real-time PCR

The primers for real-time PCR were designed with Primer3 (Koressaar and Remm, 2007; Untergasser et al., 2012). The sequenced PCR product of the primer pair CD-Ha-ACT2-fw + CD-Ha-ACT2-rv (see Table 3.3) was used to build specific actin primers of *A. tataricus* (qAstACT).

The ITS region of *P. asterica* was around 100 bp larger as any fungal sequence found in the BLASTn search (Madden, 2002) of the *P. asterica* rDNA sequence against fungi (taxid: 4751). These additional nucleic acids were close to the SSU and used for the real-time primers (qPearDNA). A primer BLAST search with these primers (Ye et al., 2012) did not result in homology with other fungi or plants.

The real-time primers for the *P. asterica* genes 1622, 4080, 4646, 5634 and 8445 spanned an intron to avoid the amplification of genomic DNA (Table 3.8).

Table 3.8: Real-time PCR primers for expression analysis.

name	sequence	size in bp	
		CDS	DNA
qAstACTfor1	CCT TCC CGA GCT ATT TAA TGT GA		160
qAstACTrev1	CGA TCA AGG CTG CAG TAG TC		
qAstACTfor2	GGA AGC AGC GGG TAT TCA TG	151	151
qAstACTrev2	TGC GGT AAT TTC CTT GCT CA		
qPearDNAfor1	AAT ATC AGT GGG TCC CCG GT		103
qPearDNArev1	CAC CTG CAA CCG AAA CTG AC		
qPeaACTgfor1	ATG GAG GAG GAG GTT GCT G	155	
qPeaACTgrev1	GGT ATG GGC CAG AAG GAC TC		
qPea1622for1	TGC GCA ATC ACT TAC TTC GG	77	
qPea1622rev1	TGT CTT TCG TTG CAT CGT GG		
qPea4080for	GTC TTG ACC GGG TTG ATG TC	82	
qPea4080rev1	TAT GGC TTG ATA CCG GTG GC		
qPea4646for1	CCG TCT ACA GCT ATG ATT GCA	155	
qPea4646rev1	AAG GTT CGG GTC ATT CAG GT		
qPea5634for1	AGA CAC TGA TTG AGC GCA T	171	
qPea5634rev1	GCG TGT CGG TAA GGA GAA AC		
qPea8445for1	TAA AGG CGC AAA CTT GGC AA	197	
qPea8445rev1	TCG GAT TGT CGG GTT GAA GA		

3.3 Substances, media and equipment

If not indicated otherwise, the chemicals were purchased from Roth, VWR and Fisher. Only specific substances like hormones, staining solutions or enzymes are listed below

(Table 3.9).

Table 3.9: **Special chemicals** with abbreviation and supplier.

name	abbreviation	company
agarose Electrophoresis Grade, Ultrapure		Invitrogen
6-benzyl-adenine	BAP	Sigma Chemicals
bovine serum albumin	BSA	MP Biomedicals
bromocresol purple		Sigma Aldrich
carboxymethyl cellulose	CMcellulose	Roanal
chitin		Sigma Chemicals
chromazurol S	CAS	Sigma Chemicals
Coomassie Brilliant Blue G-250		Merck
cresol red		Sigma-Aldrich
nuclease-free water, DEPC treated and autoclaved	DEPC water	Roth
ethidium bromide		Roth
gelatin		Sigma Chemicals
hexadecyl-trimethyl-ammonium-bromid	HDTMAB	Sigma Aldrich
Hoagland's no 2 basal salt mixture		Sigma-Aldrich
hydroxylapatite		Aldrich-Chemie
indol-3-butyric acid	IBA	Serva
iron(III) phosphate		Sigma Aldrich

name	abbreviation	company
lactophenol blue solution		Roth
malt extract		Roth
Murashige-Skoog medium with vitamins	MS	Duchefa
naphtyl acetic acid	NAA	Duchefa
phyto agar		Duchefa
potatoe dextrose bouillon		Roth
proteinase K		Roth
RNA®zol		MRC
skim milk		Fema
tartrazine yellow		Sigma-Aldrich
L-threonine		Merck

The fungal and plant media are listed below (Table 3.10). All media were sterilized at 120 °C for 15 minutes. The pH was brought to 5.8 with NaOH or HCl.

Table 3.10: Used media and their composition, with references.

medium	composition	notes
PDA	26.5 g/l potato dextrose broth 10 g/l phyto agar	PDB without phyto agar
MEA	30 g/l malt extract 10 g/l phyto agar	MEB without phyto agar
MS	4.4 g/l MS 3 % sucrose 10 g/l phyto agar	Murashige and Skoog (1962)
Hoagland	0.5 g/l MES 10 g/l sucrose 1.6 g/l Hoagland 7 g/l phyto agar	Hoagland and Arnon (1950)

Table 3.11: Special equipment used in this thesis.

application	name	company
binocular		Thalheim Spezialoptik
evaporation	Multivapor P-6	Büchi
light microscope		Zeiss JenaLab
nanodrop	ND-1000 Spektophotometer	PeqLab
real time PCR	qTower 2.2	Analytik Jena
thermocycler	Mastercycler ep gradient S	Eppendorf
UV gel documentation		Biorad
vacuum pump	VCZ 224	ILMVAC

3.4 Extraction of nucleic acids

3.4.1 Extraction of DNA from different sources

3.4.1.1 Extraction of DNA from plants and fungi

Fungal DNA was isolated from liquid cultures after a modified protocol by Möller et al. (1992). One hundred milligram tissue was ground with liquid nitrogen and after adding the DNA extraction buffer (100 mM TrisHCl, pH 7.0, 10 mM EDTA, 20 % SDS, 100 µg/ml proteinase K, 1 % 2-mercaptoethanol) the sample was transferred to an 1.5 ml Eppendorf tube. The sample was incubated at 60 °C for one hour under vigorous shaking. The salt concentration of the sample was adjusted to 1.4 M with 5 M NaCl (140 µl) and 1/10 volume of 10 % HDTMAB was added. After an incubation at 65 °C for 10 minutes under vigorous shaking, 1 volume chloroform/isoamyl alcohol (24:1) was added to the sample which was then incubated on ice for 30 minutes and centrifuged (16,000 rcf for 10 minutes at 4 °C). A half volume of CH_3COONH_4 was added to the upper phase and incubated on ice for one hour. After centrifugation (16,000 rcf for 15 minutes at 4 °C) the supernatant was transferred to a fresh tube. Remaining RNA was digested with 0.02 µg/µl RNAse A at 37 °C for 30 minutes. The DNA was precipitated with 0.6 volume isopropanol over night and then centrifuged (16,000 rcf for 20 minutes at 4°C). The pellet was washed three times with 70 % ethanol, dried at 37 °C for 10 minutes and finally dissolved in 20 µl distilled, autoclaved water.

3.4.1.2 Extraction of DNA from TAE gels

The Invisorb® Spin DNA Extraction Kit (STRATEC Biomedical) was used for the DNA extraction from TAE gels as described in the manufacturer's protocol. The DNA was eluted with 30 µl autoclaved, distilled water.

3.4.2 Extraction of RNA and synthesis of cDNA from plants and fungi

3.4.2.1 Extraction of RNA and cDNA synthesis for RT-PCR

The RNA for RT-PCR was extracted with RNAzol® as described in the instruction manual. Only one step was varied: the RNA was not precipitated within 10 minutes at room temperature, but overnight at -20 °C in a freezer.

After isolation, any remaining DNA in the RNA containing solution was digested with DNaseI, RNase free from LifeTechnologies. The sample was incubated with the following buffers and enzymes at 37 °C (see Table 3.13):

Table 3.13: DNaseI digest of RNA.

	final concentration
DEPC water	add to 40 µl
10 x DNAseI reaction buffer	1 x
40 U/µl RiboLock™ RNase Inhibitor	1 U/µl
1 U/µl DNaseI, RNase free	1 U/µg RNA
RNA sample	up to 20 µg

The reaction was stopped after 45 minutes with 2 µl 50 mM Na-EDTA at 65 °C for 10 minutes. Subsequently, the proteins had been eliminated with chloroform/isoamyl alcohol (24:1) and the RNA was precipitated with $Na(CH_3COO)$ and absolute ethanol at -20 °C over night. The pelleted RNA was then washed twice with 75 % ethanol in DEPC water, before the RNA was dried and resolved in 13 µl DEPC water. Quality and quantity of the RNA was validated by agarose gel electrophoresis and by measuring the RNA using a nanodrop.

The DNaseI digested RNA was now transcribed with RevertAid™ Reverse Transcriptase (LifeTechnologies) into cDNA according to the manufacturer's protocol.

3.4.2.2 Extraction of RNA and cDNA synthesis for quantitative real-time PCR

The RNA for quantitative real-time PCR was extracted with RNAzol solution and immediately purified with the Direct-zol™ RNA MiniPrep by ZymoResearch. The DNA was digested on the column according to the manufacturer's protocol. The cDNA was synthesized with the Maxima First Strand cDNA Synthesis Kit for RT-qPCR by LifeTechnologies.

3.5 PCR and quantitative real time PCR

3.5.1 PCR

The polymerase chain reaction (PCR) is a method to amplify and duplicate a specific DNA sequence. Primers as oligonucleotides with a known sequence bind to the specific DNA sequence and a thermostable DNA polymerase is elongating these primers according to the specific DNA sequence. This steps are repeated several times to generate multiple copies of this specific DNA sequence (Mullis et al., 1986; Mullis and Faloona, 1986). The reverse transcription PCR (RT-PCR) uses cDNA which is created by a reverse transcriptase instead of genomic DNA as PCR template.

Two different polymerases from LifeTechnologies were used for the PCR. A proof-reading polymerase, Phusion DNA Polymerase from LifeTechnologies, was used for sequencing, whereas the DreamTaq DNA Polymerase, an enhanced polymerase from *Thermus aquaticus,* was used for amplifications like halogenase search or cloning. The polymerases were used according to the manufacturer's protocol. The PCR products were then separated in a 1x TAE (80 mM TrisBase pH 8.5, 1 mM EDTA, 0.114 % v/v acetic acid) gel during agarose gel electrophoresis. If not indicated otherwise the DNA ladder used is the GeneRuler 1 kb DNA Ladder by LifeTechnologies.

3.5.2 Quantitative real-time PCR

The quantitative real time PCR (qPCR) uses fluorescence to detect the amplified DNA in real time (Gibson et al., 1996; Wittwer et al., 1997). There are different ways to label the amplified DNA. First, unspecific fluorescence dyes like SYBRGreen intercalate with double strand DNA and indicate with fluorescence the presence of double stranded DNA. Second, sequence-specific oligonucleotides can be labeled with a fluorescence reporter which only fluoresces after hybridization (see for details (Dvorak, 2006)). The qPCR can be used either for absolute quantification or for relative quantification.

The absolute quantification uses an external calibration curve to quantify the DNA amount of a specific gene (Pfaffl and Hageleit, 2001). The calibration curve pictures defined quantities of (genomic) DNA with the corresponding Ct values (crossing time). This calibration curve is used to quantify the DNA amount of a specific gene from which only the Ct values are known.

Ct values represents the amount of PCR cycles which are necessary to cross a defined fluorescence level. All samples have the same amount of newly synthesized DNA at the

Ct (Pfaffl, 2004). The higher the Ct value, the lower the DNA amount of the amplified sequence.

The relative quantification uses instead one or more reference genes to which the expression of the target gene is normalized (Rasmussen, 2001). The obtained Ct values are analyzed with the $2^{-\Delta\Delta Ct}$ method (Livak and Schmittgen, 2001). The $2^{-\Delta\Delta Ct}$ value represents the fold change of condition B to condition A. Fold changes higher than 2 show up-regulated genes, fold changes under 0.5 represent down-regulated genes.

The SensiFAST SYBR No-Rox Kit by Bioline was used for qPCR as described by the manufacturer.

3.6 Isolation and identification of a new endophytic fungus from *A. tataricus*

3.6.1 Generation of *in vitro* plants of *A. tataricus*

The inflorescence axis of one Austrian *A. tataricus* plant was surface sterilized with 70 % ethanol plus 0.1 % Triton X-100 for 30 seconds. Furthermore, the inflorescence axis was sterilized with 4.2 % sodium hypochloride for 5 to 7 minutes to kill the microorganisms in the axils and deep furrows of the axis. Afterward, the inflorescence axis was washed three times with autoclaved distilled water to remove adhering hypochloride. The sterilized inflorescence axis was cut into pieces of 1 cm in length and placed onto MS agar plates containing different phytohormones. These phytohormones, in detail naphtyl acetic acid (NAA) as well as indole-3-butyric acid (IBA) as auxins and 6-benzylaminopurine (BAP) as cytokinin, induce in combination in the sterilized tissue the cell growth. Different combination of phytohormones were tested (Table 3.14).

Table 3.14: Combination of phytohormones. These combinations of artificial and natural phytohormones in the plant media were used for the transfer of the plantlets at different time points.

	alone	in combination with
NAA	0.1 mg/l	1 mg/l BAP 3 mg/l BAP 4 mg/l BAP
	0.2 mg/l	
IBA	1 mg/l	2.5 mg/l NAA
	2.5 mg/l	
	3 mg/l	
BAP	1 mg/l	
	2 mg/l	
	3 mg/l	
	4 mg/l	

The plates were incubated in a climate chamber under long day conditions (16 hours at 23 °C with around 60 µmol/m^2s light and with 8 hours at 18 °C in the dark). The explants were transferred to fresh MS plates every second week during the first two months and then once a month.

3.6.2 Identification and phylogenetic analysis of the new endophyte

The DNA of the fungus was isolated according to the method described under section 3.4.1. The fungus isolated from the inflorescence axis of the Austrian cultivar of *A. tataricus* was identified through its rDNA sequence. Therefore, different primers were used for PCR and sequencing: NS3 and NS8 for the small subunit (SSU or 18S rDNA), ITS1 and ITS4 for the ITS1 - 5.8S rDNA - ITS2 sequence as well as LROR and LR7 for the large subunit (LSU or 28S rDNA) (Figure 3.1).

Figure 3.1: Position of primers binding to the rDNA repeat unit for identification of *P. asterica*. NS3 and NS8 bind to the small subunit (18S rDNA, SSU), LROR and LR7 bind to the large subunit (26S rDNA, LSU) and ITS1F and ITS4 bind around the internal transcribed spacer (ITS) 1 and 2 including the 5.8S rDNA.

The PCR was set up with the proof-reading Phusion polymerase. The resulting PCR product was separated on a TAE agarose gel and isolated from the TAE gel with the GE Healthcare Gel Extraction Kit according to the instruction manual. The PCR products of the rDNA (SSU, ITS and LSU) were sequenced by Eurofins MWG. The retrieved sequences were run in a BLASTn search (Madden, 2002) against fungi (taxid: 4751) with the following settings: the chosen database was Nucleotide collection (nr/nt), uncultured/environmental samples were excluded from the search and only highly similar sequences (megablast) were used. The first 250 sequences were checked for duplicates. Sequences of known fungi (including Basidiomycetes as outgroup) were aligned together with the other sequences. The alignment and the phylogenetic tree were conducted in MEGA6.0 (Hall, 2013).

A sample of the unknown endophytic fungus was sent to the DSMZ (Leibniz Institute German Collection of Microorganisms and Cell Cultures, 38124 Braunschweig, Germany) to confirm these results. A taxonomic identification of the rDNA sequence was performed.

The sequences of the ITS-LSU and the SSU were aligned using the MUSCLE method (Edgar, 2004) with the default settings. After alignment, a phylogenetic tree was built with the Maximum Likelihood method based either on the General Time Reversible model (Nei and Kumar, 2000) for the ITS-LSU or on the Kimura 2-parameter model (Kimura, 1980) for the SSU. A bootstrapping to create a consensus tree was done with 2000 replicates (Felsenstein, 1985). The evolutionary rate differences between sites were modeled with a discrete Gamma distribution (+G, parameter = 0.8144 for ITS-LSU respectively parameter = 1.7770 for SSU).

3.7 Analysis of astins

The astins were extracted using two different ways: from fresh material with acetone/methanol and from liquid culture with n-butanol. The isolated samples, dissolved

in distilled water, were measured by Thomas Schafhauser (University of Tübingen, Germany) with HPLC/MS. Both methods were developed by T. Schafhauser.

3.7.1 Extraction of astins from fresh plant material

The plant material was ground with liquid nitrogen and placed in an Erlenmeyer flask. The astins were extracted twice with 20 ml acetone/methanol (1:1) per gram fresh weight for 30 minutes under vigorous shaking. The third extraction was done with 20 ml water per gram fresh weight and collected separately. First, the acetone/methanol extract was evaporated under vacuum before the water extract was evaporated in the same flask. The sediment was then resuspended in 5 ml distilled water.

3.7.2 Extraction of astins from fungal liquid culture

The fungus is secreting almost all astins into the medium (T. Schafhauser, personal communication), so only the medium was analyzed. The mycelium was separated from the medium by centrifugation (10.000 rcf for 15 minutes at room temperature). The medium was extracted with n-butanol in an extraction funnel under vigorous shaking for 30 seconds. After phase separation, the butanol phase was collected and evaporated under vacuum. The sediment was resuspended in 1 ml distilled water.

3.8 Growth of *P. asterica* under different conditions

After isolation of *P. asterica* from *A. tataricus* cultivar Austria, several experiments were set up to enhance the growth of *P. asterica* in liquid culture. If not indicated otherwise, the fresh or dry weight and the astin profile of the dichlorinated astins A/B and C was determined. The growth rate was calculated as described in section 3.9.3. The differences were statistically analyzed with the Mann-Whitney U-test (Mann and Whitney, 1947).

3.8.1 Growth and astin profile of *P. asterica* with leaves from different plants

P. asterica was co-cultivated with surface-sterilized leaves. The leaves were sterilized using 70 % ethanol plus 0.01 % Triton X-100 for 30 seconds followed by a step with 4.2 % calcium hypochloride solution including again 0.01 % Triton X-100 for five to seven

minutes. The so sterilized leaves were washed three times with autoclaved, distilled water under the laminar hood and were cut into pieces. The leaf pieces were inoculated in 20 ml liquid PDB plus 2 ml *P. asterica* from a 28 days old liquid culture. Controls containing only *P. asterica* or the different leaf pieces were also set up. These cultures were then incubated at 28 °C under vigorous shaking for one month. Leaves of the following plants were used: *A. tataricus* cultivar Austria and Dresden, *Helianthus annuus* as well as *Symphytum officinale*. One culture per condition was set up.

3.8.2 Growth and astin profile of *P. asterica* with different *A. tataricus* plant extracts

Different plant extracts were added to the shaking culture of *P. asterica*. Leaves and roots of both cultivars of *A. tataricus* were extracted either in water or 100 % ethanol for 24 hours under vigorous shaking. The extracts were filtered to remove plant debris, followed by filter sterilization (pore size 0.22 µm) to prevent degradation of compounds in the extract during autoclaving. The sterilized extracts in different amounts were added to 20 ml liquid PDB including 2 ml *P. asterica* from a 28 day old liquid culture. The incubation was done at 28 °C under vigorous shaking for one month. This experiment was set up with one sample for each extract dilution at different time points: the first experiment was conducted in May 2013, two months after isolation of *P. asterica*; a second and third experiment were set up in summer 2013 and a fourth experiment was performed in November 2013 (eight months after isolation of *P. asterica*).

Different amounts of extract were added to the cultures. The added extract volume (e.g. 8 ml, 4 ml, 400 µl and 40 µl) was calculated according to the used biomass of fresh tissue. For example, the leaves and roots were always extracted with 4 ml water or ethanol per gram fresh weight. So, 8 ml of extract solution contain the contents of 2 g fresh weight.

3.8.3 Variability of growth between replicates

The variability between replicates inoculated with water or ethanol extract was measured. *P. asterica* was cultivated in PDB with water or ethanol extract of leaves from *A. tataricus* cultivar Dresden (for preparation see section 3.8.2) and incubated at 23°C under vigorous shaking for three weeks. Controls with only the equivalent volume ethanol or water were also measured. Ten replicates of each condition were set up.

A second experiment was performed to look if the origin of the *P. asterica* culture used

for inoculation - from solid PDA plates or from liquid PDB medium - was influencing the growth. Liquid cultures of *P. asterica* were inoculated either with *P. asterica* plugs of 6 mm in diameter from PDA or with 2 ml of *P. asterica* from a 28 days old liquid culture. After three weeks, 10 replicates of each condition were analyzed.

Only the dry weight was measured in these two experiments to determine the variability in the growth of different replicates.

3.8.4 Growth of *P. asterica* on different plates

P. asterica was growing poorly under *in vitro* conditions shortly after the isolation from *A. tataricus* cultivar Austria. To see how *P. asterica* was growing after nearly two years of *in vitro* cultivation on/in typical fungal media, an experiment on agar plates was set up in January/February 2015.

A plug of *P. asterica* (6 mm in diameter) was transferred from 21 day old plates to fresh MEA or PDA plates and incubated at 23 °C in an incubator for over 42 days. The colony diameter of 10 replicates of each condition was measured after 21 days, 28 days, 35 days and 42 days.

3.9 Further physiological characterization of *P. asterica*

To determine physiologically characters of the new endophyte, the biofertilisation of phosphate as well as iron(III), the synthesis of extracellular enzymes and the antibiosis ability of *P. asterica* were analyzed.

3.9.1 Biofertilisation of phosphates and iron

The ability of *P. asterica* to use different phosphates as substrate was tested with fungus grown on agar plates. Six millimeter plugs of *P. asterica* were transferred from MEA plates to plates with two different phosphate containing media: hydroxylapatite and iron(III) phosphate (see Table 3.15). The plates with fungus were incubated at 23 °C for two weeks. A clearing zone around the fungal colony indicates an uptake of phosphate from the medium (Sundara and Sinha, 1963). The diameter of the fungal colony and the existing clearing zone were measured. The differences in growth and clearing zone were statistically analyzed with the Mann-Whitney U-test (Mann and Whitney, 1947).

Table 3.15: Composition of phosphate media for detection of phosphate biofertilisation (Sundara and Sinha, 1963).

SS medium for phosphate biofertilisation	
0.5 g/l	ammonium sulfate
0.2 g/l	potassium chloride
0.3 g/l	magnesium sulfate
4 mg/l	manganese(II) sulfate
2 mg/l	iron(II) sulfate
10 g/l	D-glucose
0.5 g/l	yeast extract
0.1 g/l	chloramphenicol
10 g/l	phyto agar
additives	
0.5 g/l	hydroxylapatite or
0.5 g/l	iron(III) phosphate

P. asterica was transferred also to agar plates to analyze the fertilization of iron(III). Beside an iron source, the fungal growth media (PDA and MEA) contained CAS and HDTMAB (Table 3.16). The HDTMAB stabilizes the blue complex of CAS and iron. Fungal siderophores form a complex with the iron and release thereby the CAS from the blue complex. This leads to a color change of the medium from blue into orange (MEA) or pink (PDA). A production of siderophores by the fungus *P. asterica* was therefore indicated by a color change (Schwyn and Neilands, 1987). The plates with 6 mm plugs of *P. asterica* were incubated at 23 °C for four weeks. *Aspergillus* sp. was used as a positive control.

Table 3.16: Composition of CAS medium for siderophore production (Schwyn and Neilands, 1987).

CAS medium for iron(III) biofertilisation	
PDA-CAS	1/20 PDA 80.8 mg/l CAS 5.41 mg/l $FeCl_3$ 97.2 mg/l HDTMAB
MEA-CAS	1/20 MEA 80.8 mg/l CAS 5.41 mg/l $FeCl_3$ 97.2 mg/l HDTMAB

3.9.2 Determination of exoenzymes

Typical exoenzymes of microorganisms (cellulase, chitinase and different proteases) were analyzed for enzymatic activity. A 6 mm plug of *P. asterica* was transferred to agar plates containing different media (Tables 3.17, 3.18 and 3.19) to detect chitinase, cellulase and protease activity. Ten plates of each type were incubated at 23 °C for two weeks.

Chitin degradation could be seen directly on the plate through the pH indicator bromocresol purple. Bromocresol purple changes its color depending on the pH value in the plates (pH < 5.2 yellow, pH > 6.8 violet to purple). A breakdown of colloidal chitin into N-acteyl glucosamine increases the alkalinity and leads to a color-change around the fungal colony from yellow into violet (Agrawal and Kotasthane, 2012). As positive control served *Trichoderma* sp. (Harman et al., 1993).

Table 3.17: Composition of medium to detect chitinase activity (Agrawal and Kotasthane, 2012).

chitinase activity	
0.3g/l	$MgSO_4$
3g/l	$(NH_4)_2SO_4$
2g/l	KH_2PO_4
1g/l	citric acid monohydrate
10g/l	phyto agar
200µl	tween 80
4.5g/l	colloidal chitin
0.15g/l	bromocresol purple

Extracellular endoglucanases - one of different cellulase activities - were detected with carboxymethyl (CM) cellulose. CM-cellulose is a cellulose ether with carboxymethyl groups instead of hydroxyl groups (Thielking and Schmidt, 2000). CM-cellulose was used to assess endoglucanase activity (Wood and Bhat, 1988), in this case CM-cellulase. The remaining CM-cellulose in the medium which was not degraded by the fungi was detected with Schulze's solution (chloroiodide of zinc) (Schulze, 1924; Kunike, 1925). A degradation of CM-cellulose would be visible as a clearing zone around the fungal colony after staining. *Schizophyllum commune* was the positive control (Willick et al., 1984).

Table 3.18: Composition of medium to detect cellulase activity (Kasana et al., 2008).

cellulase activity	
0.2 %	$NaNO_3$
0.1 %	KH_2PO_4
0.05 %	$MgSO_4 \cdot 7H_2O$
0.05 %	KCl
0.2 %	carboxymethyl cellulose
0.02 %	peptone
1.0 %	phyto agar

The diameter of the fungal colony on plates to determine the protease activity was measured. Additionally, the plates were stained with 0.25 % Coomassie Brilliant Blue G-250 in methanol/acetic acid/water (5:1:4) and destained twice with methanol/acetic acid/water (5:1:4) for 15 minutes and over night. Coomassie Brilliant Blue G-250 is a blue stain at pH values from 2 to neutral and binds non-covalently to proteins forming

complexes. This dye/protein complex stabilizes the blue form of Coomassie Brilliant Blue G-250 and proteins are visible as a blue staining (De St. Groth et al., 1963). Therefore, a clearing zone around the fungal colony indicated a depletion of the specific protein from the agar (casein, BSA or gelatin). *Schizophyllum commune* was used as positive control (Hummel et al., 1998).

Table 3.19: Composition of medium to detect protease activity.

protease activity	
1/20	MEA
additives, either	
1%	BSA,
1%	gelatin or
5%	skim milk

3.9.3 Antagonism between *P. asterica* and other fungi

An experiment was performed on agar plates (once on MEA and once on PDA) to test whether *P. asterica* can inhibit the growth of other fungi by secreting antibiotic compounds. The interaction plates contained the fungi (see Table 3.2) in co-culture with *P. asterica*. The distance between two fungi was 4 cm and the plugs of the fungi were 2.5 cm away from the plate edge. *P. asterica* was growing very slowly and for that reason, the agar plug of *P. asterica* was cultivated for three weeks alone on the interaction plate before the testing fungi were transferred to the plate. Parallel to the interaction plate, control plates were set up. The control plates contained only the fungus (2.5 cm away from the plate edge) which grew together with *P. asterica* on the interaction plate (Table 3.2). *P. asterica* was put on its control plate three weeks in advance compared to the other control plates of the fungi (see Figure 3.2). Five replicates of each plate were done.

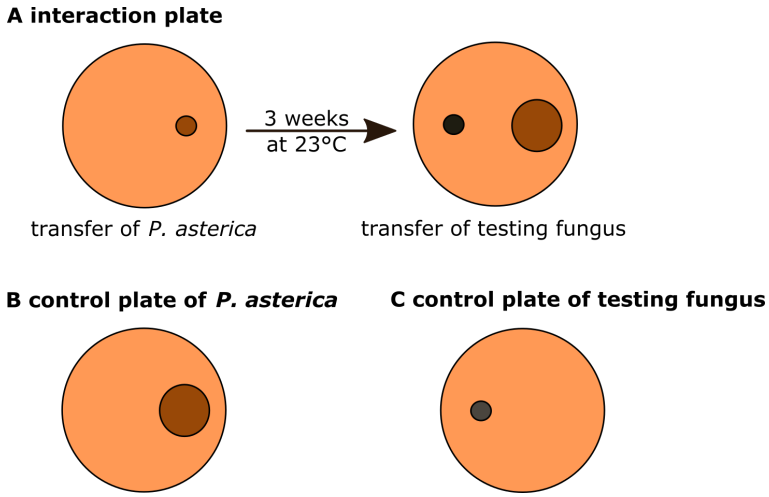

Figure 3.2: Scheme of fungal interaction assay. A *P. asterica* was transferred onto the interaction plate three weeks in advance of the testing fungus because of its slow growth. B The control plate of *P. asterica* was three weeks older than the control plates of the respective testing fungi (under C).

All plates were cultivated at 23 °C for one month. Every three to four days the growth of the testing fungi and of *P. asterica* was analyzed. To define the growth of the respective fungus and *P. asterica*, the diameter of fungal colony, the distance between fungus and *P. asterica* as well as the kind of growth of the different fungi (e.g. was the fungus growing over *P. asterica* or was there a developing inhibition zone between the two fungi) were estimated.

The growth rate of the fungal colonies was calculated after the following equation:

$$\text{growth rate} = \frac{\text{diameter past} - \text{diameter present}}{\text{diameter present}}$$

Due to the small sample size of only five replicates a normal distribution could not be guaranteed and a t-test could not be performed. Hence, the data were statistically analyzed with the Mann-Whitney U-test (Mann and Whitney, 1947) to determine if the differences in fungal growth are significant. This test did not need a normal distribution of the data and can be used for small sample sizes ($n < 10$).

3.10 Detection of *P. asterica* in *A. tataricus*

The *P. asterica* DNA was detected with qPCR in different plant cultivars. One plant of the Austrian cultivar (plant SS4-1) and two plants of the Dresden cultivar of *A. tataricus*

were analyzed. The two Dresden cultivar plants differ in their cultivation time in the greenhouse: One plant was grown from seeds and cultivated for nearly four years in the greenhouse (plant BG2-2) and the other plant was brought in fresh from the Botanical Garden in Dresden to the greenhouse and cultivated only for half a year there (plant oBG12).

The qPCR was conducted as described above (section 3.5.2) with different primers. The fungal primer pair qPearDNAfor1 + qPearDNArev1 amplified the fungal ITS region only present in genomic DNA and indicated so fungal DNA. The plant primer pair qAstACTfor1 + qAstACTrev1 amplified the plant DNA of *A. tataricus* to exclude any PCR inhibitors. The total DNA extracted from *A. tataricus* was measured by Nanodrop ND1000.

For absolute quantification of the fungal DNA, a calibration curve was set up with genomic DNA of *P. asterica* and the two fungal primers qPearDNAfor1 + qPearDNArev1. The PCR efficiencies of each primer pair in each run were analyzed. Only qPCR runs with PCR efficiencies between 0.95 and 1.05 were validated and analyzed. The calibration curve and each sample were run three times in triplicates in the qPCR. The mean and the standard deviation of all nine Ct values belonging to one sample were calculated. The fungal DNA amount was determined with the help of the calibration curve and the relative fungal DNA amount of the total DNA was calculated. Additionally, the astin profile of the analyzed samples were determined as well.

3.11 Induction of astin production in plants and fungi

3.11.1 Infection of *A. tataricus* with *P. asterica*

Plants from the Dresden cultivar where astins were not detectable were cultivated on autoclaved soil in a two-compartment system. The two-compartment system is a tank divided into two parts by a wall containing holes. This wall is covered with gauze (pore size 80 µm) permeable for the fungus, but not for the plant. The plant grew on the one side, whereas the soil at the other side was inoculated with *P. asterica* from a 21 days old liquid culture (PDB shaking culture at 23 °C). The fungus was now able to grow to the plant and infect the roots (see Figure 3.3). The two-compartment system - with the separated plant and fungus - was incubated in the climate chamber under long day conditions and was watered with autoclaved water. An infection of *A. tataricus* by *P. asterica* can be measured by the production of astins (see section 3.7 for extraction of astins). After three months, the plant organs were harvested and analyzed for astins.

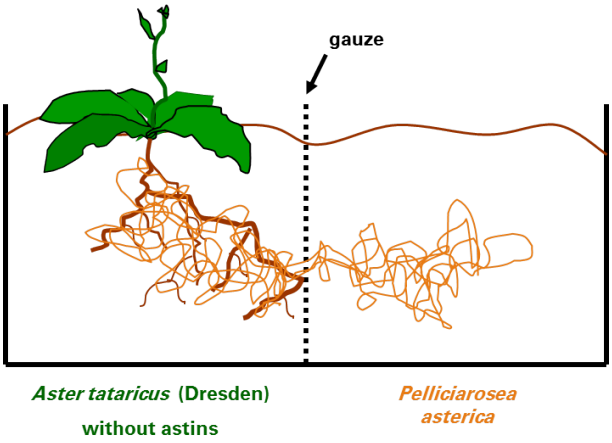

Figure 3.3: Two compartment system used for infection of *A. tataricus* with *P. asterica*. The plant was set in one side, the fungus into the other side. Both were separated by a gauze (pore size 80 µm). The roots could not grow through the gauze but the fungus could.

3.11.2 Cultivation of *A. tataricus* in different sized pots

One of the *A. tataricus* varieties (cultivar Dresden) showed during the first two years of cultivation in the greenhouse no detectable astins. During the cultivation in the greenhouse, the astin synthesis was somehow induced. The influence of the pot size on the astin production was therefore analyzed.

Whole plants of *A. tataricus* cultivar Dresden were harvested in the Botanical Garden Dresden and cultivated in different sized pots in the greenhouse under long day condition. The pots had a size in diameter of 16 cm, 22 cm and 28 cm. Before the plants were cultivated in the greenhouse, the astin profile was determined as described in section 3.7 to guarantee that only plants without detectable astins were cultivated. Every 21 weeks, leaves and roots of the plants were harvested and the astin profile was determined.

3.11.3 Feeding experiment with *P. asterica*

The fungus *P. asterica* was synthesizing only astins C, F and G. However, additional astins, above all astin A/B, were found in the plant *A. tataricus*. The difference between all three dichlorinated astins A, B and C is the second, respectively fifth amino acid (α-aminobutyric acid against *allo*threonine). Therefore, an experiment was set up to look if the fungus is producing other astins when the medium was supplemented with L-threonine.

P. asterica was grown in liquid PDB plus different concentrations of L-threonine (0 mM, 5 mM as well as 250 mM). These cultures were harvested after three or eight days. The dry weight of the fungus and the astin concentration and profile in the liquid medium were analyzed.

3.12 Identification of a halogenase gene

3.12.1 Alignment of different bacterial halogenases

The alignment was conducted with Geneious 8.1.5 (Kearse et al., 2012). The Muscle method was used to align the nucleic acid sequences of different halogenase.

The phylogenetic tree of the amino acid sequence of different halogenases was conducted in MEGA6. The amino acid sequences were aligned using the MUSCLE method (Edgar, 2004) with the default settings. The phylogenetic tree was built with the Maximum Likelihood method based on the Le-Gascuel model (Le and Gascuel, 2008). A bootstrapping to create a consensus tree was done with 2000 replicates (Felsenstein, 1985). The evolutionary rate differences between sites were modeled with a discrete Gamma distribution (+G, parameter = 2.4607).

3.12.2 PCR with putative halogenase primers

Different primers were designed (Table 3.7) to identify a halogenase gene from *A. tataricus* and *P. asterica*. Each primer pair was tested on cDNA and genomic DNA of *A. tataricus* and *P. asterica*. Additionally, each forward primer was combined with one of the reverse primers to get a PCR product. The preparation and cycling program for the PCR was taken from the instruction manual of the DreamTaq polymerase.

3.12.3 cDNA library construction

A. tataricus and *T. islandicus* contain both dichlorinated cyclic pentapeptides (astins and cyclochlorotine). Due to the high similarity of astins with cyclochlorotine, both organisms have to synthesize NRPS and flavin-dependent halogenases for the astin biosynthesis. Hence, it was decided to create cDNA libraries of both organisms, the plant and the fungus, to find possible biosynthetic genes of these chlorinated, cyclic pentapeptides.

After several attempts to generate a cDNA library with the In-Fusion SMARTer Directional cDNA Library Construction Kit (Clontech), mRNA was sent to evrogen (Moscow, Russia)

for generation of cDNA libraries from *A. tataricus* cultivar Austria roots and *T. islandicus*. The double strand cDNA of *A. tataricus* and *T. islandicus* was cloned into the vector pAL17.3 (3 kb).

3.12.4 Southern and colony blot

A Southern blot is a method to detect DNA sequences after separating the DNA on an electrophoresis gel with a hybridization probe (Southern, 1975). The probe is either chemically or radioactively-labeled. The Southern and colony blot was done in the laboratories of the Institute of Biochemistry (TU Dresden, Germany) after the protocol of Milbredt (2010).

The restricted DNA of *A. tataricus* was separated on a 1xTAE agarose gel (section 3.5.1) for six hours at 50 V. The separated DNA of the gel was then blotted onto a nylon membrane (Amersham Hybond NX from GE Healthcare). After cross-linking of DNA and membrane, the blotted membrane was hybridized with the probe in the hybridization buffer for 16 hours. Several steps with washing buffer followed, before the membrane was placed in blocking solution which contained the antibody anti-DIG-AP from Roche. The antibody bound to the DIG-labeled probe which was itself bound to the cross-linked DNA on the membrane. The including alkaline phosphatase of the anti-DIG-AP was incubated onto the washed membrane with the chemiluminescent substrate CSPD (Roche). The resulting signals were detected with an X-ray film (Amersham Hyperfilm ECL from GE Healthcare) in the dark room for one to 16 hours.

The colony blot used colonies which were blotted from an agar plate onto a nylon membrane. The cells on the membrane were disrupted and the DNA was cross-linked to the membrane. The following steps are the same as in the Southern blot.

The probe for the Southern and colony blot was designed based on the tryptophan motif (WXWXIP) due to the higher conservation and the lower variance in the nucleic acid sequence. The glycine from the GXGXXG motif is encoded by four different codons (GGA, GGC, GGG, GGU) and only three out of six amino acids are conserved. Whereas the tryptophan is encoded by only one codon (UGG) and four out of six amino acids are conserved. Isoleucine and proline are as well encoded by more than one codon (isoleucine: three codons, proline: four codons). The tryptophan motif was amplified with the PCR primers PeiHALBfor2 and PeiHALBrev1 binding around the tryptophan motif and amplifying a fragment of 268 bp. The probe was labeled with the DIG High Prime® (Roche).

Two different approaches were performed to find the halogenase gene by Southern blot.

First, genomic DNA from *A. tataricus* cultivar Austria was used (for DNA extraction see section 3.4.1). The DNA was digested with *Hae*III as well as *Vsp*I and separated on a 1xTAE gel. This gel was used in a Southern blot. The probe was hybridized at 40°C. The light signals of the alkaline phosphatase and the CSPD substrate were detected over night. Positive controls were the probe itself and the halogenase gene of *T. islandicus* (amplified with PeiHALfor1 + PeiHALrev1 from genomic DNA).

Second, the cDNA libraries of *A. tataricus* and *T. islandicus* were cut with *Sfi*I to release the cDNA from the vector pAL17.3. The digested fragments of the cDNA libraries were separated on a 1xTAE gel and used for Southern analyzes. The hybridization temperature was 45 °C, the detection time 2.5 hours. The probe served as positive control.

3.12.5 Genome sequencing of *P. asterica*

The DNA of *P. asterica* was isolated according to section 3.4.1. The genomic DNA was sent to the University of Bielefeld, Center for Biotechnology (CeBiTec), Germany. Two different approaches were done to obtain the complete genome of *P. asterica*. First, a whole-genome-shotgun PCR free (Nextera DNA Sample Preparation Kit, Illumina) and second, a 8k mate pair library (Nextera Mate Pair Sample Preparation Kit, Illumina) were generated according to the manufacturer's protocol. The resulting libraries were sequenced on the Illumina MiSeq system (2x 300bp). The sequenced and processed data were assembled *de novo* using the GS De Novo Assembler software (release version 2.8) from Roche with default settings.

The resulted genome of *P. asterica* was analyzed within GenDBE (Rupp et al., 2014) - a software tool from the Justus-Liebig-Universität Gießen, Germany.

3.13 RNA sequencing of *P. asterica*

Previously experiments (e.g. the growth of *P. asterica* in culture including leaves or plant extracts) showed an increased astin production in the presence of plant parts or extracts. Therefore, *P. asterica* culture were set up with plant extract to increase the astin production and to find possible astin biosynthetic genes in the analyzed RNA sequencing data.

3.13.1 RNA sequencing of different *P. asterica* cultures

P. asterica was cultivated in shaking culture under different conditions for three weeks: a 21 days old shaking culture in PDB (referred to as control), a 51 days old shaking culture in PDB (51 days old culture), a 21 days old shaking culture in PDB including water extract of leaves of *A. tataricus* cultivar Austria (Austrian leaf extract), a 21 days old shaking culture in PDB including water extract of leaves of *A. tataricus* cultivar Dresden (Dresden leaf extract) and a 21 days old shaking culture in MEB (MEB). The fungus of the 51 days old culture was used for inoculation of the different 21 days old cultures.

After harvesting, the fungus was separated from the medium which was used to determine the astin profile of *P. asterica* under the different conditions. The main part of the fungal biomass was freeze-dried and the dry weight was measured. A small part of the fungal biomass was sent to vertis Biotechnologie AG (Freising, Germany) to create a cDNA libraries using TruSeq adaptors for Illumina sequencing. These libraries were sequenced by CeBiTec in Bielefeld (Germany). The RNA sequencing data were analyzed using the platform ReadXplorer (Hilker et al., 2014). *P. asterica* cultivated for 21 days in PDB was the reference sample for the differential expression analyzes which were done using the DEseq package (Anders and Huber, 2010).

The p value was the probability calculated by the DEseq package (Anders and Huber, 2010) to observe the result arising by chance ($p < 0.01$ very strong presumption against null hypothesis, $p < 0.05$ strong presumption against null hypothesis, $p < 0.1$ low presumption against null hypothesis, $p > 0.1$ no presumption against null hypothesis). Therefore, only expression data which showed a significant regulation ($p < 0.05$) were considered.

3.13.2 Validation of RNA sequencing with qPCR

Some of the differentially expressed genes were validated with the relative quantification of the qPCR. A reference gene was chosen from the RNA sequencing data which showed no regulation under the different conditions of the RNA sequencing: the fungal γ-actin coded by gene.g7825. The analyzed genes were gene.g1622, gene.g4080, gene.g4646, gene.g5634 and gene.g8445. All of them showed a differential expression in the RNA sequencing under at least one condition. The resulting Ct values of the qPCR were analyzed with the $2^{-\Delta\Delta Ct}$ method (Livak and Schmittgen, 2001).

Each culture except the 51 days old culture were performed in duplicate. The 51 days old culture was set up with one culture. Each gene of each culture was analyzed with at

least three qPCR runs in triplicate. Each run in a 96-well plate contained in the upper part the cDNA of the different fungal cultures (A to D) plus three different primer pairs and the primer pair of the reference gene. The lower part included a cDNA mix of the different cultures in different volumes (8 µl, 4 µl, 2 µl and 1 µl) to create a small calibration curve for each primer pair for evaluating the PCR effiency. All samples were run in triplicate (Figure 3.4). Such a qPCR run was repeated three times before other primer pairs and/or other cDNA were tested. The reference gene (γ-actin) and the reference sample (control) were included in every qPCR run.

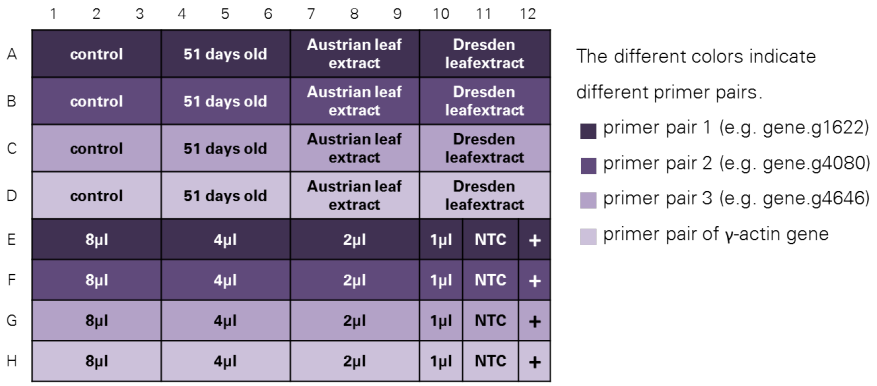

Figure 3.4: Pipetting scheme for the qPCR as an example. Each line labeled with the same color contained the same primer pair (1 to 3). The fourth primer pair was always the reference primer pair for the γ-actin. The upper part of the 96-well plate was filled with the cDNA of the different cultures in triplicate, whereas the lower part contained triplicates of a cDNA mix of the used cultures in different amounts (8 µl, 4 µl, 2 µl and 1 µl). The mix included the cDNA of all measured fungal cultures in the same amount. NTC no template control, + positive control.

Only Ct values from qPCR runs with a PCR efficiency between 0.95 and 1.05 were chosen for the analysis. Ct values of one gene were averaged for each run separately and the respective $2^{-\Delta\Delta Ct}$ values (= fold change after Livak and Schmittgen (2001)) were calculated for each run. The resulting $2^{-\Delta\Delta Ct}$ values - a total of six values for each duplicate culture - were again averaged and the standard deviation of these $2^{-\Delta\Delta Ct}$ values was determined to show the variation of the fold change. A fold change above 2 indicated an up-regulation, while a fold change beneath 0.5 showed a down-regulation. Genes with a fold change between 0.5 and 2 were not differentially regulated.

4 Results

4.1 A new endophytic fungus *Pelliciarosea asterica* from *Aster tataricus*

4.1.1 Isolation of *P. asterica* from the inflorescence axis

The inflorescence axis of *A. tataricus* cultivar Austria was sterilized and cultivated *in vitro* on MS medium (A). After one month of sterile cultivation, a fungus was growing out of the explants (B). Using several antimycotics like nystatin (50 µg/ml for four months) or antibiotic antimycotic solution (including amphotericin B for one month), it was tried to get rid of the fungus. After several transfers to antimycotic containing MS or Hoagland plates, the fungus was still growing out of the plant explants. Therefore, the endophyte was isolated on two fungal media, PDA (C) and MEA at 28 °C.

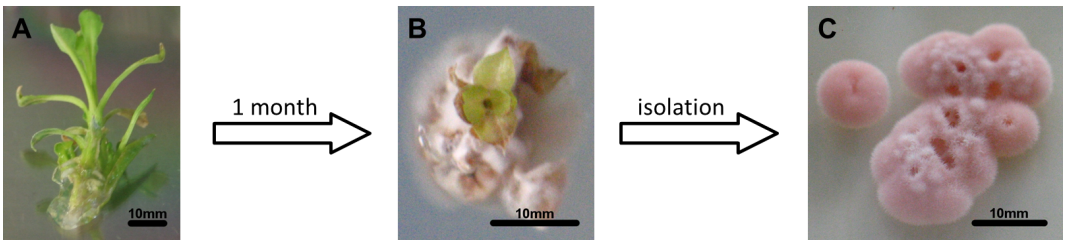

Figure 4.1: Isolation of *P. asterica* from *A. tataricus* cultivar Austria. Details see text above.

4.1.2 Phylogenetic relationship of *P. asterica*

The rDNA region of *P. asterica* was used to determine the phylogenetic relationship with other fungi. The BLASTn search (Madden, 2002) of the sequenced PCR products revealed a distinct relationship either with Dothideomycetes (SSU) or with Lecanoromycetes (ITS-LSU). The ITS sequence of *Pelliciarosea asterica* showed a partial match with *Pleopsidium chlorophanum* and *Acarospora smaragdula*, both of them belong to the Lecanoromycetes. The LSU sequence showed a higher match to sequences of

Umbilicaria species (Lecanoromycetes), whereas the SSU sequence was more related to *Acarospora smaragdula*, *Trapelia involuta* and *Cyanodermella viridula* (see Table 4.1).

Table 4.1: Results of the BLASTn search of the rDNA cluster.

	species	accession number	query cover in %	ident	e-value
SSU	*Acarospora smaragdula*	AY552543.1	78	91	0.0
	Trapelia involuta	AF119499.2	78	91	0.0
	Cyanodermella viridula	U86583.1	78	91	0.0
ITS	*Pleopsidium chlorophanum*	DQ525472.1	41	100	$1 \cdot 10^{97}$
	Acarospora smaragdula	EU870652.1	38	86	$4 \cdot 10^{97}$
LSU	*Umbilicaria crustulosa*	HM161593.1	99	88	0.0
	Umbilicaria haplocarpa	HM161534,1	99	88	0.0

The DSMZ confirmed these results. In their analysis, a 95 % identity to *Cyanodermella viridula* (HM244763 and U86583 in GenBank) was found for both subunits (SSU and LSU). For the ITS sequence, two other organisms showing homology were found: *Skyttea nitschkei* (UDB016230 in UNITE database) and *Geltingia associata* (UDB015045 in UNITE database).

Both phylogenetic trees - one for the ITS-LSU sequence, one for the SSU sequence - clustered *Pelliciarosea asterica* together with other ostropalean fungi from the Stictidaceae lineage (*Stictis, Cryptodiscus, Conotrema, Schizoxylon, Cyanodermella*) (see Figures 4.2 and 4.3). Thirteen percent of all replicate trees in the bootstrapping clustered the ITS-LSU sequence of *P. asterica* to the ones from the ostropalean fungi. Already 38 % of all replicate trees based on the SSU sequences clustered the SSU sequence to the one from *Cyanodermella viridula*.

Based on the results of the rDNA analysis, the new endophytic fungus was classified as

new genus and species *Pelliciarosea asterica* (order Ostropales, family Stictidaceae).

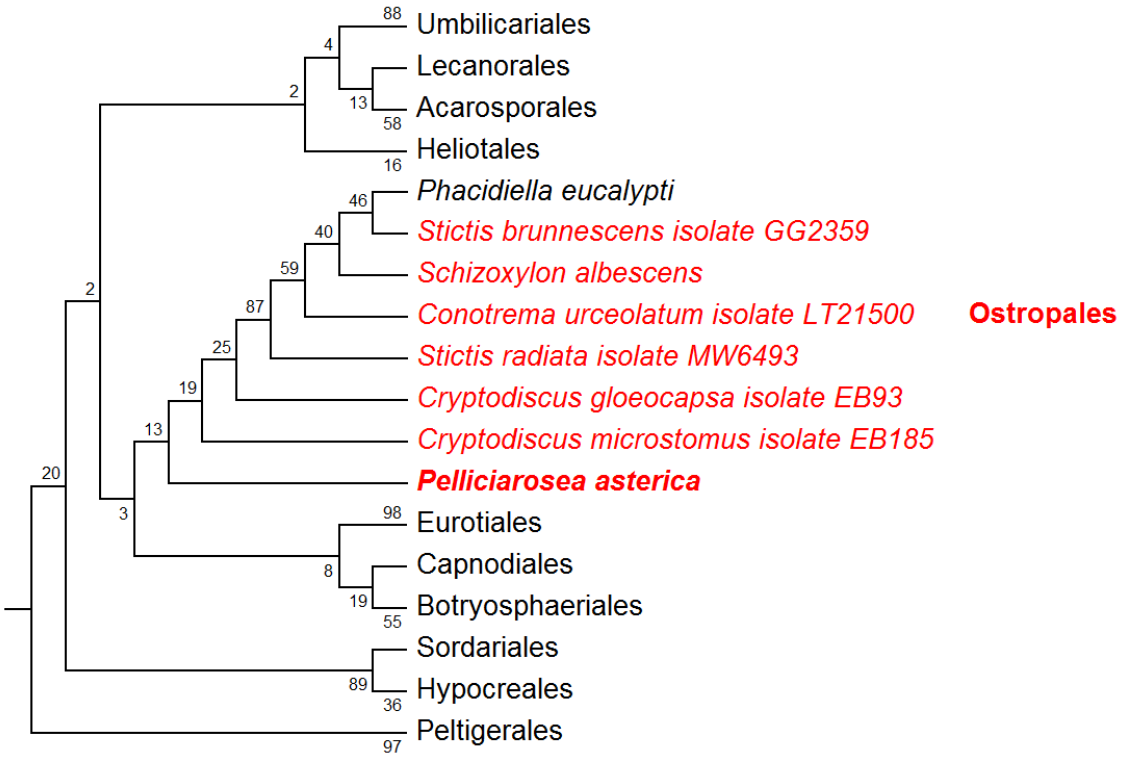

Figure 4.2: Phylogenetic relationship of *P. asterica* based on its LSU-ITS sequence. The evolutionary history was inferred by using the Maximum Likelihood method based on the General Time Reversible model (Nei and Kumar, 2000). The bootstrap consensus tree inferred from 2000 replicates is taken to represent the evolutionary history of the taxa analyzed (Felsenstein, 1985). Branches corresponding to partitions reproduced in less than 50 % bootstrap replicates are collapsed. The percentage of replicate trees in which the associated taxa clustered together in the bootstrap test are shown next to the branches. Initial tree(s) for the heuristic search were obtained by applying the Neighbor-Joining method to a matrix of pairwise distances estimated using the Maximum Composite Likelihood (MCL) approach. A discrete Gamma distribution was used to model evolutionary rate differences among sites (5 categories (+G, parameter = 0.8144)). The analysis involved 110 nucleotide sequences. All positions with less than 95 % site coverage were eliminated. That is, fewer than 5 % alignment gaps, missing data, and ambiguous bases were allowed at any position. There were a total of 363 positions in the final data set. Evolutionary analyzes were conducted in MEGA6 (Tamura et al., 2013).

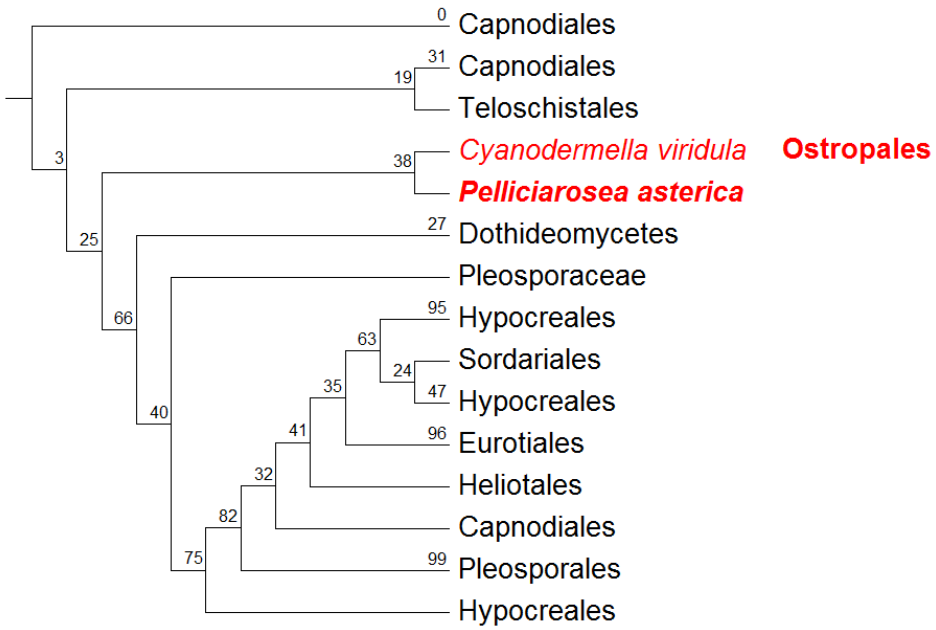

Figure 4.3: Phylogenetic relationship of *P. asterica* based on the SSU sequence. The evolutionary history was inferred by using the Maximum Likelihood method based on the Kimura 2-parameter model [1]. The bootstrap consensus tree inferred from 2000 replicates is taken to represent the evolutionary history of the taxa analyzed (Felsenstein, 1985). Branches corresponding to partitions reproduced in less than 50 % bootstrap replicates are collapsed. The percentage of replicate trees in which the associated taxa clustered together in the bootstrap test are shown next to the branches. Initial tree(s) for the heuristic search were obtained by applying the Neighbor-Joining method to a matrix of pairwise distances estimated using the Maximum Composite Likelihood (MCL) approach. A discrete Gamma distribution was used to model evolutionary rate differences among sites (5 categories (+G, parameter = 1.7770)). The analysis involved 160 nucleotide sequences. All positions with less than 95 % site coverage were eliminated. That is, fewer than 5 % alignment gaps, missing data, and ambiguous bases were allowed at any position. There were a total of 326 positions in the final data set. Evolutionary analyzes were conducted in MEGA6 (Tamura et al., 2013).

4.1.3 Morphology of *P. asterica*

P. asterica is a filamentous endophytic fungus from *A. tataricus* and could be cultivated on typical fungal media like PDA and MEA. The colony pattern and the growth behavior was different in both media. The fungus was growing as pink colony on PDA. Young colonies (14 days old) of *P. asterica* were still white (N 9.00) to pale pink (2.5R 9.00/2.00). After one month the color turned from pale pink into light pink (2.5R 8.00/6.00). Old colonies (over 50 days old) additionally developed colors of deep pink (2.5R 6.00/10.00) and vivid red (5.00R 4.00/14.00). *P. asterica* grew with much less color intensity on

MEA than on PDA. Young colonies on MEA (seven to 14 days old) were usually white to colorless (N 9.00). Older colonies (over 50 days old) were colored in light pink (Figure 4.4A-E). The colors of *P. asterica* were indicated after the Munsell Color System (Munsell, 1905).

No sporulation could be observed in culture, therefore no information on the type of spores was available. The asexual hyphae were 1.5 to 2.0 µm in width (Figure 4.4F + G).

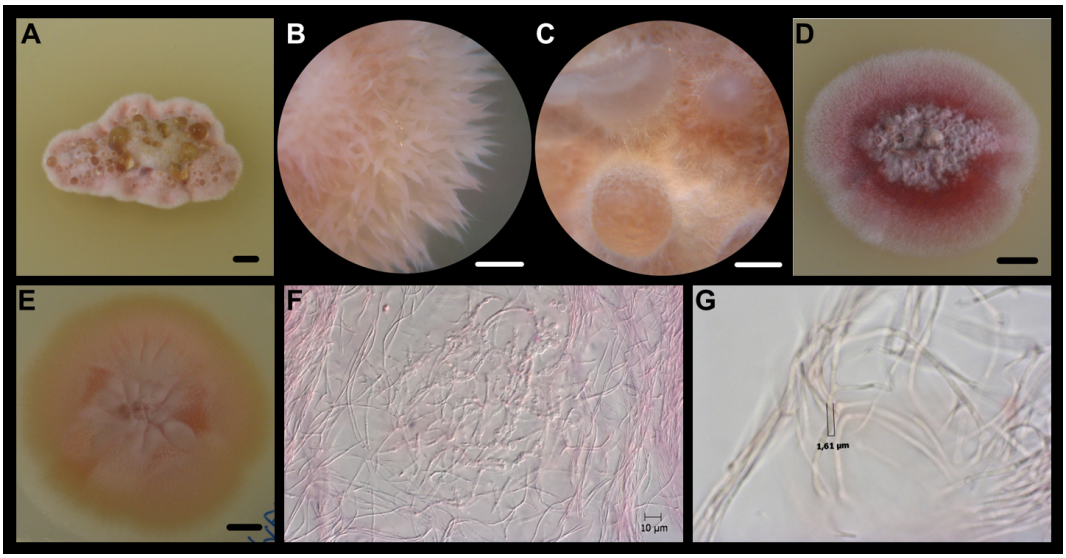

Figure 4.4: Morphology of *P. asterica*. A – D *P. asterica* on PDA and E on MEA. The filamentous structure can be seen in B. Hyphae enveloped water drops and appeared as globalized structure on the plate (A and C). After evaporation of the water, the hyphae stayed as remains of the water drops in form of holes (C and D). F – G microscopic view of *P. asterica* stained with congo red, cultivated in a shaking culture with PDA. The bars indicate 5 mm (A, D and E) or 1 mm (B and C).

The genus name *Pelliciarosea* derived from its appearance on the first isolation medium PDA. The Latin word pellicius -a, -um meant fluffy whereas roseus -a, -um stood for the color rose/pink. The epithet *asterica* derived from the plant *A. tataricus* from which *P. asterica* was isolated first.

4.1.4 Distribution of *P. asterica* throughout *A. tataricus* plants

Dying leaves of both cultivars from *A. tataricus* were microscopically screened for sporulation structures of *P. asterica*, but nothing was visible so far. Only dark areas on the leaves and on the leaf hairs were detected (shown for cultivar Austria in Figure 4.5). These dark brown spots turned out to be the excrement of thrips and small flies

contaminating the plants in the greenhouse. The leaves and also the leaf hairs were screened under the binocular and microscope but these structures were only colonized by single hyphae. The hyphae did not form any structure similar to an ascus or any kind of spore.

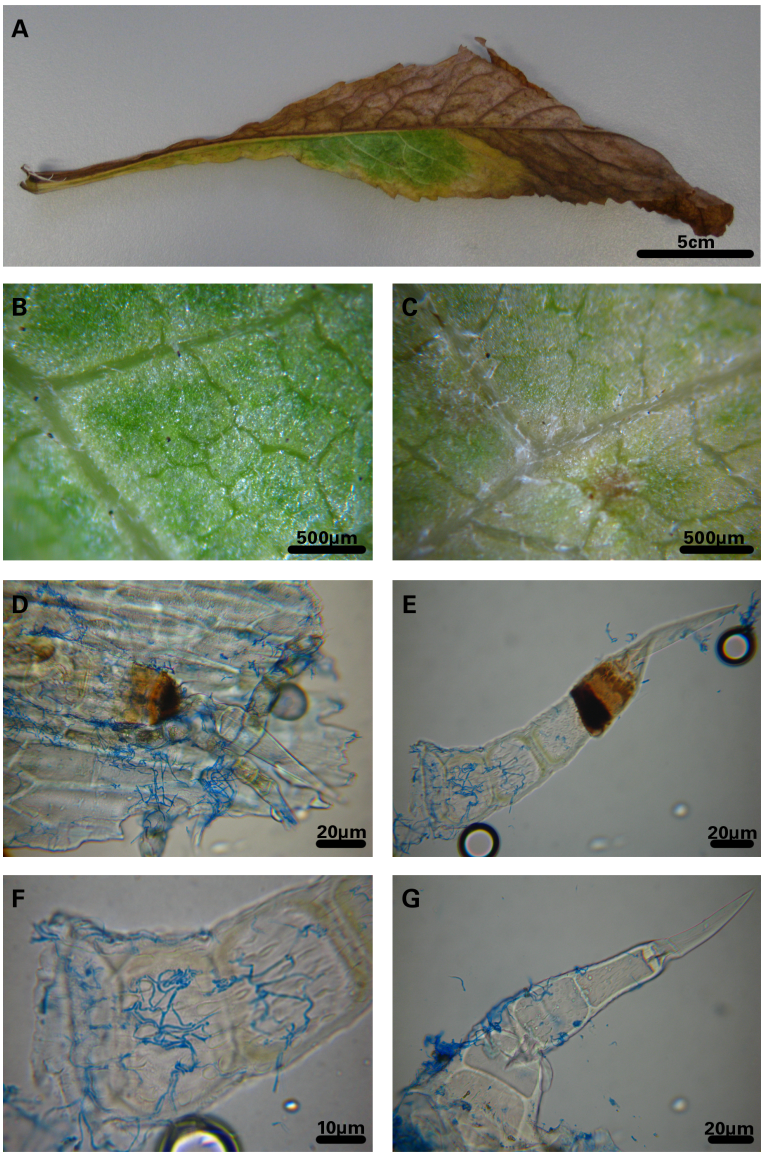

Figure 4.5: Details of the lower side of leaves from *A. tataricus* cultivar Austria. A Overview over one of the analyzed leaves. B and C Lower side of a leaf with leaf hairs with and without brown spots. D to G Lower side of a leaf and leaf hairs stained with lactophenol blue to visualize fungal hyphae. D Lower side of a leaf with leaf hairs and mycelium. E and F Leaf hair with a brown tip. The fungal mycelium seems to colonize the leaf hair. G Leaf hair without a brown tip, also colonized by mycelium.

4.2 The new fungus *P. asterica* produces astins

4.2.1 Astins in the host plant *A. tataricus*

Astins were up to now only isolated from dried roots and rhizomes of *A. tataricus*. Therefore, different cultivars of *A. tataricus* were analyzed whether astins can be detected not only in dried roots and rhizomes but also in fresh leaves, roots and other plant organs.

Different astins were detected in the organs of *A. tataricus*. The Dresden cultivar of *A. tataricus* showed a different pattern than the Austrian cultivar (Figure 4.6). The Austrian cultivar showed an astin profile of astins A/B, C, E/H, G and F (variant 2). Astins D and I were not detected in this *A. tataricus* (cultivar Austria). The main astins were astin A/B, the other detected astins were just minor constituents. In contrast to the Austrian cultivar, the Dresden cultivar was different. No astins were detected in plants which were sown on soil and analyzed after one and two years (spring 2013). Only after three years on soil (spring 2014), astins could be detected. This astin profile was similar to that of the Austrian cultivar but with much less intensity.

The HPLC/MS protocol used for detection and analysis cannot differ between astins A and B. Astins A and B share the same mass and the same molecular structure. They differ only in the hydroxylation of the second or fifth amino acid (α-aminobutyric acid or *allo*threonine). The same is true for astins E and H. Hence, it was referred to astins A and B respectively astins E and H as astin A/B and astin E/H.

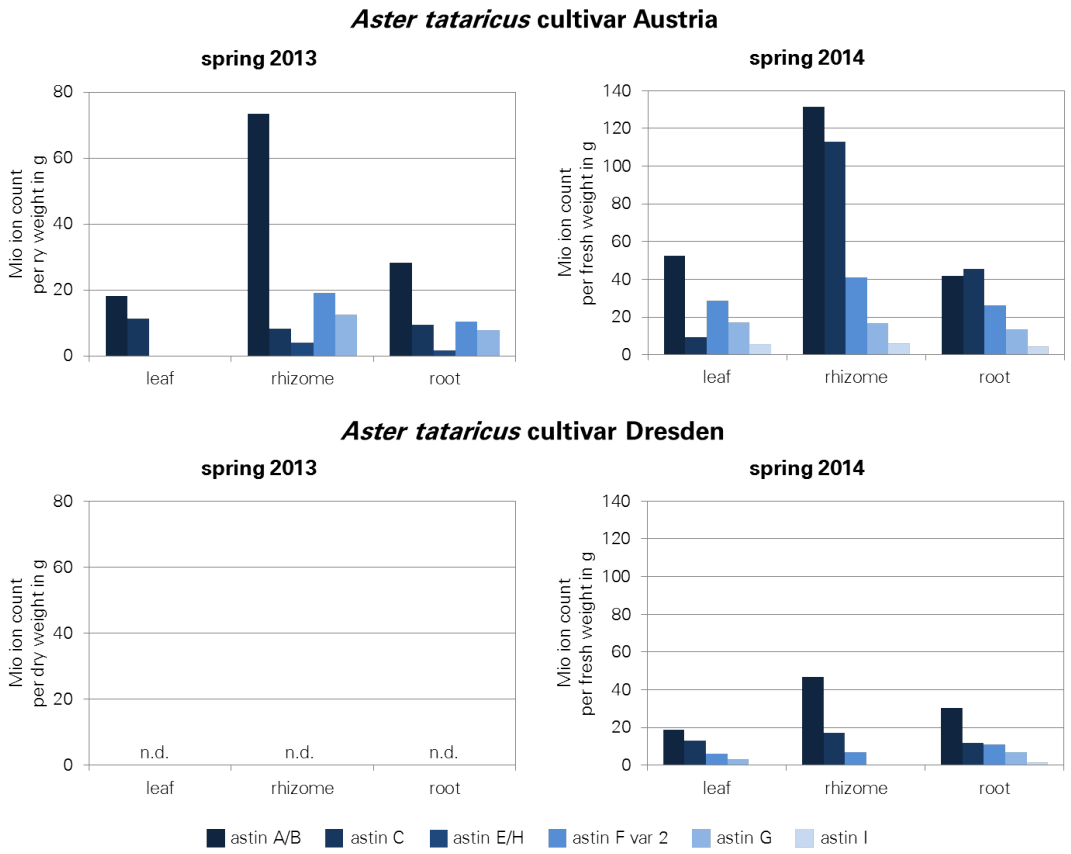

Figure 4.6: Astin profile of the two different cultivars of *A. tataricus* over one year. The Austrian cultivars shows from the beginning detectable amounts of astins. Seven astins were detected. Astins A and B cannot be differentiated with the HPLC/MS method used for analysis. The Dresden cultivar shows no detectable astins in spring 2013. During one year, astin synthesis in *A. tataricus* cultivar Dresden was induced. The astin profile was very similar to that in the Austrian cultivar. Only the intensity of several astins is lower as in the Austrian cultivar. n.d. samples were measured but astins were not detectable in the HPLC/MS.

4.2.2 Astins in the endophyte *P. asterica*

The newly isolated endophytic fungus *P. asterica* was analyzed for its astin profile. *P. asterica* produced as well some of the astins found in the plant. The fungus was cultivated in different media like PDB, MEB or liquid MS, but in all media only astins C, F (variant 1) and G could be detected (Figure 4.7).

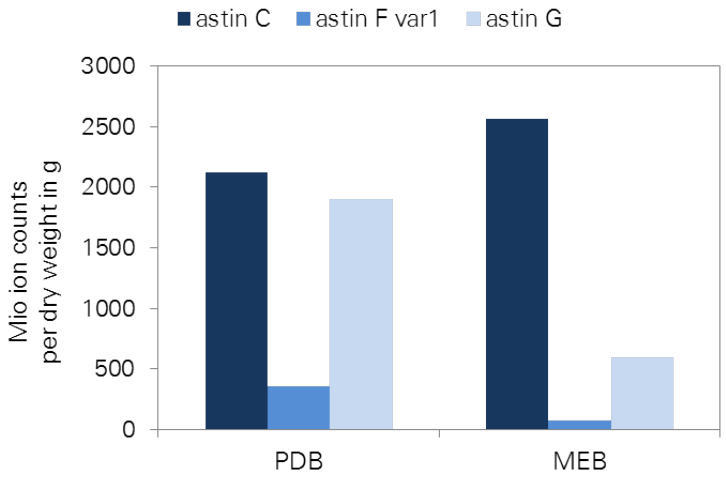

Figure 4.7: Astin profile of *P. asterica* in PDB and MEB. Only astins C, F and G were found in *P. asterica*.

The comparison of the astin profile of *A. tataricus* and *P. asterica* showed two different variants of astin F (see Figures 4.6 and 4.7). Astin F variant 2 (astin F var2) needed longer from the injection of the sample to detection of the astin (retention time of 6.7 to 7.1 minutes) than the first variant (astin F var1) with 6.4 to 6.7 minutes. Both variants had the same m/z value of 536. No other astins showed a m/z value of 536 like astin F. Thus, it was referred to these two variants of astin F as variant 1 and variant 2.

4.3 Growth of *P. asterica* under different *in vitro* conditions

4.3.1 Growth of *P. asterica* supplemented with different leaves

P. asterica grew after isolation detectably only in the presence of *A. tataricus* leaves within one month (Figure 4.8). No growth was detected in the presence of the leaves of *Helianthus annuus* and *Symphytum officinale*. The corresponding astin profile showed that astins were only synthesized in the presence of *A. tataricus* leaves. The high amount of astin A/B in the Austrian sample came from the leaf itself. The amount of astin C was very low in the sample containing the leaf of the Austrian cultivar despite the high biomass. Therefore, *P. asterica* produced no astins in the presence of the these leaves. All detected astins were derived from the Austrian leaf. In contrast to that, the growth of *P. asterica* with the leaf of Dresden cultivar was slowly but instead it produced much astin C which was not coming from the leaf of the Dresden cultivar.

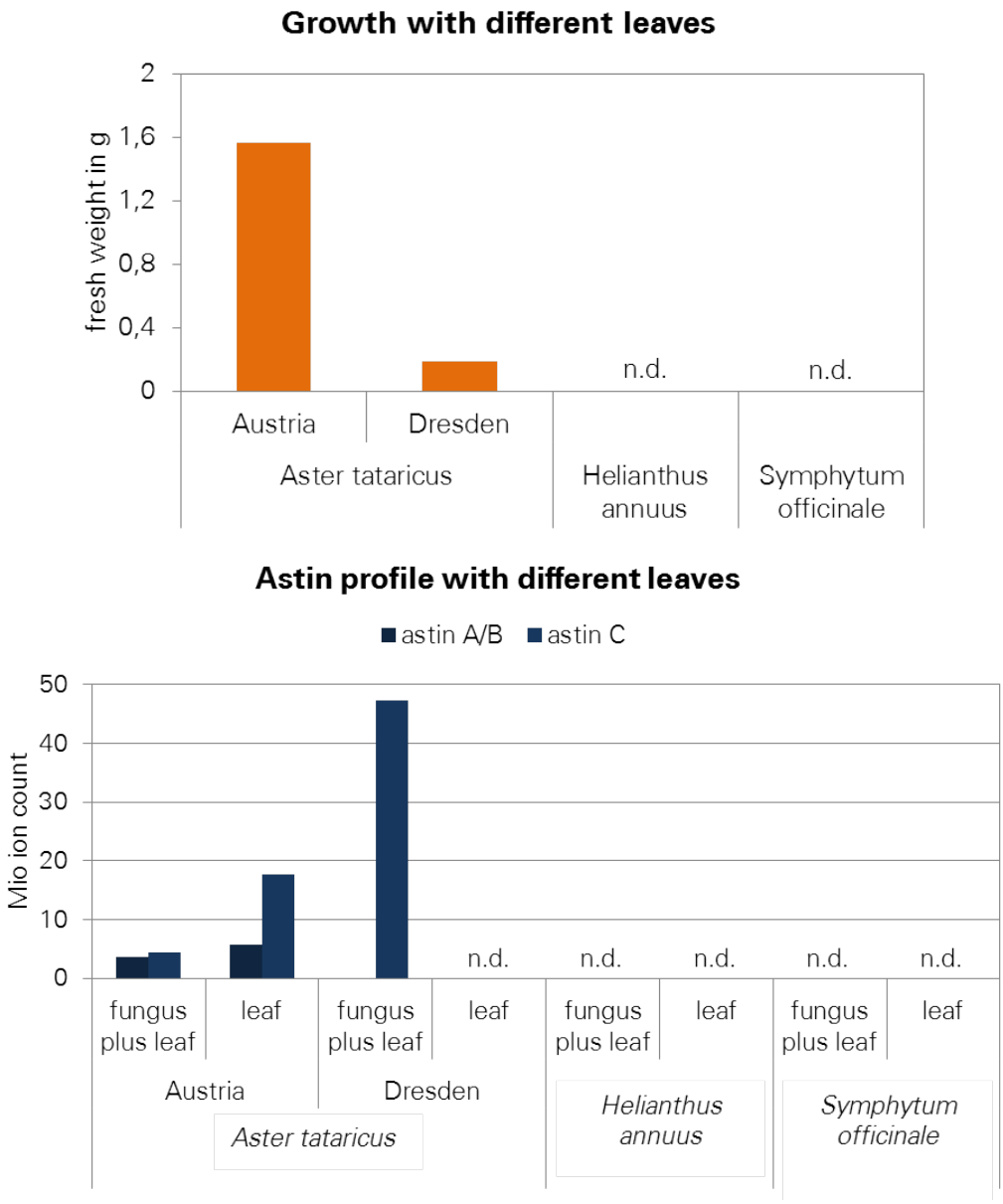

Figure 4.8: Growth and astin profile of *P. asterica* grown in liquid culture plus different leaves in May 2013. *P. asterica* grew detectable only in the presence of *A. tataricus* leaves. Astins were only detected in these samples. The astins in the sample with the Austrian leaf were derived from the Austrian leaf and not from the fungus. Astin production was only found in the *P. asterica* culture including the leaf of the Dresden cultivar. The fresh weight shown was that of one culture (per condition) and the astin profile represents raw data which were not calculated per fresh weight to show the astin content in the controls as well. n.d. not detectable.

4.3.2 Growth and astin production of *P. asterica* within different extracts of *A. tataricus*

Preliminary tests with leaves of *A. tataricus* had shown that *P. asterica* grew better in the presence of *A. tataricus* (see section 4.3.1). Thus, it was tested, if *P. asterica* would grew faster in medium containing different extracts of *A. tataricus* organs.

The first experiment in May 2013 - done two months after the isolation of *P. asterica* - showed no detectable, reproducible growth of *P. asterica* (data not shown). Only a few samples showed detectable growth, to be specific *P. asterica* grown in the water extract of leaves from *A. tataricus* cultivar Dresden. A growth of *P. asterica* was clearly visible in these samples (Figure 4.9).

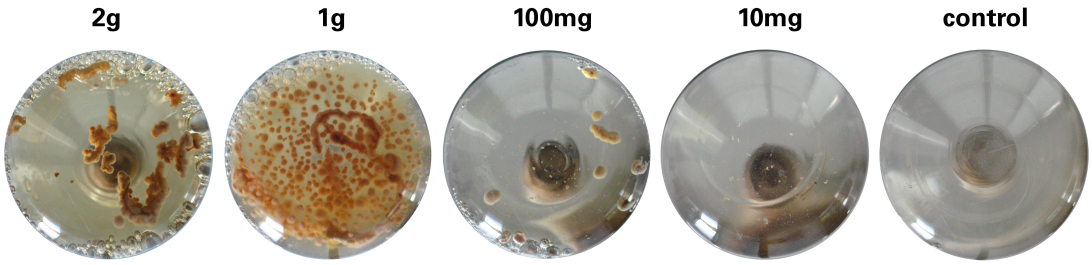

Figure 4.9: Growth of *P. asterica* in PDB including aqueous leaf extract from *A. tataricus* cultivar Dresden two months after isolation. *P. asterica* grew visible within 2 g to 100 mg aqueous leaf extract. The control culture contained no *P. asterica* and showed that the extract was not contaminated. The weight specifications above the cultures indicate the added extract volume calculated to the added plant fresh weight (see section 3.8.2).

The analyzed astin profile of the different samples showed an astin production - especially of astin C - by *P. asterica* in the medium containing aqueous leaf extract of the Dresden cultivar (data not shown). Samples containing ethanol extract showed as well a small amount of astin production. At higher ethanol concentrations, no astin production was detectable. Astin production was found only at lower ethanol concentrations.

Due to the fact that only one sample per condition could be set up, the experiment had to be repeated. The experiment was repeated twice but at both time points the cultures got contaminated with other microorganisms. Therefore, a fourth attempt was done to repeat this experiment in November 2013.

The experiment repeated in November 2013 (eight months after isolation of *P. asterica*) should verify the results from May 2013. Surprisingly, *P. asterica* was now able to grow in all cultures, regardless of the different added plant extracts (Figure 4.10). No pattern was clearly visible, aqueous as well as ethanol extracts of roots and leaves of both

cultivars seemed not to influence the growth of *P. asterica*. The control of *P. asterica* grown without any extract showed a dry weight of around 5 mg, whereas most samples showed a biomass much higher than 5 mg. Therefore, the plant extracts of *A. tataricus* enhanced the growth of *P. asterica* but no pattern depending on plant, organ or extraction method was visible.

The astin profile (only astins A/B and C) of the samples from November 2013 showed higher amounts than in May 2013 (Figure 4.11). Astins could be detected in many more samples than in May 2013, but still not all samples showed a fungal astin production. The displayed astins were the ones produced by the fungus. The extract-derived astins, contained in the extracts due to the extraction method, were subtracted from the overall astin profile according to the added volume. It was conspicuously that all ethanol samples showed a higher astin production (especially of astin C) as the corresponding water samples and this with even lower extract concentrations. Some samples showed also high astin A/B amounts although *P. asterica* produced in single culture no astin A/B.

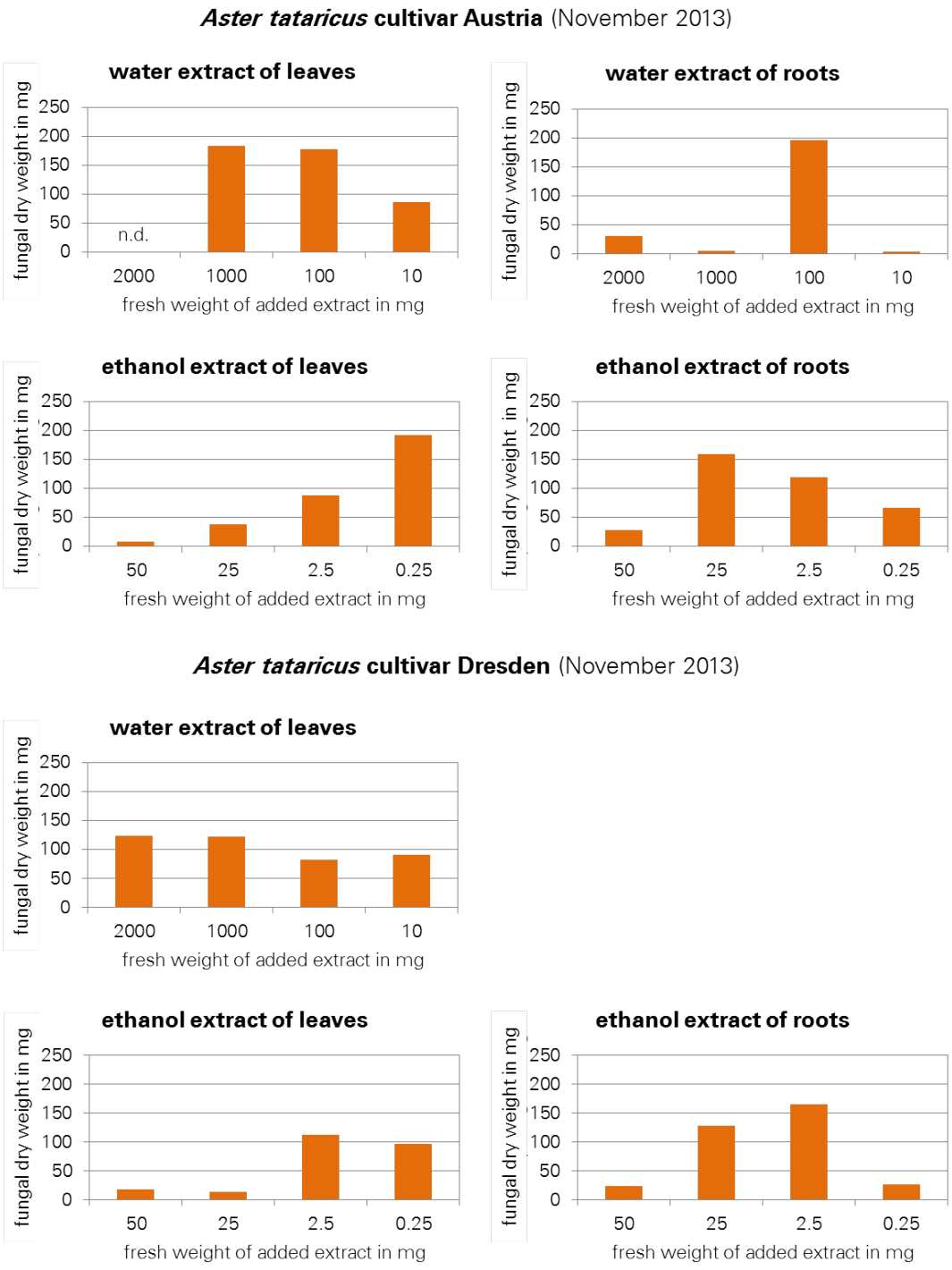

Figure 4.10: Growth of *P. asterica* in cultures containing different extracts of *A. tataricus* eight months after isolation. *P. asterica* was now growing much better in culture as in May 2013, shortly after the isolation, where only few cultures showed a visible/detectable growth. n.d. growth was not detectable.

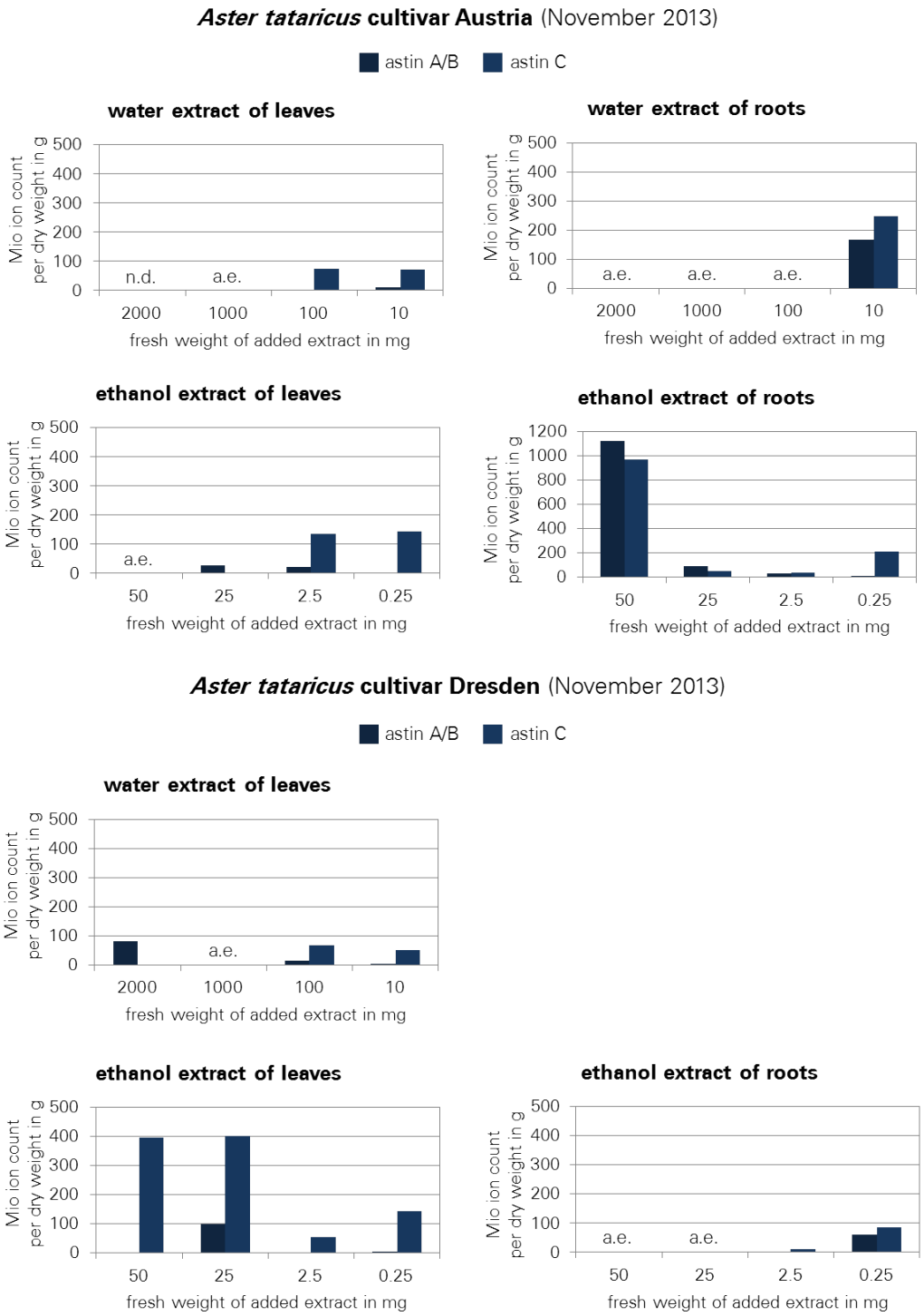

Figure 4.11: Astin profile of *P. asterica* in cultures containing different extracts of *A. tataricus* eight months after isolation. The charts show the astins produced by *P. asterica* per fungal dry weight. The extract-derived astins were subtracted from every sample according to its added volume of plant extract. *P. asterica* grew not only better but also produced more astins, too. n.d. astins were not detectable in HPLC/MS. a.e. astins were detectable in the HPLC/MS but the astins were extract-derived and not produced by *P. asterica* itself.

Control samples were carried during both experiments. These control samples contained PDB including the respective plant extract (without any fungus) to show that the extracts were sterile. The astin profile of the control samples (Figure 4.12) did not show the astins produced by the fungus *P. asterica* but the astins produced by *A. tataricus*. The plant astins were carried over into the fungal culture through the plant extracts. The Austrian cultivar showed in May as well as in November 2013 high amounts of astins A/B and C. In contrast, the Dresden cultivar showed in May 2013 only in the aqueous root extract low amounts of astin C. In November 2013, the Dresden cultivar produced more and more astins, detectable in relatively high amounts of astins A/B and C in leaf and root extracts. These controls showed that the Dresden cultivar of *A. tataricus* was now able to produce astins.

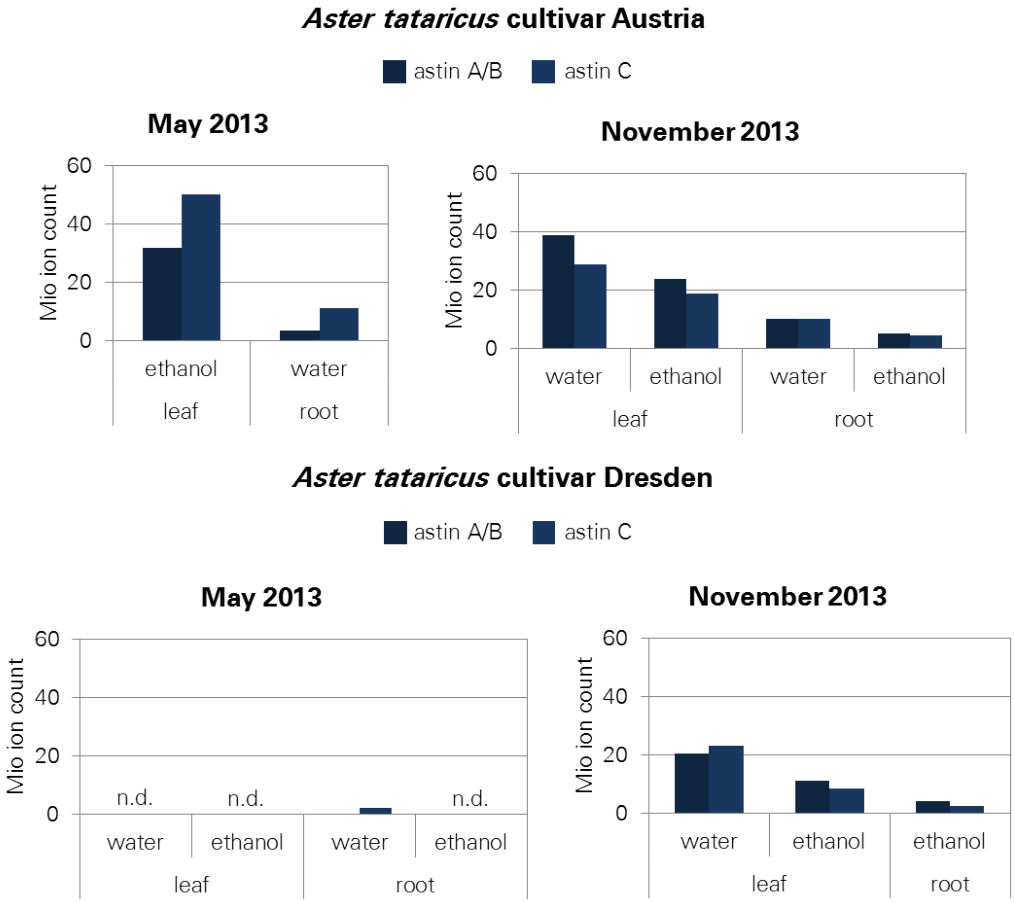

Figure 4.12: Astin profile of the control cultures including plant extract without *P. asterica* two and eight months after the isolation. The plant extracts of the Austrian cultivar contained astins in varying amounts at both time points. The Dresden cultivar of *A. tataricus* showed astins for the first time in November 2013. n.d. astins were not detectable in the HPLC/MS.

4.3.3 Variability of fungal growth through cultivation conditions

The growth experiments of *P. asterica* with different additives of *A. tataricus* (leaves or extracts) were carried out only with one culture per each condition. Therefore, it was necessary to determine the variability of growth of *P. asterica* in liquid cultures.

P. asterica showed a high variability regardless how the cultivation conditions were chosen (Figure 4.13). If *P. asterica* was co-cultivated with leaf extracts of the Dresden cultivar, the variability - measured as standard deviation - was very high (aqueous leaf extract: over 65 %, ethanol leaf extract: over 55 %). The water control showed a smaller standard deviation of about 32 %. In contrast, the ethanol control had also a very high variation of over 57 %. The cultures which were inoculated with *P. asterica* either from liquid (over 36%) or solid medium (51 %) showed a high standard deviation as well.

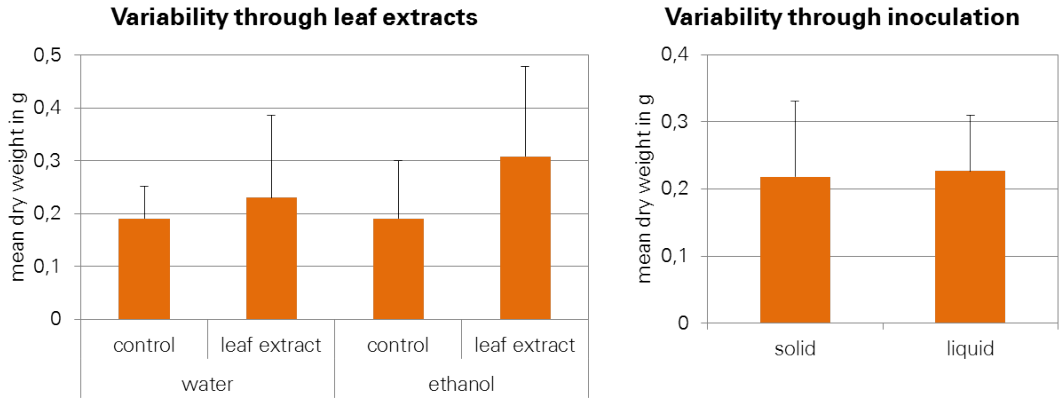

Figure 4.13: Variability of growth through different cultivation conditions. Left side: Liquid PDB was inoculated with *P. asterica* plus different leaf extracts of *A. tataricus* cultivar Dresden. Right side: Liquid PDB was inoculated with *P. asterica* from different sources - from solid PDA plates as well as from liquid PDB culture.

4.3.4 Growth of *P. asterica* on plates

An experiment (January/February 2015) was conducted to investigate the growth of *P. asterica* nearly two years after the isolation from *A. tataricus* cultivar Austria (see Figure 4.14). The growth on MEA and PDA was not significantly different but *P. asterica* grew on PDA with a higher variability as on MEA (indicated by the standard deviation).

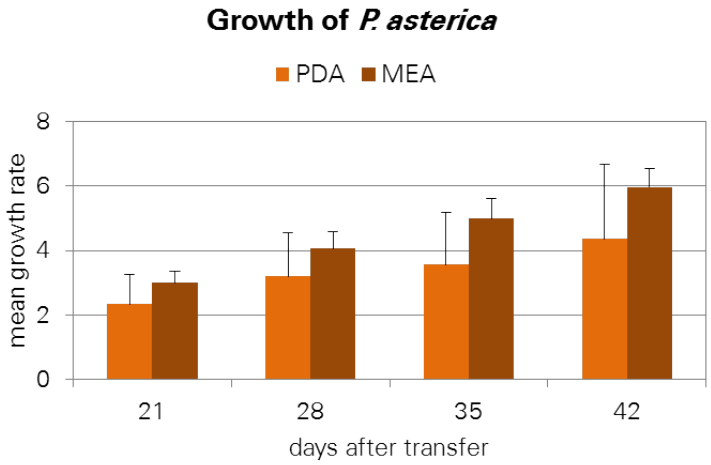

Figure 4.14: Growth rate of *P. asterica* on PDA and MEA in comparison. The fungus was cultivated on plate containing the appropriate medium for over one month. *P. asterica* grows with a smaller variance on MEA. The growth rate on PDA is more variable.

Summarizing the growth experiments of *P. asterica*, it was shown that *P. asterica* was growing after the isolation from *A. tataricus* very slowly (no visible growth within one month in liquid culture). After several months and the possibility to adapt to the new *in vitro* environment, *P. asterica* grew much better under *in vitro* conditions. Two years after the isolation, *P. asterica* was growing visible in liquid culture as well as on agar plate within one month.

4.4 Further physiological characterization of the new endophyte *P. asterica*

4.4.1 Solubilization of phosphates and iron(III) by *P. asterica*

Some endophytes supply their host plant with additional nutrients in this way that they solubilize nutrients like phosphates or iron(III) which are usually poorly available for plants.

Fungi which are able to solubilize hydroxylapatite or iron(III) phosphate grow on these agar plates (Tables 3.15) with a clearing zone around the fungal colony. This clearing zone indicates a depletion of the phosphate from the medium. *P. asterica* was producing such clearing zones around its fungal colony on medium containing hydroxylapatite as well as iron(III) phosphate (Figure 4.15). The fungal endophyte grew significantly ($\alpha = 0.001$)

better on hydroxylapatite than on the control plate without any phosphate. The fungus cultivated on medium containing iron(III) phosphate grew significantly ($\alpha = 0.001$) slower than on the control plate. The clearing zone around the fungal colony as indicator for phosphate solubilization was significantly ($\alpha = 0.001$) larger on the hydroxylapatite containing plate than on the iron(III) phosphate containing plate. The positive control *Acremonium alternatum* grew on hydroxylapatite with a clearing zone around the fungal colony after two weeks. Both phosphate sources - hydroxylapatite and iron(III) phosphate - could be degraded by *P. asterica*.

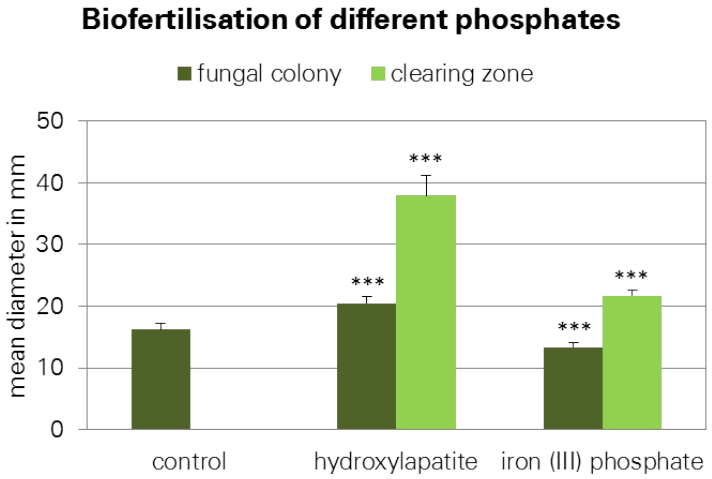

Figure 4.15: Biofertilisation of phosphates through *P. asterica*. Different phosphate sources (hydroxylapatite and iron(III) phosphate) could be used successful by *P. asterica*. The clearing zone around the fungal colony indicated the grade of phosphate degradation. * * * $\alpha = 0.001$.

The solubilization of iron(III) by the production of siderophores leads to a color change from blue to orange-red on the CAS medium (Table 3.16) containing $FeCl_3$. Such a color change was not detected on the plates with *P. asterica* (Figure 4.16). *P. asterica* did not grow on the CAS medium. Only the positive control with *Aspergillus* sp. was developing an orange-red zone around the growing colony. *P. asterica* was not able to produce siderophores for the chelating of iron(III).

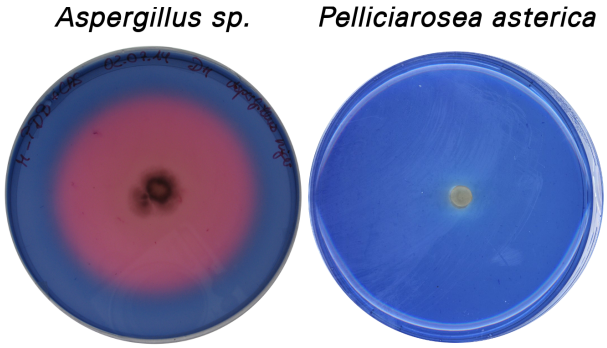

Figure 4.16: Solubilization of iron(III) through *P. asterica* on MEA. The positive control with *Aspergillus* sp. showed an orange-red zone around the fungal colony after seven days. *P. asterica* was not showing such a zone after 14 days, indicating that *P. asterica* was not able to use the iron(III) from the CAS medium by siderophore production.

4.4.2 Production of exoenzymes by *P. asterica*

Fungi secrete enzymes into their environment for different purpose: cellulases can be used for infiltration of plant hosts through the plant cell wall, chitinases can be used to attack possible phytopathogenic or competing fungi and proteases can be used in the defense of the host plant. Therefore, it is interesting if *P. asterica* produces such extracellular enzymes.

Fungi which produce extracellular chitinases developed on the chitinase medium (Table 3.17) a color change around the fungal colony from yellow into red. A color change was not detectable on the agar plates on which *P. asterica* was grown (Figure 4.17). Only the positive control with *Trichoderma* sp. showed a color change around the fungal colony from yellow into red. *P. asterica* was therefore growing on the chitinase medium but without degrading the colloidal chitin.

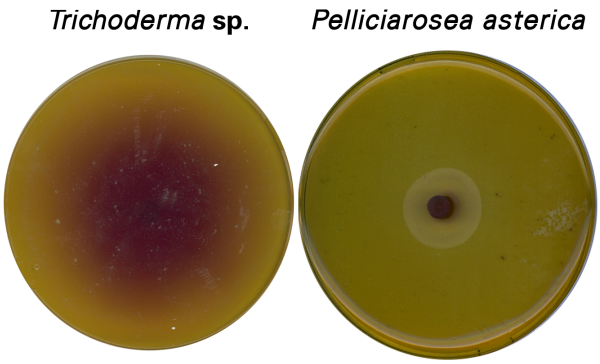

Figure 4.17: Test for chitinase activity by *P. asterica* after 14 days. A chitinase activity (indicated by a color change around the fungal colony from yellow into red) as seen for *Trichoderma* sp. after three days could not be determined for *P. asterica* (after 28 days).

CM-cellulose was detected on the agar plates with Schulze's solution which stains the CM-cellulose dark violet. A clearing zone around the fungal colony would indicate a degradation of the CM-cellulose. The results on the cellulase plates with *P. asterica* showed no clear cellulase activity (Figure 4.18). Positive controls like *Bjerkandera adust*a or *Schizophyllum commune* were carried out but the staining with chloroiodine of zinc showed not the expected staining. The positive controls as well as *P. asterica* showed after staining with chloroiodine of zinc a clearing zone around the colony, but the whole plate was stained brown instead of dark violet (indicating cellulose in the plate). The repeated assay showed no other results. Therefore, a cellulase activity could not be determined but could as well not be excluded.

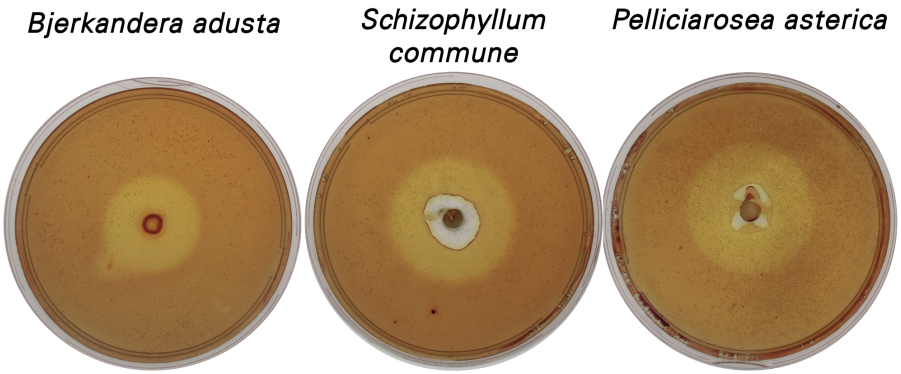

Figure 4.18: Test for cellulase activity by *P. asterica*. The control plates of *Bjerkandera adusta* and *Schizophyllum commune* were analyzed after three days. *P. asterica* was analyzed after 14 days. Cellulose is indicated with a dark violet stain by zinc chloroiodide and a cellulase activity is seen as clearing zone around the fungal colony. The plates were stained brownish instead of dark violet outside of the clearing zone.

The activity of extracellular proteases was detected with a clearing zone around the fungal colony after staining the agar plate with Coomassie Brilliant Blue G-250. *P. asterica* produced different extracellular proteases to degrade the protein source in the MEA medium (shown 21 days after transfer, Table 4.2). The differences in growth between the different protein media (BSA, gelatin and skim milk) were significant ($\alpha = 0.05$ or smaller) (Table 4.2). *P. asterica* grew significantly ($\alpha = 0.01$) slower on media including protein sources (compared to the control plate). The growth of *P. asterica* on the protein containing media were declining in the following order: BSA, skim milk and gelatin. Clearing zones after staining the plates with Coomassie Brilliant Blue G-250 were visible on gelatin and skim milk containing media (Figure 4.19). A clearing zone was visible after staining with Coomassie Brilliant Blue G-250 on the BSA containing medium only on some plates. The control of *P. asterica* on $\frac{1}{20}$ MEA showed no clearing zone around the fungal colony as well. The positive control with *Schizophyllum commune* showed after three days a clearing zone around the colony on medium containing skim milk (without staining). After staining the BSA and skim milk containing media with Coomassie Brilliant Blue G-250, a clearing zone around the fungal colony of *Schizophyllum commune* was visible. *Schizophyllum commune* did not develop such a clearing zone on medium containing gelatin. *P. asterica* was able to use different protein sources like gelatin or skim milk from growth media. The use of BSA by *P. asterica* was not clearly visible on all plates.

Table 4.2: Growth of *P. asterica* on MEA with different protein sources. The MEA plates were analyzed 21 days after transferring of *P. asterica*. Statistical analysis were done with the Mann-Whitney U-test and the significance level α is indicated for the comparison of all different protein sources among each other.

medium	diameter in mm		significance level α				clearing zone
	mean	SD	control	BSA	gelatin	skim milk	
control	35.09	2.21	-	0.01	0.01	0.01	no
BSA	26.36	1.43	0.01	-	0.01	0.01	yes
gelatin	21.33	3.08	0.01	0.01	-	0.05	yes
skim milk	22.30	1.70	0.01	0.01	0.05	-	yes

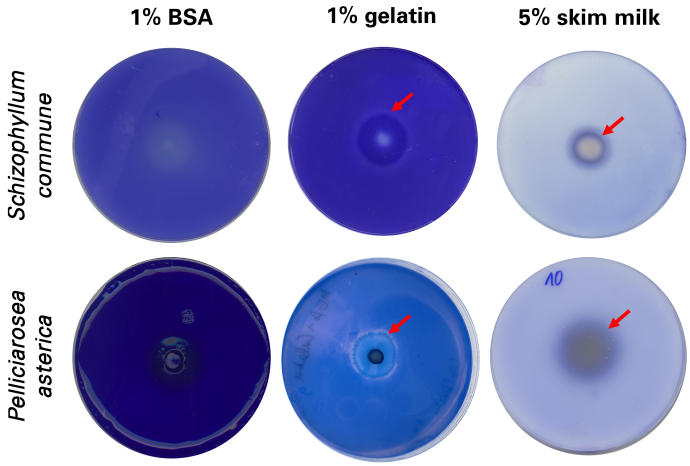

Figure 4.19: Test for protease activity on different protein sources by *P. asterica*.The upper line shows the positive control *Schizophyllum commune* (after three days) and the lower line shows *P. asterica* (after three weeks) on the different protein containing media (BSA, gelatin and skim milk). A clearing zone indicated by a red arrow was seen on the gelatin and skim milk containing media for *P. asterica* as well as *Schizophyllum commune*.

To summarize this section, *P. asterica* was able to grow on media containing chitin as carbon source and gelatin as well as skim milk as nitrogen source. *P. asterica* did not show a clear cellulase and protease activity on BSA.

4.4.3 Antagonism against other fungi by *P. asterica*

The fungi used in this experiment (Table 3.2) were confirmed by PCR with fungal primers binding to the ITS region (Table 3.4) and species-specific primers (Table 3.5). Only fungi that were identified without doubt were used in this experiment.

The antagonism of *P. asterica* against different fungi was tested and analyzed 14 days after transferring the fungal plugs to MEA (Figure 4.20). All wood decaying fungi (*Bjerkandera adusta*, *Daedalea quercina*, *Gloeophyllum sepiarium*, *Postia placenta* and *Schizophyllum commune*) were growing significantly slower in the presence of *P. asterica*. Nearly all tested endophytic fungi were significantly inhibited by *P. asterica*. Only the fungus *Trichoderma* sp. was not influenced by *P. asterica*. The phytopathogenic *Fusarium avenaceum* and the sporulating fungi (*Aspergillus* sp. and *Ceratorhiza hydrophila*) were growing similar to their control plates. However, important phytopathogenic fungi like *Fusarium culmorum* and *F. graminearum* or *Macrophomina phaseolina* were significantly inhibited in their growth by *P. asterica*.

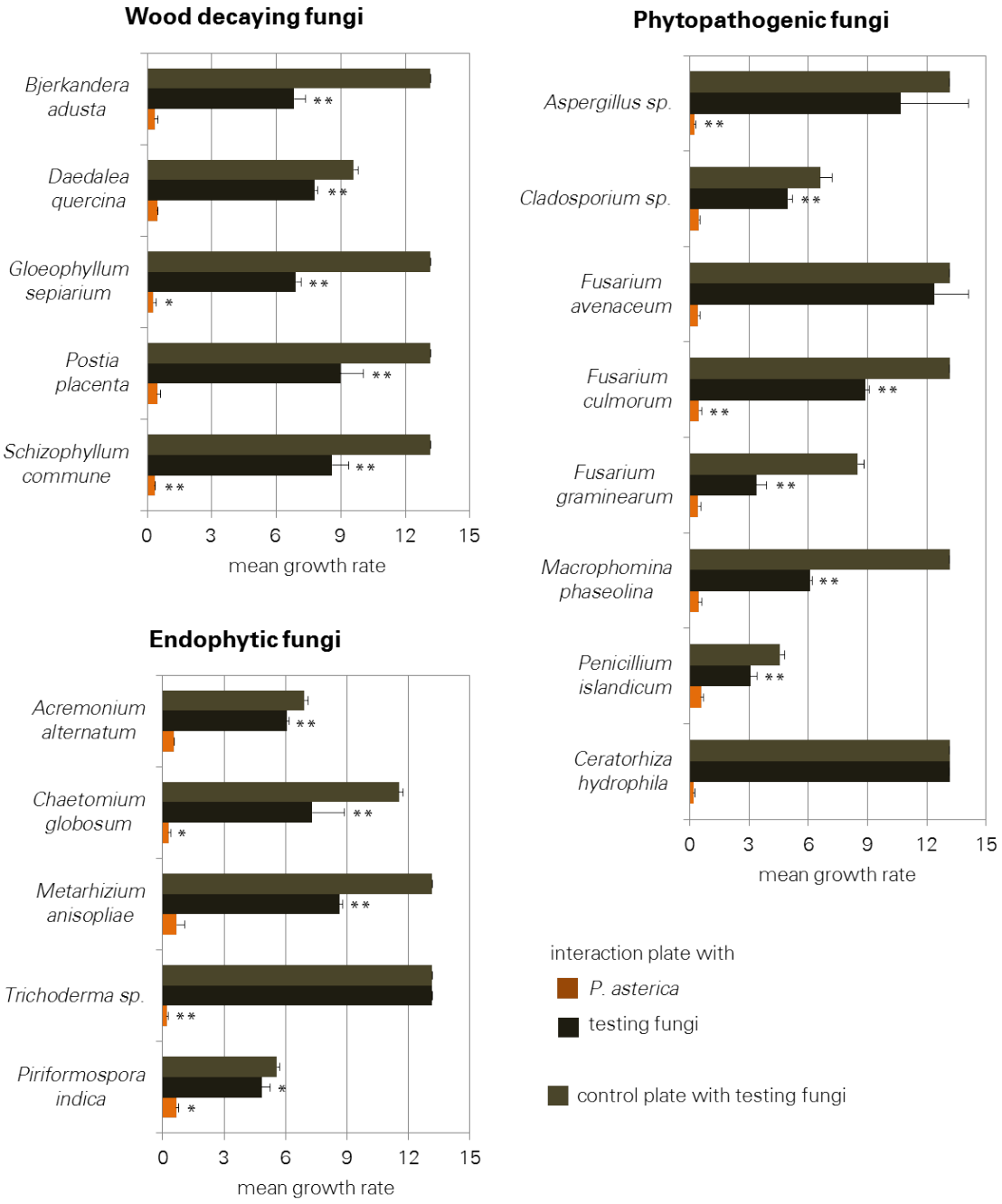

Figure 4.20: Interaction between *P. asterica* and different fungi after 14 days of co-cultivation. Data were statistically analyzed by a Mann-Whitney U-test (Mann and Whitney, 1947) ($\alpha = 0.05$ (*), $\alpha = 0.01$ (**)). See text for a detailed explanation.

P. asterica was also inhibited in its growth by other fungi (Figure 4.20 and Table 4.3). *Gloeophyllum sepiarium*, *Schizophyllum commune*, *Chaetomium globosum*, *Trichoderma* sp., *Aspergillus* sp. and *Fusarium culmorum* led to a significant growth inhibition of *P. asterica*. *Piriformospora indica* enhanced the growth of *P. asterica* significantly ($\alpha = 0.05$) to some extent.

Table 4.3: Influence of different fungi on the growth of *P. asterica* on MEA. The mean growth rate of five replicates and the standard deviation is shown for plates cultivated for 14 days. The growth rate of the control plate of *P. asterica* was statistically compared to the growth rate of the indicated interaction plates by a Mann-Whitney U-test (Mann and Whitney, 1947). The different significance levels α are indicated with ** for $\alpha = 0.01$ and * for $\alpha = 0.05$.

species on interaction plate	growth rate	
	mean	SD
control	0.50	0.06
Aspergillus sp.	0.22**	0.09
Chaetomium globosum	0.28*	0.11
Trichoderma sp.	0.21**	0.07
Ceratorhiza hydrophila	0.17**	0.08
Gloeophyllum sepiarium	0.28*	0.15
Piriformospora indica	0.66*	0.11
Schizophyllum commune	0.35**	0.04

Beside the growth rate also the growth of the different fungi in the presence of *P. asterica* was interesting. Many fungi just grew over *P. asterica*, even if they were inhibited in their growth speed (*Aspergillus* sp., *Trichoderma* sp., *Ceratorhiza hydrophila*, *Daedalea quercina* and *Schizophyllum commune*). Others in turn grew around *P. asterica* - with (*Fusarium graminearum*, *Macrophomina phaseolina*, *Postia placenta*) or without an inhibition zone (*Chaetomium globosum*, *Fusarium avenaceum*, *Fusarium culmorum* and *Metarhizium anisopliae*). Other fungi were strongly inhibited in growth by *P. asterica* so that they grew only on their side of the plate (*Cladosporium* sp.) or faster to the opposite side than to the endophyte side (*Fusarium graminearum*, *T. islandicus*, *Bjerkandera adusta* and *Gloeophyllum sepiarium*).

The inhibition zone of fungi which kept a distance to *P. asterica* was developing over the time (Figure 4.21).While for some fungi the inhibition zone remained more or less constant over the time (*Fusarium graminearum*, *T. islandicus*), other fungi grew towards *P. asterica* within three weeks (*Chaetomium globosum*, *Cladosporium* sp., *Macrophomina phaseolina*, *Bjerkandera adusta*, *Gloeophyllum sepiarium* and *Piriformospora indica*).

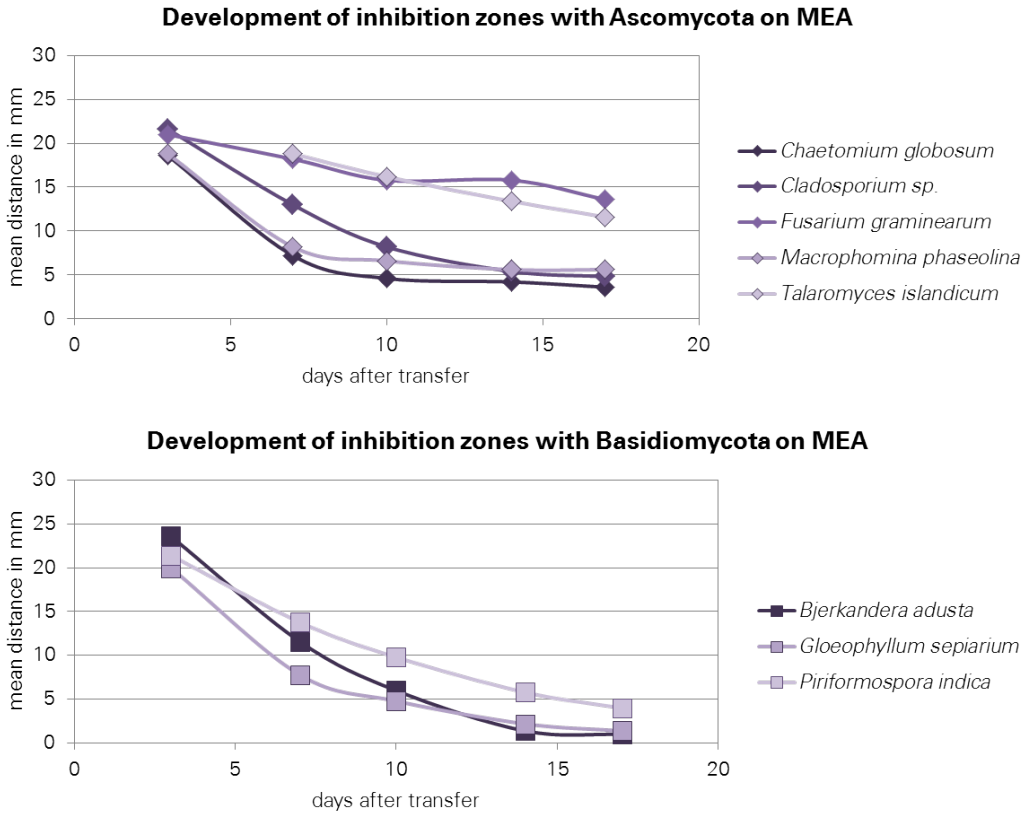

Figure 4.21: Inhibition zone between *P. asterica* and different fungi on MEA over 17 days of co-cultivation. This inhibition zone was sometimes larger and some other time smaller. All indicated fungi preserved this inhibition zone up to 17 days of co-cultivation.

The experiment was performed not only on MEA but also on PDA (data not shown). The inhibition of fungi by *P. asterica* on PDA showed a very similar pattern to that on MEA. Only *Acremonium alternatum*, *Cladosporium* sp. and all three *Fusarium* species behaved differentially than on MEA. *Acremonium alternatum*, *Fusarium culmorum* and *Fusarium graminearum* showed no reduced growth on PDA in the presence of *P. asterica*. However, *Fusarium avenaceum* was inhibited otherwise in growth by *P. asterica* on PDA. *P. asterica* was itself inhibited in growth by the following fungi: *Bjerkandera adusta*,

Schizophyllum commune, *Metarhizium anisopliae*, *Trichoderma* sp., *Aspergillus* sp., *T. islandicus* and all three *Fusarium* species. An inhibition zone was developed between *P. asterica* and *Cladosporium* sp., *T. islandicus*, *Bjerkandera adusta*, *Daedalea quercina*, *Gloeophyllum sepiarium* as well as *Piriformospora indica* (some examples are shown in Figure 4.22).

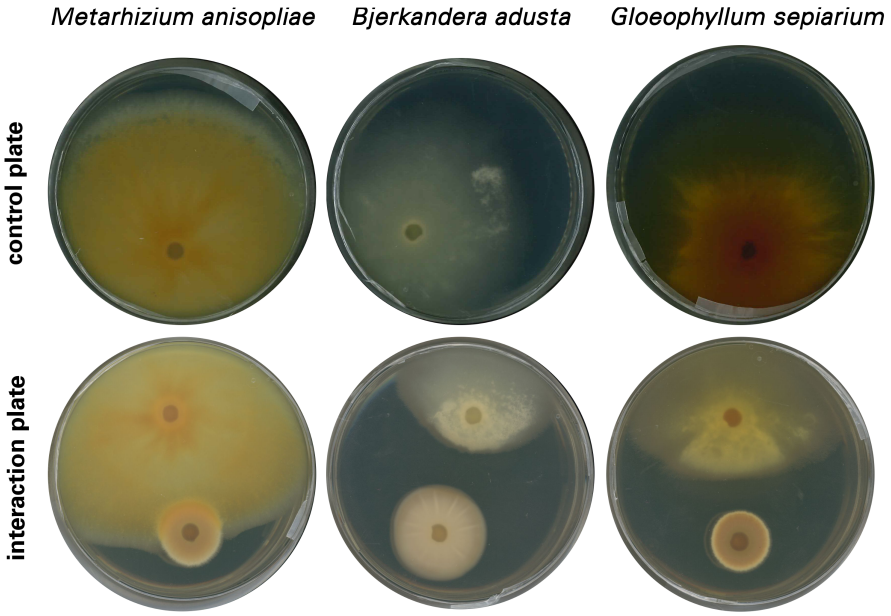

Figure 4.22: Interaction between *P. asterica* and different fungi on PDA after 14 days of co-cultivation. The upper line shows the control plates, the lower line the interaction plates with *P. asterica* and the corresponding fungus. The endophyte *P. asterica* is always the fungal colony at the bottom of the antagonism plate. *Bjerkandera adusta* and *Gloeophyllum sepiarium* were strongly inhibited in growth by *P. asterica*.

4.5 Detection of *P. asterica* in *A. tataricus*

4.5.1 Fungal DNA in different *A. tataricus* cultivars

The fungus *P. asterica* was detected in different plants of *A. tataricus*. One plant of the Austrian (plant SS4-1) and two plants of the Dresden cultivar. The two plants of the Dresden cultivar differ in their cultivation time in the greenhouse. The plant BG2-2 was cultivated for over three years, whereas the plant oBG12 was cultivated only for two months in the greenhouse.

All three plants were analyzed with RT-PCR if *P. asterica* genomic DNA can be amplified

with the specific primers (data not shown). No PCR product was detected in the plant of the Dresden cultivar cultivated for two months (plant oBG12). Therefore, the more sensitive qPCR was used to detect and quantify the amount of fungal DNA.

The suitability of the DNA samples (between 5 ng to 8 ng) for the qPCR was tested with qPCR primers for the plant gene actin of *A. tataricus* (qAstACTfor1 + qAstACTrev1). These results showed for all samples a mean Ct between 22 and 26 while the Ct of the no template control was not detectable. Therefore, the PCR was not influenced by inhibitors ("Plant primers"). The Ct values of the fungal primer pair qPearDNAfor1 + qPearDNArev1 were translated with a calibration curve into fungal DNA concentrations ("Fungal DNA"). The calibration curve for the fungal primer pair was set up with fungal DNA of *P. asterica* (Figure 4.23). The lowest DNA amount detectable with the fungal primer pair was between 5 pg and 2 pg. All Ct values over 29 to 30 were above the detection limit.

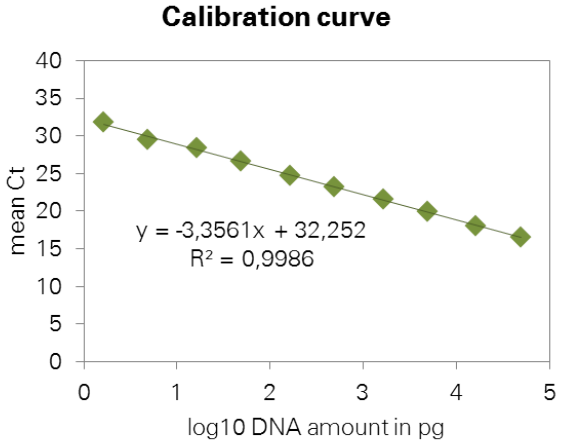

Figure 4.23: Calibration curve of fungal primers qPearDNAfor1 + qPearDNArev1.

The presence of *P. asterica* could be verified in all organs of the Austrian plant SS4-1 (Figure 4.24). Only 0.11 % of the total DNA was presented by fungal DNA. The rhizome showed a lower fungal DNA amount (12.47 %) than the above-ground parts of the plant like leaves (38.94 %) and inflorescence (23.51 %).

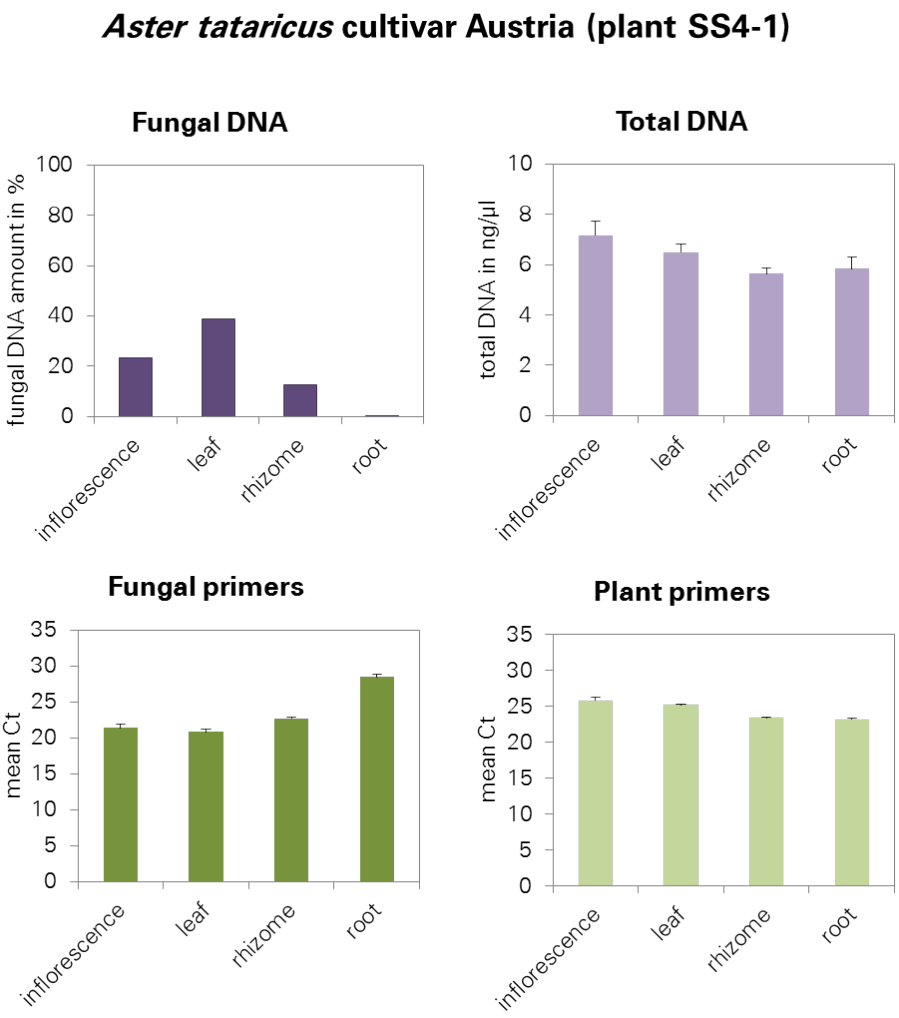

Figure 4.24: Detection of *P. asterica* in *A. tataricus* cultivar Austria (plant SS4-1). Fungal DNA was detected in all analyzed organs but in roots far below the detection limit. Therefore, roots contained almost no fungal DNA of *P. asterica*. Leaves showed the highest amount of fungal DNA, followed by the inflorescence and rhizomes (Fungal DNA). Similar amounts of genomic DNA (Total DNA) were used in and are suitable for the qPCR (Plant primers).

A similar pattern was found in the Dresden plant BG2-2 (Figure 4.25). The roots showed with 0.17 % similar low data as the Austrian plant. The only difference to the Austrian plant was that in the Dresden plant - cultivated for over three years in the greenhouse - the rhizome (24.33 %) showed the highest amount of fungal DNA compared the above-ground parts. Leaves (14.06 %) and inflorescence (7.83 %) showed lower values than the rhizome.

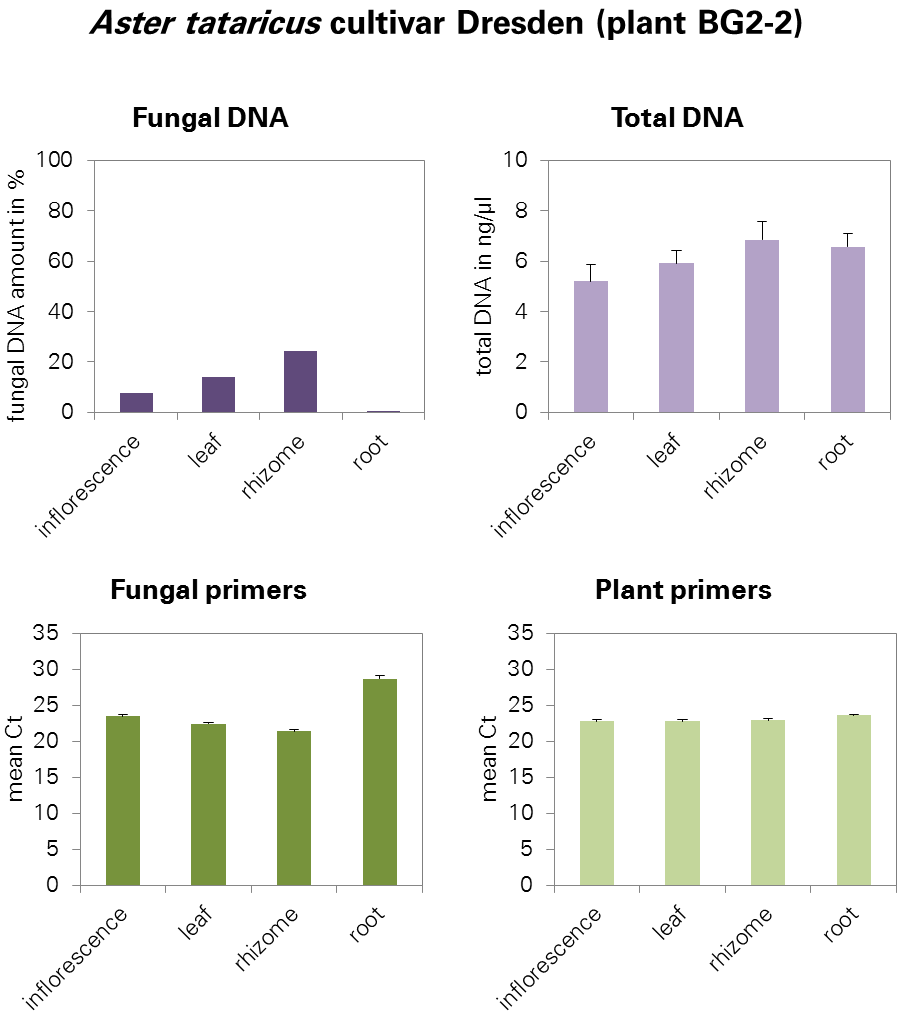

Figure 4.25: Detection of *P. asterica* in *A. tataricus* cultivar Dresden (plant BG2-2). Fungal DNA was detected in varying amounts (Fungal DNA). Almost no fungal DNA was detected in the roots (due to the detection limit of the fungal primers). The rhizomes, leaves and inflorescence showed - in this order - declining astin amounts (Fungal DNA). The genomic DNA as PCR template was suitable for qPCR (Plant primers).

The Dresden plant cultivated for only two months in the greenhouse (plant oBG12) showed even lower values than the two other aster cultivars in leaves (0.07 %) and roots (0.08 %) (Figure 4.26). The Ct values of the fungal primers were with around 30 very high and lied above the detection limit of the fungal primers which was seen in the calibration curve (see Figure 4.23).

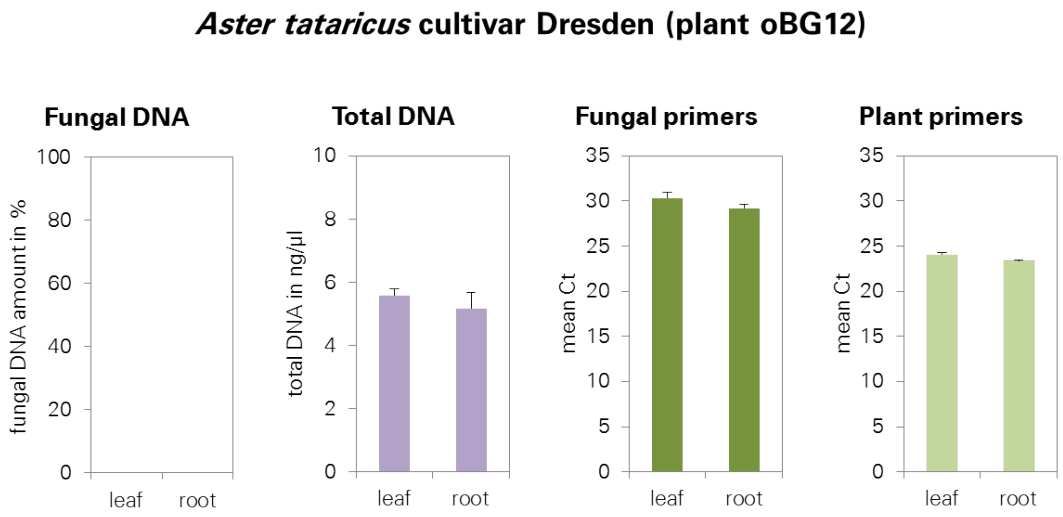

Figure 4.26: Detection of *P. asterica* in *A. tataricus* cultivar Dresden (plant oBG12). Fungal DNA was detected but below the detection limit of the fungal primers (Fungal DNA). The PCR templates were all suitable for qPCR which was shown with plant primers for the actin gene (Plant primers). The total DNA amount was comparable to the other samples (Total DNA).

Summarizing this part, fungal DNA of *P. asterica* was detected in the Austrian plant SS4-1 and in the Dresden plant BG2-2 cultivated for over three years in different organs like inflorescence, leaves and rhizomes. Almost no *P. asterica* DNA could be detected in the roots of both cultivars (plants SS4-1 and BG2-2) and in the Dresden plant which was cultivated for two months in the greenhouse (plant oBG12).

4.5.2 Corresponding astin profile

As already seen in section 4.2.2, *A. tataricus* (cultivar Austria plant SS4-1 and cultivar Dresden plant BG2-2) showed a broad spectrum of astins. Astin A/B and astin C were the main variants present in the different organs. Astins E/H, F (variant 2), G and I were minor constituents in the analyzed samples (Figures 4.27 and 4.28).

The highest concentrations of the dichlorinated astins were found in the roots of both cultivars (plant SS4-1 and plant BG2-2). The difference between both plants was that the Dresden cultivar had a much higher astin concentration in the roots as the Austrian cultivar. Vice versa, the Austrian cultivar showed in the above-ground organs the higher astin concentration. No astins were detectable in the Dresden plant (plant oBG12) cultivated only for two months in the greenhouse.

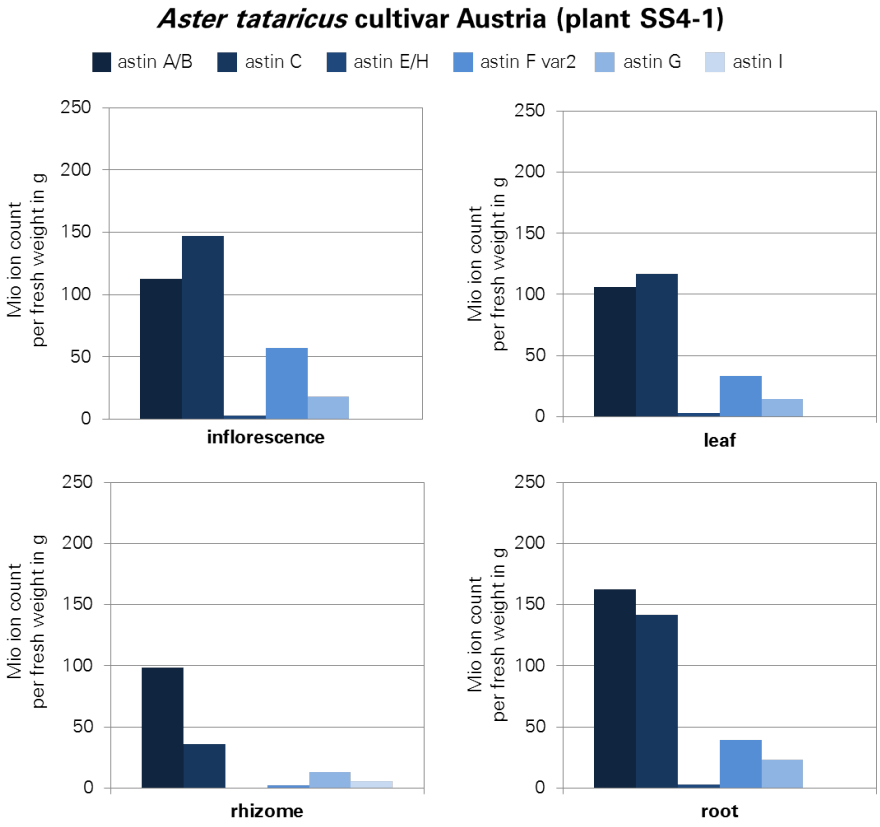

Figure 4.27: Astin composition of the *A. tataricus* cultivar Austria (plant SS4-1). All analyzed plant organs contained detectable amounts of astins. Roots and inflorescence indicated similar high amounts of astins, whereas rhizomes and leaves showed similar low, but still high amounts.

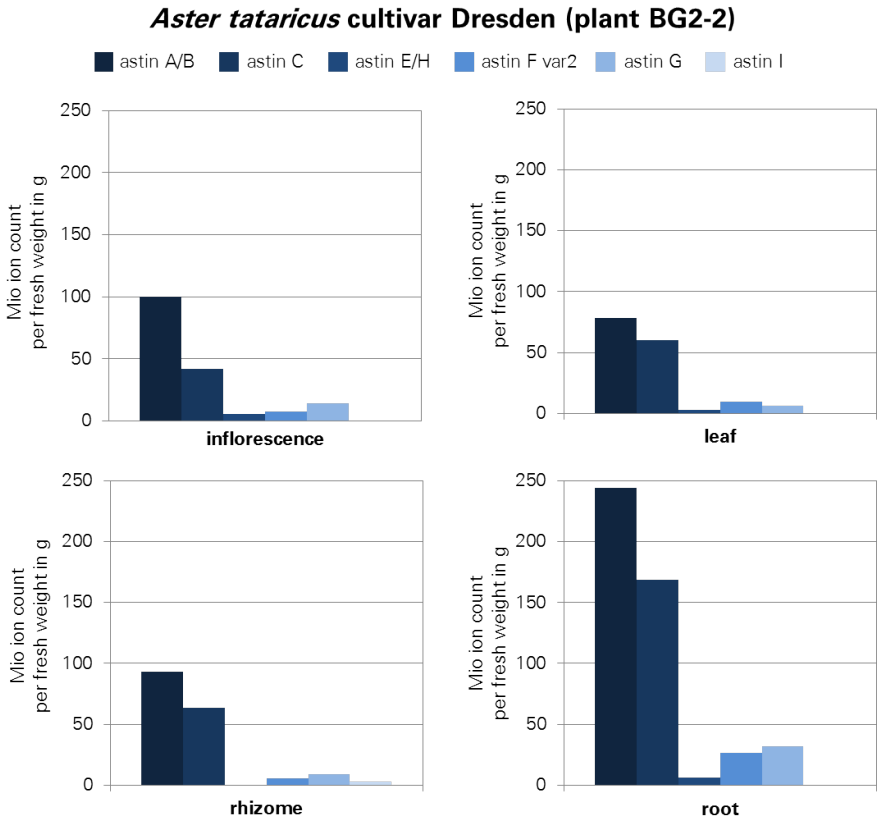

Figure 4.28: Astin composition of the *A. tataricus* cultivar Dresden (plant BG2-2). Astins were detected in all four organs. The highest amount of astins were found in the roots, followed by rhizomes and inflorescence. The leaves contained least astins.

4.6 Induction of astin synthesis in plants or fungi

4.6.1 Infection of *A. tataricus* with *P. asterica*

Plants of *A. tataricus* cultivar Dresden were infected with *P. asterica* in a two-compartment system. These plants were cultivated for two years in the climate chamber and showed no detectable astin profile. Detectable amounts of different astins were found after the infection with *P. asterica* (Figure 4.29). The main astins are as well astins A/B and C. Compared to the astin profiles of other plants (Austrian and Dresden cultivars), the amounts were much lower but the composition is similar. Only in one plant (plant 2) astins were detectable in all three organs. This plant had also the highest astin level of all three infected plants. Plant 1 showed astins only in roots and plant 3 only in leaves.

The control plant - cultivated in the same way as the others, but without inoculation with *P. asterica* - showed no detectable astins. The main astins were astins A/B and C, as already seen in the other plants. Astins E/H, G, F and I were only minor constituents within the astin profile.

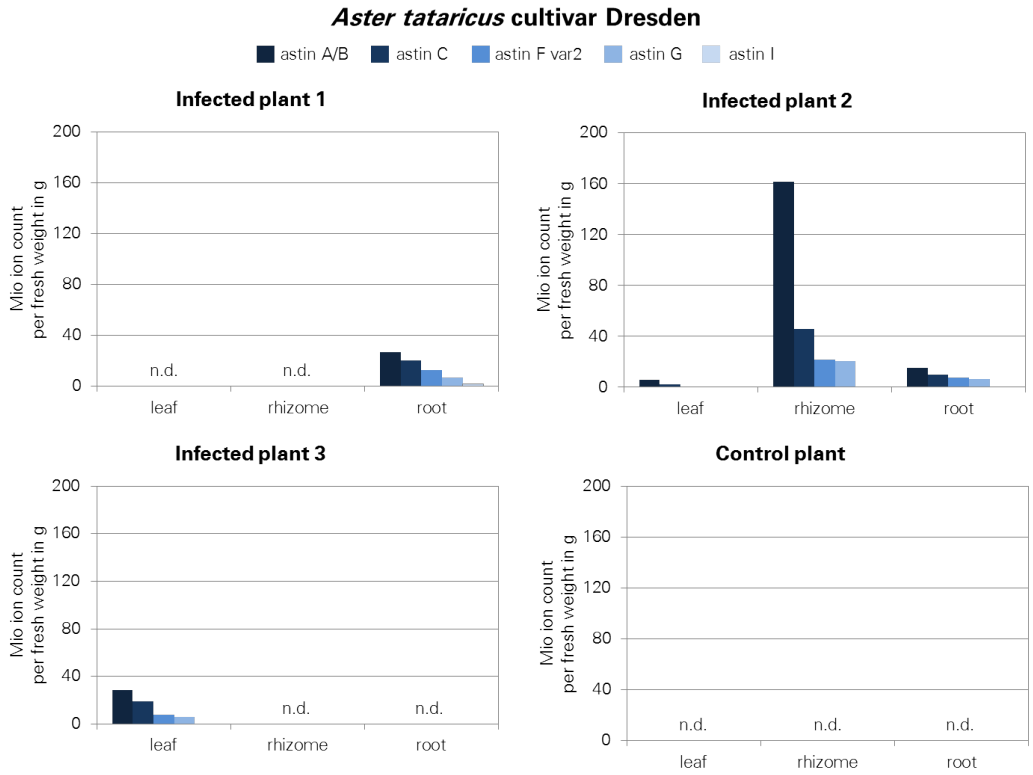

Figure 4.29: Astin profile of infected *A. tataricus* cultivar Dresden plants. The infection of astin-free plants with *P. asterica* leads after three months cultivation to detectable amounts of all astins which were found in *A. tataricus* cultivar Austria. The control plant which was not infected with *P. asterica* shows no detectable astins. n.d. samples were measured but astins were not detectable.

4.6.2 Growth of *A. tataricus* in different sized pots

A. tataricus cultivar Dresden plants directly from the Botanical Garden were cultivated in different sized pots to see if the pot size influences the astin level in plants. The measured astin profiles over the time (Table 4.4) showed an induction of astin production during the winter months (after 24 and after 36 weeks) in the greenhouse in some plants. Only astins A/B, C and F (variant 2) were detected in these plants. The first astins occurred in plant 12 after 24 weeks cultivated in a pot of 22 cm in diameter. Astins A/B,

C and F were detected in the roots, not in the leaves. After 36 weeks, there are already three plants with detectable astins: plant 12 (roots), plant 8 (leaves and roots) as well as plant 9 (leaves and roots). Again, only astins A/B, C and F were detected.

Table 4.4: Developing astin production in *A. tataricus* plants (cultivar Dresden) cultivated in the greenhouse.

pot size in cm	plant	organ	Mio ion count of astins per fresh weight in g					
			after 24 weeks			after 36 weeks		
			A/B	C	F var2	A/B	C	F var2
22	12	leaf	0	0	0	0	0	0
		root	1.81	0.83	0.44	23.73	0	2.82
28	8	leaf	0	0	0	1.01	0	0
		root	0	0	0	21.65	2.87	4.11
	9	leaf	0	0	0	9.49	5.89	0
		root	0	0	0	72.36	12.56	17.00

The experiment is ongoing and the astin profile of the plants will be further detected. Up to now, no influence of the pot size on the astin production can be determined. But the time period of cultivating the plants in the greenhouse seems to be relevant.

4.6.3 Feeding of *P. asterica* with L-threonine

Astins A and B contain as second respectively fifth amino acid an *allo*threonine. It was reasoned that maybe the amino acid might be a limiting factor in culture, but could be supplied by the plant. To determine if L-threonine was limiting, *P. asterica* cultures were incubated with different concentrations (0 mM, 5 mM and 250 mM) of L-threonine for three and eight days. The analyzed astin profiles of these cultures did not change by the addition of L-threonine into the liquid culture (Figure 4.30).

The growth of *P. asterica* was calculated as mean of three liquid cultures, whereas the astin profile is shown only from one culture. No additional astins - beside the known fungal astins C, F and G - were detected, neither three days nor eight days after cultivation in liquid media containing different amounts of L-threonine. The only

difference to the other astin profiles of *P. asterica* was that astin F appeared with both variants. The growth was not statistically analyzed due to the low amount of replicates (only three).

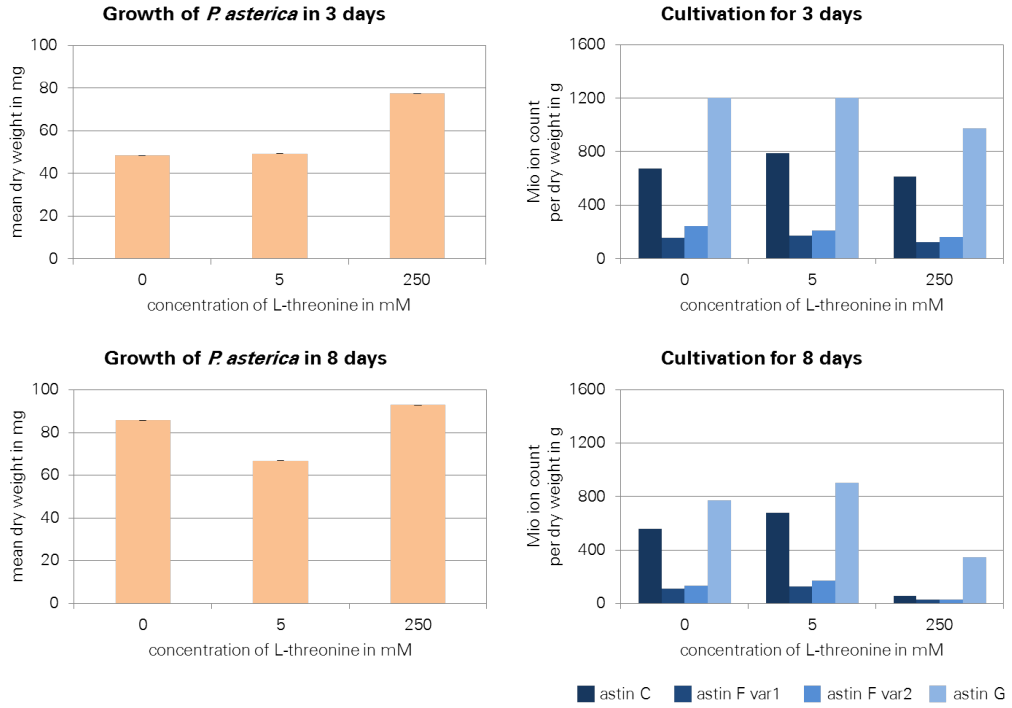

Figure 4.30: Growth of *P. asterica* in liquid culture containing different concentrations of L-threonine. The growth represents the mean of three replicates, whereas the astin profile is shown only from one sample. The astin profile showed no additional astins like astin A/B which would be synthesized with L-threonine.

4.7 Search for a halogenase in *A. tataricus* and *P. asterica*

The chlorinated proline in the astins indicates the presence of a flavin-dependent halogenase. Hence, different approaches were done to find such a halogenase either in *A. tataricus* or *P. asterica*.

4.7.1 Phylogenetic relationship of bacterial halogenases to the *T. islandicus* halogenase

The nucleic acid sequence of different bacterial halogenases used for the primer design were aligned with the nucleic acid sequences of the putative halogenase from *T. islandi-*

cus (Figure 4.31). The FAD-binding (GXGXXG) and the tryptophan (WXWXIP) motifs were clearly visible and conserved throughout the different bacterial halogenases. The alignment of the bacterial halogenases with the putative halogenase from *T. islandicus* showed a high conservation in the two known motifs.

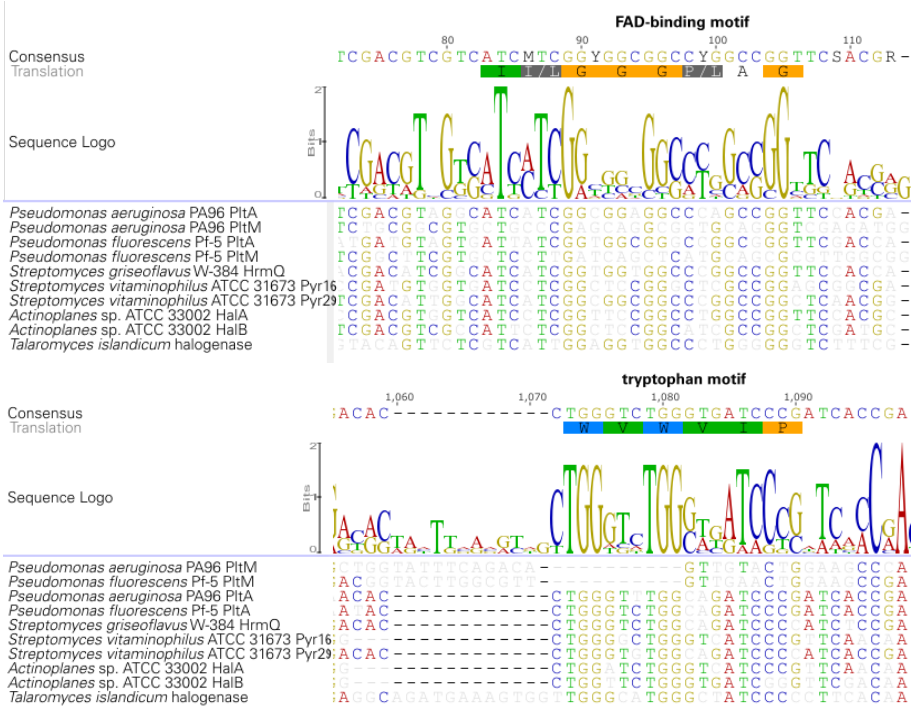

Figure 4.31: Alignment of the nucleic acid sequence of different bacterial halogenases with the putative halogenase of *T. islandicus*. The two known domains could be identified as tryptophan (WXWXIP) and FAD-binding motif (GXGXXG). These were conserved in the bacterial halogenases as well as in the putative halogenase from *T. islandicus*.

The phylogenetic tree of the bacterial halogenases with the putative halogenase of *T. islandicus* showed no relationship between these halogenases (Figure 4.32). The putative halogenase of *T. islandicus* was not clustered together with the bacterial halogenases in any bootstrap tree which was indicated by a branch without any number. These numbers indicating the percentage of replicates trees in which the two taxa are clustered together.

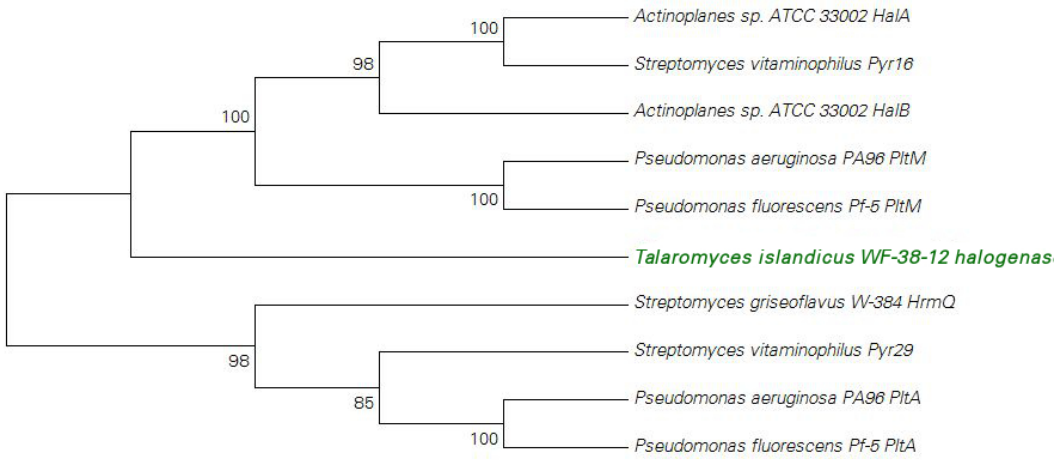

Figure 4.32: Phylogenetic relationship of the putative halogenase from *T. islandicus* with different bacterial halogenases based to their amino acid sequences. The evolutionary history was inferred by using the Maximum Likelihood method based on the Le-Gascuel model (Le and Gascuel, 2008). The bootstrap consensus tree inferred from 2000 replicates is taken to present the evolutionary history of taxa analyzed (Felsenstein, 1985). The percentage of replicates trees in which the associated taxa clustered together in the bootstrap test (2000 replicates) are shown next to the branches. Initial tree(s) for the heurestic search were obtained by applying the Neighbor-Joining method to a matrix of pairwise distances estimated using a JTT model. A discrete Gamma distribution was used to model evolutionary rate differences among sites (5 categories (+G, parameter = 2.4607)). The analysis involved 10 amino acid sequences. All positions contained gaps and missing data were eliminated. There were a total of 414 positions in the final data set. Evolutionary analyzes were conducted in MEGA6 (Tamura et al., 2013).

Despite this, the primers of the bacterial halogenases could be used to identify a possible halogenase gene in *A. tataricus* and *P. asterica* even if the bacterial halogenase were not related to the halogenase of *T. islandicus*.

4.7.2 PCR results

Different primers were tested to identify a possible candidate gene of a halogenase. The primers derived from known bacterial halogenases (degenerated primers named LFHAL), from putative halogenases of *Penicillium marneffei* (PemHAL) as well as *T. islandicus* (PeiHAL) and from a hypothetical halogenase of *Ricinus communis* (RicHAL).

PCRs with these primer pairs showed no specific PCR product of a halogenase gene in *A. tataricus,* neither in the Dresden cultivar nor in the Austrian one (Figure 4.33). A control PCR with plant primers (AstSHSf2 + AstSHSr2) was conducted to analyze the templates for inhibitors and resulted in PCR products of the expected size. The

resulting PCR products (indicated by a red arrow) were sequenced and compared in BLASTn (Madden, 2002) with other sequences but none of them showed a similarity to halogenases. The strong bands of the RicHAL PCR products turned out to be sequences of the plant 26S rRNA.

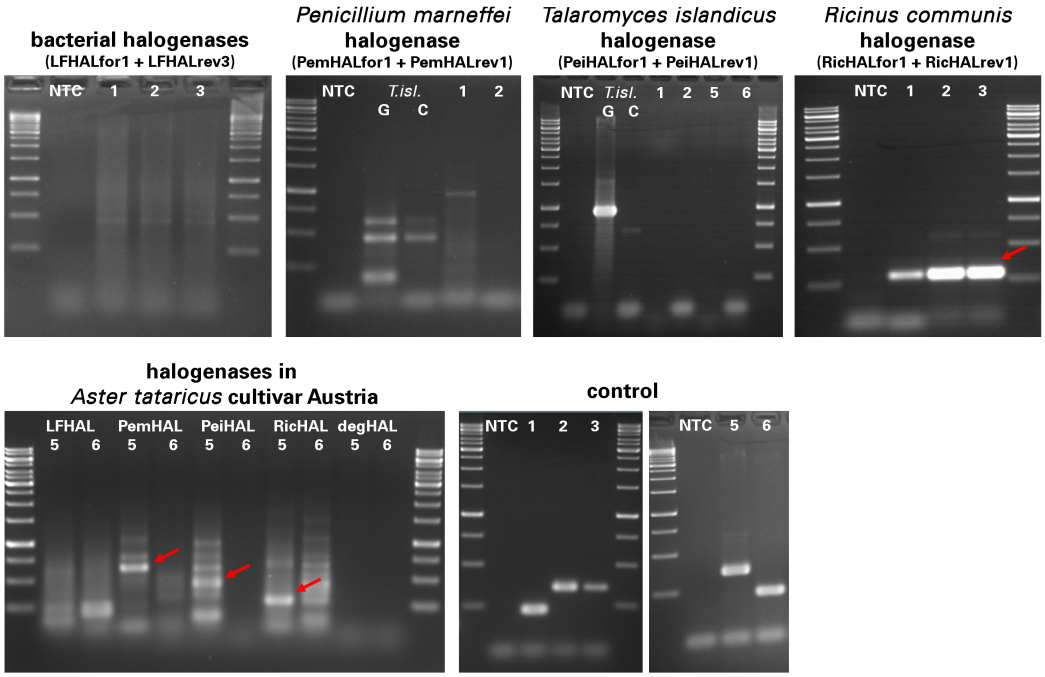

Figure 4.33: PCR results obtained with different halogenase primers for *A. tataricus*. The PCRs were carried out with genomic DNA as well as cDNA of both cultivars (DreamTaq, 40 cycles). The control PCR was done with AstSHSfor2 + AstSHSrev2. The PCR products indicated with a red arrow were cut out and sequenced. For detailed information see text. NTC no template control, 1 cDNA root cultivar Dresden, 2 genomic DNA leaf cultivar Dresden, 3 genomic DNA root cultivar Dresden, 5 cDNA root cultivar Austria, 6 genomic DNA root cultivar Austria, T.isl. *T. islandicus* with genomic DNA (G) and cDNA (C).

Different primer combinations were used to identify the halogenase in *A. tataricus* (see Figure 4.34). A PCR with plant primers (control, AstSHS3Uf1 + AstSHS3Ur1) was performed to exclude inhibition of the PCR reaction through substances extracted from the plant. Each tested sample showed a PCR product with the right size. None of the halogenase primer combinations revealed a sequence related to a halogenase. Only two PCR products (around 300 bp and 620 bp, indicated with a red arrow) appeared with the RicHALrev1 primer in all primer combinations. These were 26S rDNA sequences from the plant rDNA cluster and were amplified only by the reverse primer RicHALrev1.

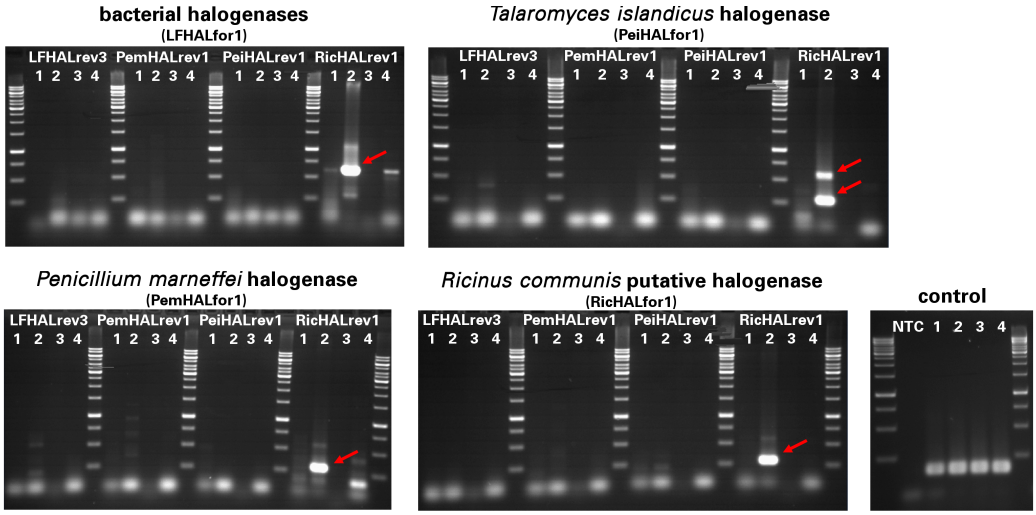

Figure 4.34: PCR results with different primers for halogenases in *A. tataricus*. Different combinations of halogenase primers were tried (DreamTaq, 40 cycles). 1 genomic DNA root of Dresden plant, 2 cDNA root of Dresden plant, 3 genomic DNA root of Austrian plant, 4 cDNA root of Austrian plant, NTC no template control.

P. asterica was analyzed as well by PCR for a halogenase gene (Figure 4.35). The halogenase primers, especially LFHAL and PeiHAL, revealed strong bands in the electrophoresis (indicated by a red arrow). However, the sequencing and analysis showed no hit for a halogenase gene and the two conserved motifs of the halogenase could not be detected.

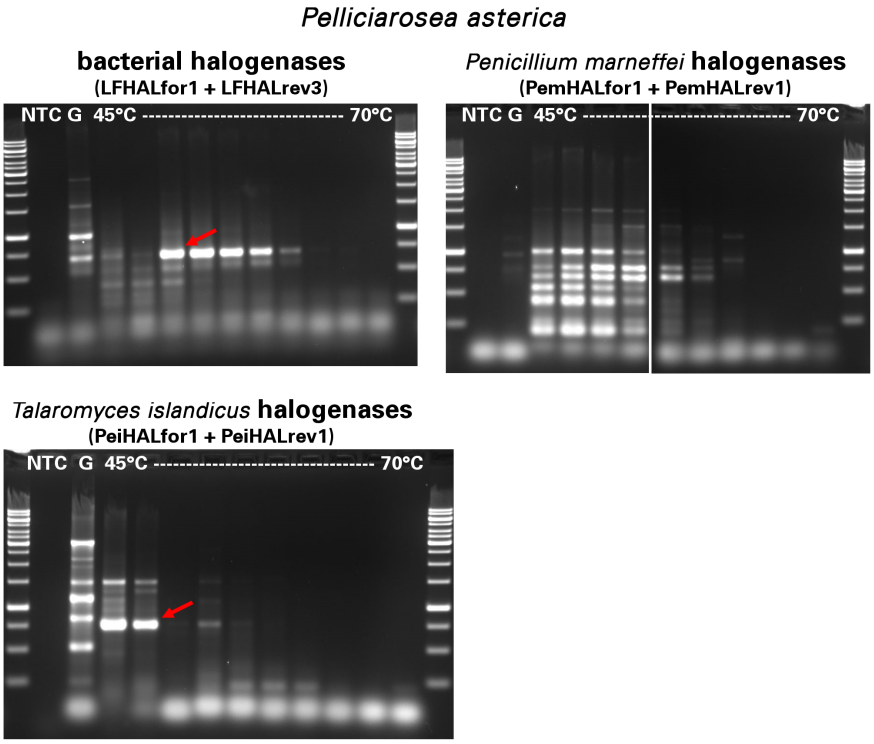

Figure 4.35: PCR results with halogenase primers on *P. asterica*. The PCR was carried out with DreamTaq and cDNA of *P. asterica* under a temperature gradient from 45 °C to 70 °C in temperature steps of 2 to 3 °C (40 cycles). The bands indicated with a red arrow were cut out and sequenced. The sequence analysis revealed no candidate gene for a halogenase. NTC no template control, G genomic DNA of *P. asterica*.

4.7.3 Southern blot analysis

Southern analysis of the genomic DNA from *A. tataricus* revealed a weak band on the X-ray film of around 1.5 kb (Figure 4.36, indicated by a red arrow). The positive controls, probe and genomic DNA of *T. islandicus*, worked well. The expected signals with the right size were detected (probe 268 bp, *T. islandicus* halogenase 949 bp).

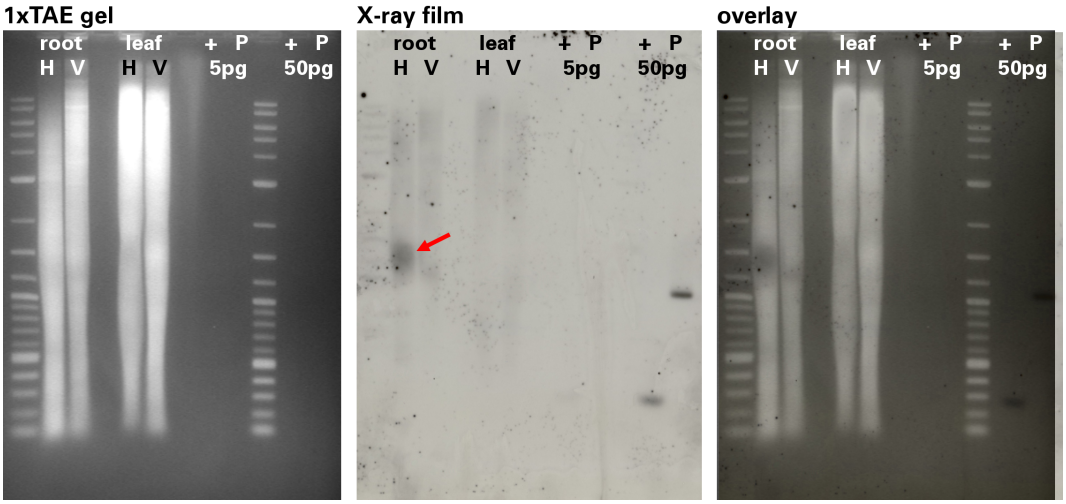

Figure 4.36: Southern blot of *A. tataricus* cultivar Austria with a faint signal on the film (1.5kb in size). The genomic DNA of leaves and roots was digested with *Hae*III or *Vsp*I. Positive controls were at the one hand the probe itself and at the other hand the putative halogenase of *T. islandicus*. root *A. tataricus* cultivar Austria gDNA of roots, leaf *A. tataricus* cultivar Austria gDNA of leaves, + probe, P *T. islandicus* halogenase, H restriction enzyme *Hae*III, V restriction enzyme *Vsp*I. 2-log DNA Ladder (0.1 - 10.0 kb) was used as DNA ladder.

4.7.4 cDNA Library and Colony Blot

A Southern blot with the two cDNA libraries was performed. The plant RNA should contain fungal RNA as well (due to the extraction method) so that a possible fungal halogenase might be detected within the plant cDNA library.

After detection of the hybridization signal from the membrane, some bands (750 bp, 900 bp and 1.4 kb, indicated by red arrows) were visible on the X-ray film (Figure 4.37).

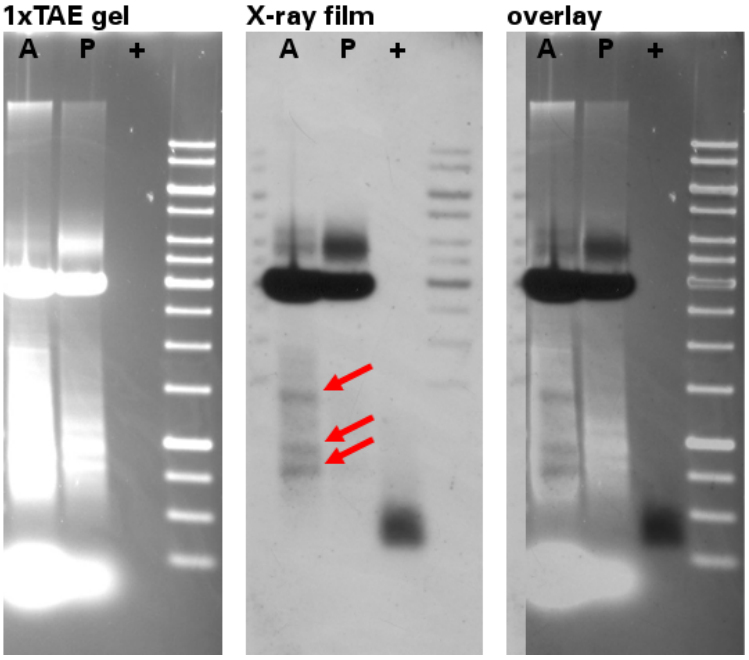

Figure 4.37: Southern blot with the cDNA library of *A. tataricus*. Hybridization was done at 45 °C, detection of signals for 2.5 hours. The probe binds unspecific but strong to the vector backbone pAL17.3 of the cDNA library (3 kb). Additional bands are visible at 750bp, 900 bp and 1.4 kb. A digested cDNA Library of *A. tataricus*, P digested cDNA library of *T. islandicus*, + probe (5 pg).

The bands visible in the Southern blot were cut out, cloned into pGEM-T easy and transformed into *Escherichia coli* XL1-Blue. Nearly all colonies streaked onto LB plates including IPTG and X-Gluc were blue. A blot of these colonies was done (Figure 4.38 C and D). The problem was that the probe for the halogenase - even it was not aligning to the vector backbone of pGEM-T easy - was binding to the vector pGEM-T easy at a hybridization temperature of 45°C (as shown in Figure 4.38A and B). The temperature could not be increased because of the low consensus between probe and hypothetical halogenase.

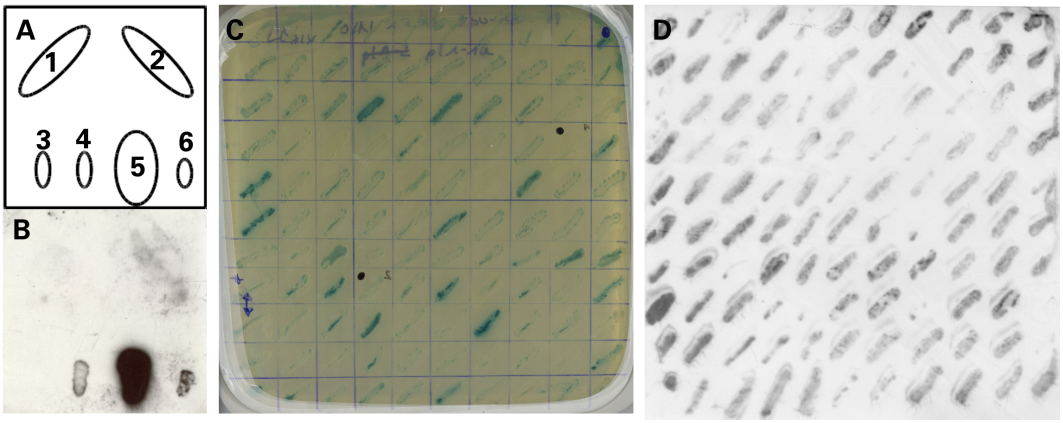

Figure 4.38: Colony blot of fragments (750bp-1kb) transformed into *E. coli*. The whole plate (C) was blotted onto a membrane, hybridized with halogenase probe and detected for 2.5 hours on a X-ray film (D). Unfortunately, the probe is binding at this low hybridization temperature to the vector backbone of pGEM-T easy (A and B). 1 *E.coli* XL1-Blue, 2 pGEM-T easy in *E.coli* XL1-Blue, 3 DNA of *E.coli* XL1-Blue, 4 linearized pGEM-T easy, 5 cDNA sequence of the probe cloned into pGEM-T easy, 6 probe as PCR product.

4.7.5 Genome sequencing of *P. asterica*

Since it was not possible to identify a putative halogenase from plant or fungus, it was decided to sequence the genome of P. asterica. Halogenase sequences should be possible to identify according to their conserved motifs. The annotated genome was searched for a halogenase candidate gene. Unfortunately, so far no candidate gene was found containing both conserved motifs (GXGXXG and WXWXIP).

4.8 RNA sequencing of *P. asterica*

It might be possible that the genome of *P. asterica* is not complete yet. Thus, RNA from samples which produced astins might contain a halogenase candidate gene. Therefore, the RNA of *P. asterica* was isolated from culture grown under different conditions which were a 21 days old culture in PDB (referred to as control), a 51 days old culture in PDB (51 days old), two 21 days old cultures in PDB containing aqueous leaf extract from *A. tataricus* once cultivar Austria (Austrian leaf extract) and once cultivar Dresden (Dresden leaf extract) and a 21 days old culture in MEB (MEB). The reference for the following analyzes was the control culture in which *P. asterica* was grown for 21 days in PDB.

4.8.1 Growth rate and astin profile of RNA sequencing samples

The RNA sequencing samples were harvested in March 2014, whereas the qPCR samples were harvested in February 2015. Despite the one year time-lag between both analyzes, *P. asterica* showed very similar dry weights (Figure 4.39). The data for the qPCR samples were the mean of two separately prepared sets of flasks.

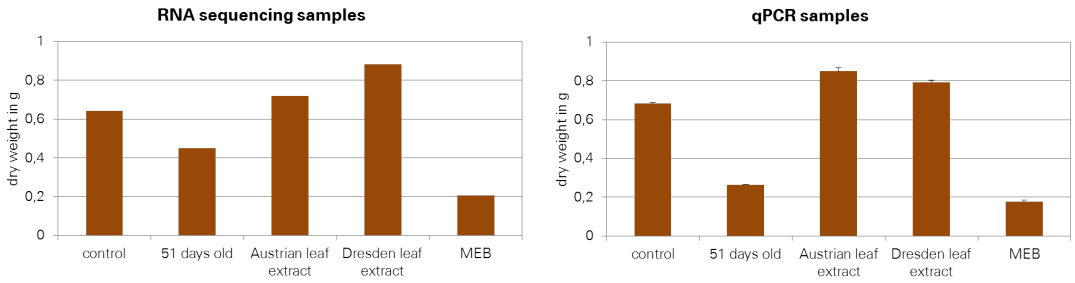

Figure 4.39: Growth of *P. asterica* in the cultures used for RNA sequencing and qPCR. Despite the one year time-lag between the harvesting of these samples, the cultures used for RNA sequencing showed a similar growth pattern as the cultures used for qPCR.

The astin profile of the liquid cultures of *P. asterica* used for RNA sequencing and qPCR showed astins C, D, F (both variants) and G (Figures 4.40 and 4.41). The fungal cultures used for RNA sequencing (Figure 4.40) showed additional astin D in their profiles. Astin C in the RNA sequencing samples was higher concentrated in the cultures including plant extract. The control culture without any additives showed the lowest astin C concentration. The mono- and non-chlorinated astin forms (astins D, F and G) were higher concentrated in the 51 days old *P. asterica* culture.

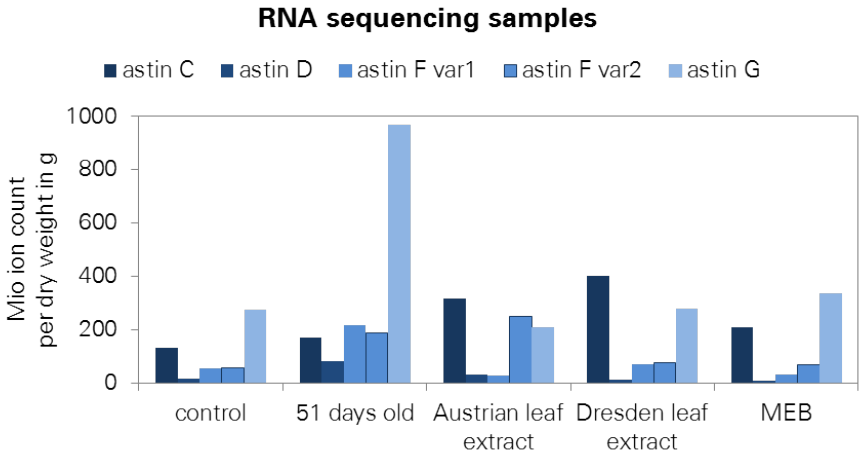

Figure 4.40: Astin profile of fungal samples used for RNA sequencing. For details see text above.

The qPCR samples (Figure 4.41) harvested one year later showed much higher astin concentrations than the fungal samples used for RNA sequencing. The highest concentration of astin C was found in the control and MEB culture. The addition of plant extract led not to a higher astin C concentration in the qPCR samples (compared to the control culture) as was seen in the RNA sequencing samples. The 51 days old culture showed higher amounts of mono- and non-chlorinated astin forms compared to all other analyzed samples indicating degraded dichlorinated astins. The usually minor constituents (astins D to I) represent the majority in the 51 days old culture.

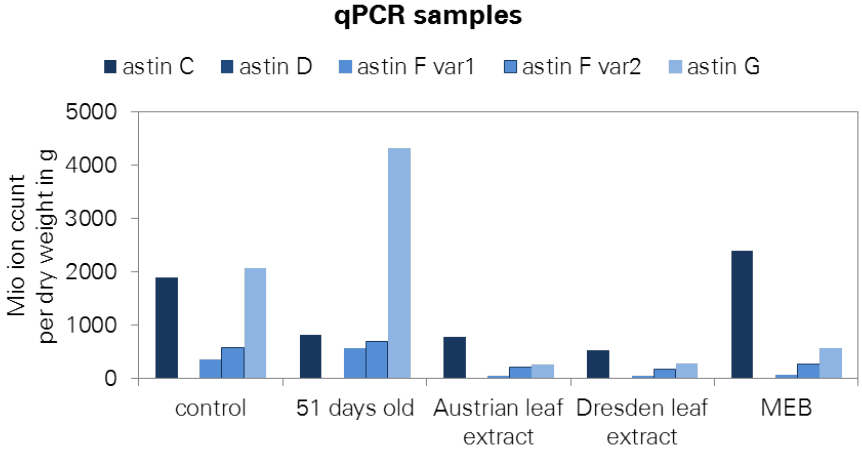

Figure 4.41: Astin profile of fungal samples used for qPCR. For details see text above.

4.8.2 Quality assessment of RNA sequencing data

Before the RNA sequencing data could be analyzed the quality of the RNA sequencing had to be verified. Therefore, differential analyzes were done which showed that only few genes are significantly differentially expressed.

The scatter plots of the differentially expressed genes showed the normalized mean expression against the log2 fold change (Figure 4.42). The further away a gene from 0 on the y axis and the higher the normalized mean expression of the gene, the more probable is the differential gene expression of this gene. Most genes were located around 0 of the y axis (indicated by the red line) meaning that they showed no change in their expression level between both compared conditions.

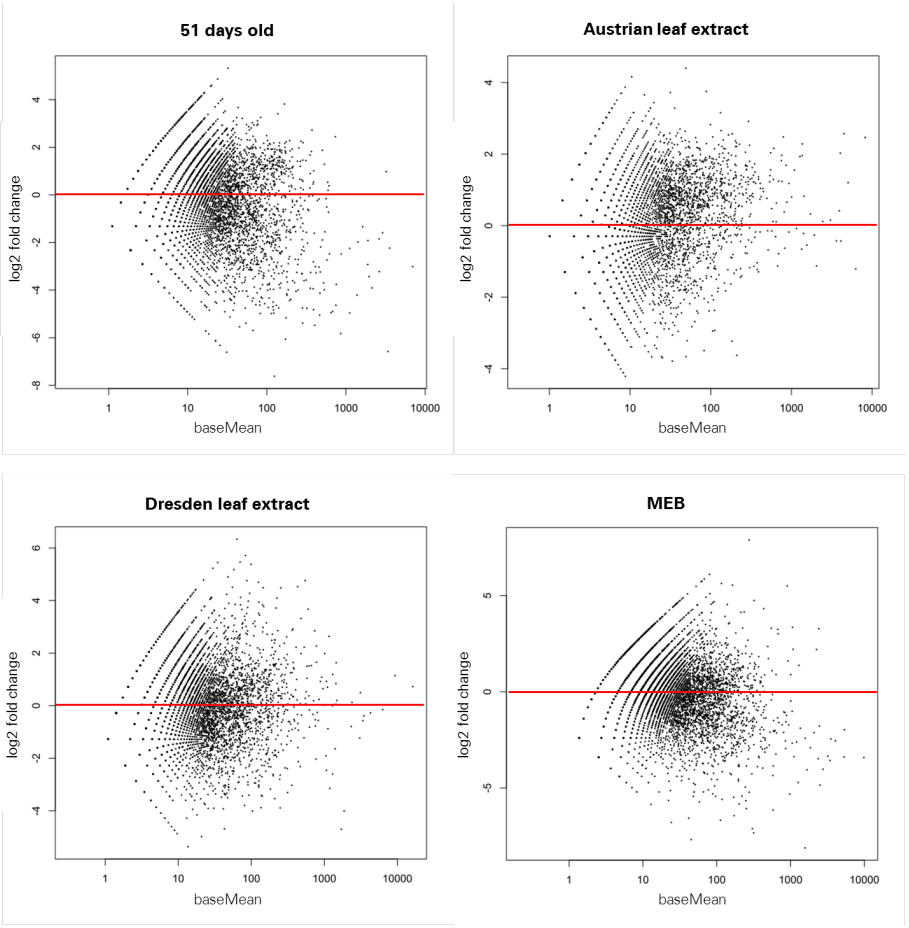

Figure 4.42: Scatter plots of the normalized mean expression (A) against log2 fold change (M). The red line indicates the base line of the y axis. The 21 days old culture in PDB served as reference.

The histogram of the different p values (Figure 4.43) showed that the majority of the expressed genes were not significantly differentially expressed. Only differentially expressed genes with a p value smaller than 0.05 were considered in the analysis. P values higher than 0.05 indicate a low or no presumption against the null hypothesis which states that the compared expressions of one gene between two samples are not different. Only a few genes showed a differentially gene expression according to these criteria.

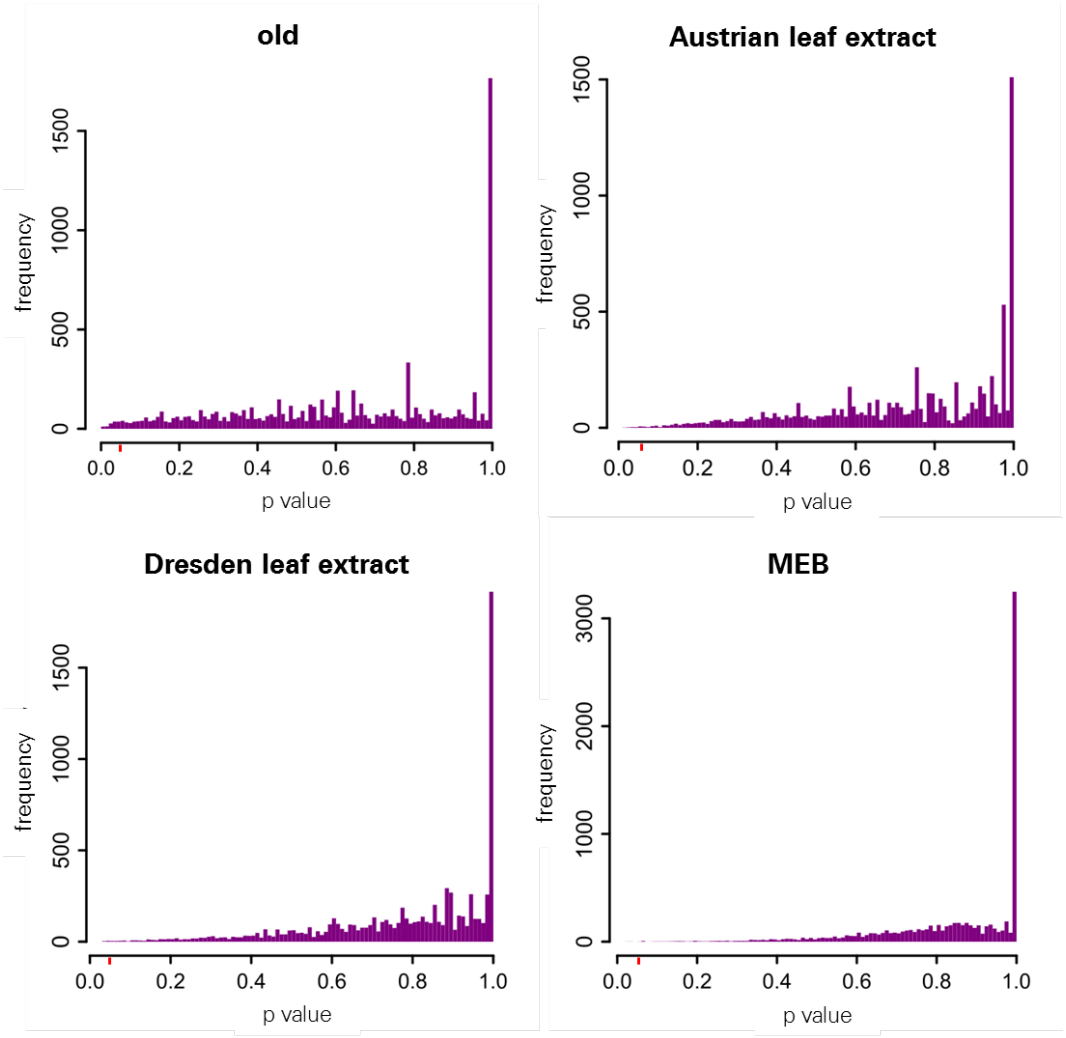

Figure 4.43: Histogram of the frequency of the different p values. Most of the genes are not significantly differentially expressed (p values smaller than 0.05, indicated by a red tick mark).

4.8.3 Differential gene expression analysis with ReadXplorer

The analyzes with ReadXplorer revealed in every culture over 7,500 expressed genes (Figure 4.44). However, only a few of them were differentially expressed and thus regulated ($p < 0.05$). The most differentially regulated genes were found in 51 days old culture (122 differentially expressed genes). Surprisingly, the addition of plant leaf extracts to the cultures did not change the expression of many genes. Only nine (Austrian leaf extract) respectively eight (Dresden leaf extract) genes were differentially expressed. The cultivation in MEB changed the expression of two genes.

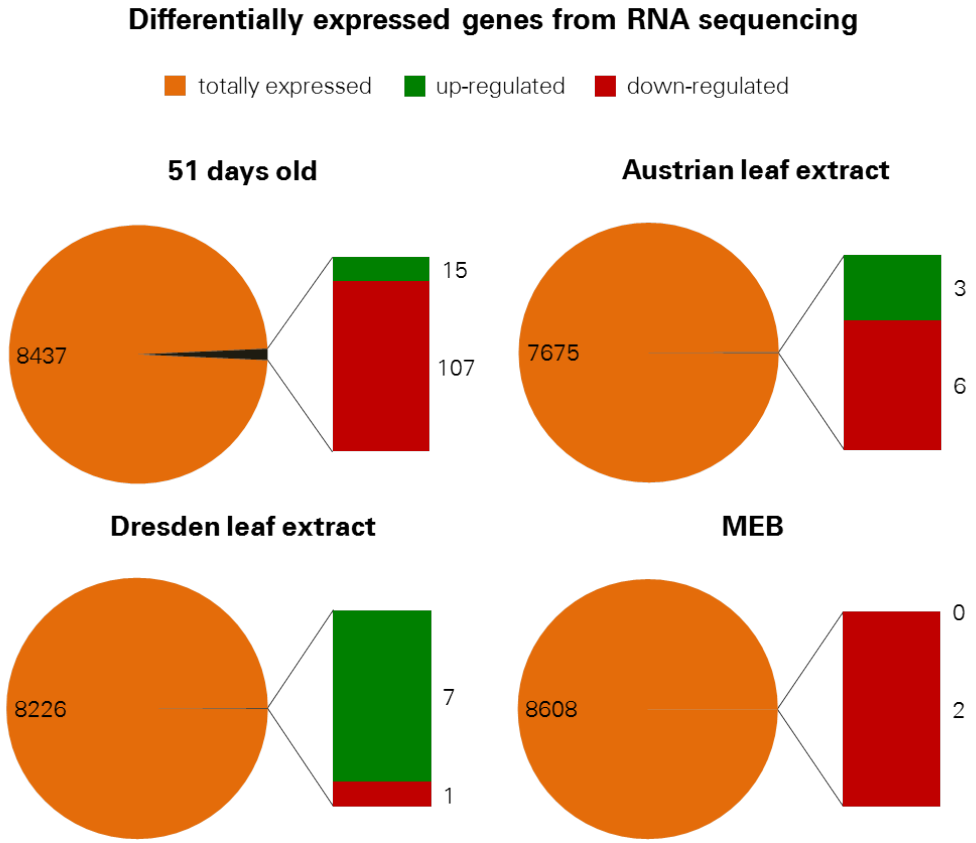

Figure 4.44: Up- and down-regulation of genes between the different conditions. Reference condition was the 21 days old *P. asterica* culture in PDB. Shown are only results with at least strong presumption against the null hypothesis ($p > 0.05$). Totally expressed genes are shown in orange, whereas the differentially expressed genes are in green (up-regulation) or red (down-regulation).

All in all, only a few genes were differentially expressed under the chosen conditions. The differentially expressed genes in the 51 days old *P. asterica* culture belonged to

different metabolic pathways and covered a wide range of different functions. Many differentially expressed genes coded for hypothetical proteins. Encoding genes were involved in cell cycle, regulation of gene expression, transport or stress response.

The *P. asterica* culture inoculated with Austrian leaf extract showed an up-regulation of different genes - a flavin-dependent monooxygenase (gene.g1622), a peroxisomal membrane protein (gene.g5259) and a histone promoter control 2 protein (gene.g8314). The down-regulated genes coded for proteins of the protein biosynthesis (gene.g642 and gene.g80), a protein of the oxidative stress response (gene.g1742) and a fungal hydrophobin protein (gene.g3074) responsible for forming of a hydrophobic coat on surfaces.

The seven up-regulated genes in the Dresden leaf extract belonged to the mitosis (gene.g679 and gene.g6567), transcription (gene.g6350), cytoskeleton (gene.g331) and a zinc-type alcohol dehydrogenase (gene.g6876). Two of them encoded hypothetical proteins (gene.g4599 and gene.g4094). The down-regulated gene was as well a hypothetical gene (gene.g8445).

Differential gene expression in the MEB culture was only seen for a hypothetical gene (gene.g9076) and a gene encoding a subunit of RNA polymerases, Rpb8 (gene.g7084). All other genes showed no differential gene expression which was statistically significant ($p < 0.05$).

No gene was found which may be involved in the astin biosynthesis even though the genome sequence showed a candidate gene for a NRPS (gene.g10100). The most differentially expressed genes in the RNA sequencing belonged to the primary metabolism.

4.8.4 Differential gene expression analysis with qPCR

A few genes of the RNA sequencing which showed a differential gene expression under the different conditions were chosen for confirmation by qPCR (Figure 4.45). The reference condition for all samples was the fungal culture grown in PDB for only 21 days. The five chosen genes were: 1622 (flavin-dependent monooxygenase), 4080 (survival factor 1 for oxidative stress, Svf1-like), 4646 (activator of stress genes 1, transcription factor), 5634 (beta subunit of a signal recognition particle receptor) as well as 8445 (hypothetical protein). Differentially regulated genes in the RNA sequencing with an at least strong presumption against the null hypothesis ($p < 0.05$) were indicated with an asterisk in the chart.

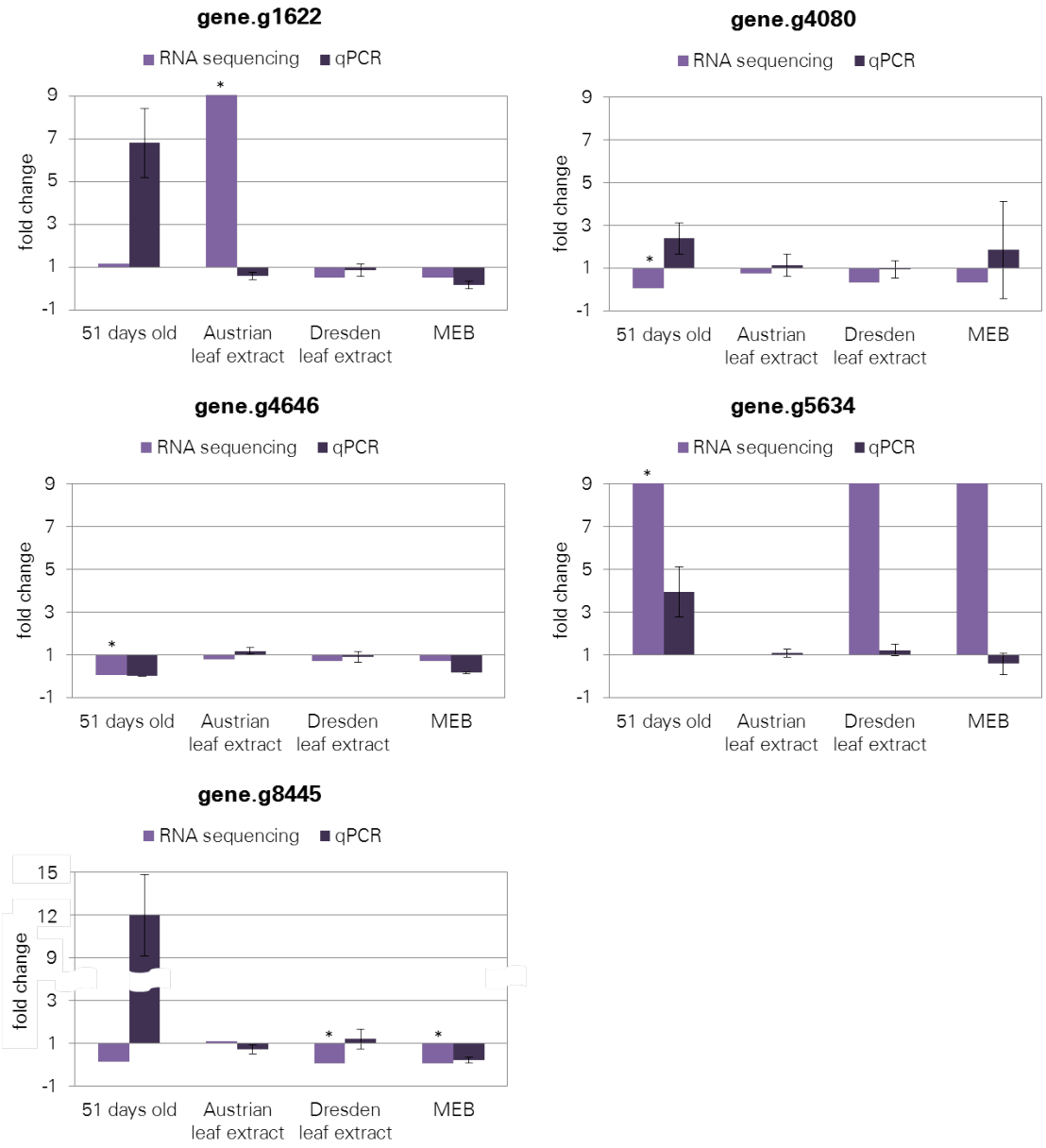

Figure 4.45: Comparison between RNA sequencing and qPCR results. Reference sample was the 21 days old *P. asterica* culture grown in liquid PDB. The RNA sequencing data with a very strong or strong presumption against the null hypothesis were indicated with an asterisk. Genes are up-regulated with a fold change > 2 and down-regulated with a fold change < 0.5. A fold change between 0.5 and 2 represents no differential expression. For a detailed explanation see text above.

The results of the qPCR analysis of the gene of a flavin-dependent monooxygenase (gene.g1622) was different from the RNA sequencing results. The gene expression of

the flavin-dependent monooxygenase was confirmed by qPCR only for the Dresden leaf extract, the gene was not regulated in this sample by both analyzes. The results of the RNA sequencing and qPCR differed in all other samples including the 51 days old, the Austrian leaf extract and MEB culture. The qPCR data showed for the the gene of the monooxygenase an up-regulation in the 51 days old culture and a down-regulation in the MEB culture. The addition of aqueous plant leaf extract of the Austrian plant did not change the expression level of this gene (qPCR). The RNA sequencing data showed for the monooxygenase gene only in the Austrian leaf extract culture a significant up-regulation. However, this up-regulation was not confirmed by qPCR. The genes of the monooxygenase in all other cultures showed in the RNA sequencing no significant differential regulation compared to the reference.

The differential expression of the survival factor 1-like gene for oxidative stress (gene. g4080) showed different results in the RNA sequencing and qPCR. The addition of plant leaf extract (Austrian leaf extract and Dresden leaf extract) did not lead to a differential expression in both analyzes. The qPCR data indicated no differentially regulation of this gene in all four samples. In contrast, the RNA sequencing data showed a strong down-regulation for the gene in the 51 days old culture which could not be confirmed with the qPCR. The survival factor 1-like gene had a high standard deviation in the gene expression of the MEB culture analyzed with qPCR. This allowed no clear prediction of a differential expression in this culture.

The gene of the stress-related transcription factor (gene.g4646, activator of stress genes 1) showed in the qPCR as well as in the RNA sequencing analyzes a very strong down-regulation in the 51 days old PDB. Furthermore, the addition of plant leaf extract did not change the expression pattern of this gene in both analyzes. Different to the results of the RNA sequencing were that the gene is not regulated in MEB culture according to the RNA sequencing data. The qPCR results indicated a strong down-regulation of this gene in the MEB culture. The gene expression of the stress-related transcription factor was inhibited by fungal aging and by growth in another medium (MEB).

The gene of a subunit of the signal recognition particle receptor (gene.g5634) showed a similar pattern in the RNA sequencing and the qPCR analyzes. An up-regulation of this gene was seen for the 51 days old culture, all other cultures showed no differential expression of the gene. The gene.g5634 was not expressed in the control culture according to the RNA sequencing data. Hence, the fold change of this gene was very high in the 51 days old culture. Both analyzes (RNA sequencing and qPCR) showed an up-regulation of this gene in the 51 days old culture. The addition of aqueous leaf extract of the Dresden cultivar (Dresden leaf extract) or the change of the medium (MEB)

did not change the expression pattern of the signal recognition receptor subunit gene. The Austrian leaf extract culture showed in the RNA sequencing no expression at all of this gene, but the qPCR data revealed an expression which was not different to the reference. Therefore, the gene of the signal recognition particle receptor subunit was expressed differentially induced by the aging of the fungal culture.

The gene encoding for a hypothetical protein (gene.g8445) showed also different results in the RNA sequencing and qPCR. The gene was down-regulated in the MEB culture according to both analyzes. The addition of Austrian leaf extract to the fungal culture did not change the expression pattern of this gene. The 51 days old and Dresden leaf extract cultures showed diverse results in the RNA sequencing and the qPCR. The gene was up-regulated in the 51 days old culture according to the qPCR data. The RNA sequencing data showed no regulation of this gene in the 51 days old culture. The addition of Dresden leaf extract to the fungal culture led to a strong up-regulation of this gene after the RNA sequencing, but the qPCR showed in this culture no regulation.

Summarizing this part, some result of the RNA sequencing were confirmed by qPCR but some remains still different. Therefore, the data of the RNA sequencing had to be confirmed by qPCR before any prediction of a gene expression could be made.

5 Discussion

With the beginning of this work, it was so far known that astins occurred in dried roots of *A. tataricus* (Morita et al., 1993a,b, 1994; Itokawa et al., 1994; Morita et al., 1995a). Some of these astins showed an antitumor activity against different human cell lines (Morita et al., 1996; Itokawa et al., 2000; Rossi et al., 2004; Saviano et al., 2004). However, only very few amounts of astins could be isolated from dried roots. Therefore, the aim of this work was to identify possible candidate genes involved in the astin biosynthesis and to express them heterologous in organ cultures of *A. tataricus* to increase the astin production.

Plants of *A. tataricus* were cultivated under different conditions: in the greenhouse or climate chamber and *in vitro* on plant medium. Astins were detected in the first year of cultivation only in the Austrian cultivar. To prove if the sterile plants of the Austrian cultivar produced astins as well, *in vitro* plants had to be generated due to the fact that no seeds were available. The *in vitro* plants of the Austrian cultivar got contaminated with a fungus during the cultivation process. This fungus was a newly, undescribed fungus named *P. asterica* able to produce astins.

5.1 A new endophytic fungus from *A. tataricus* - *Pelliciarosea asterica*

The new endophyte *P. asterica* isolated from the inflorescence axis of *A. tataricus* is phylogenetically clustered to the Stictidaceae lineage of the ostropalean fungi. The Ostropales contain lichenized and non-lichenized fungi. Non-lichenized ostropalean fungi live parasitic, saprotrophic or as parasymbionts on lichen (Sherwood, 1977a,b; Lutzoni et al., 2004; Wedin et al., 2004, 2006; Grube and Hawksworth, 2007). Nearly all Ostropales have a special type of hemioangiocarpous ascoma (Henssen, 1976, 1995; Henssen and Lücking, 2002; Grube et al., 2004; Schmitt et al., 2009) and form very small fruiting bodies (diameter under 1 mm and 0.5 mm) (Baloch et al., 2010). Therefore, they were not studied by many mycologists and not much is known about them.

The closest neighbors of *P. asterica* were listed below including some information about life style and distinguishable characters (Table 5.1). The Stictidaceae lineage of the Ostropales (including *Stictis*, *Cryptodiscus* and *Schizoxylon*) includes saprobes, parasites and optionally lichenized species (Figure 5.1). *Stictis*, *Cryptodiscus* and *Cyanodermella* are fungi living together either way with other organisms. *Sticits radiata* and *Stictis brunnescens* are living on dead material of plants whereas *Cryptodiscus gloeocapsa* and *Cryptodiscus microstomus* live in symbiosis with algae as lichen. Unfortunately, no information is available about *Cyanodermella viridula*.

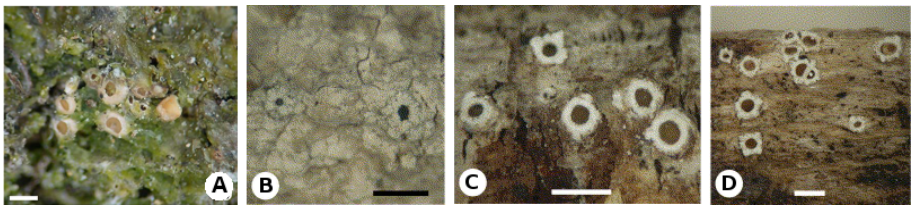

Figure 5.1: Morphology of the nearest neighbors of *P. asterica* (Wedin et al., 2006; Baloch et al., 2009). A Habitus of *Cryptodiscus gloeocapsa*. B Young fruiting bodies of *Schizoxylon albescens*. C Ascoma of *Stictis brunnescens* on wood. D *Stictis radiata* ascoma. The bar indicates 1 mm.

5.2 Astin production in *A. tataricus* by a fungal endophyte

Sixteen different astins are known so far (astin A to P) (Morita et al., 1993b; Xu et al., 2013). These astins were isolated from commercially available dried roots of *A. tataricus* obtained from different pharmaceutical suppliers. The main dichlorinated astins found in these roots varied depending on the supplier of the root material. Morita et al. (1996), Shen et al. (2011) as well as Xu et al. (2013) identified in their root material always astins A, B and C. The root material used by Liu et al. (2012) did not contain any astin A, only astin B and C were detected. Therefore, the astin profile of the roots depends on the *A. tataricus* plant used for the analysis.

Astins could be found in *A. tataricus* in all organs - roots, rhizomes, leaves and inflorescences - in different amounts. It could not be differed between astins A and B. Therefore, it is not clear if only astin A, astin B or both astins were synthesized. The astin structure shows clearly the involvement of NRPS and flavin-dependent halogenases which are so far only known from bacteria and fungi (Finking and Marahiel, 2004; Walsh, 2007; van Pée, 2001). The isolated endophytic fungus from *A. tataricus*, *P. asterica*, was able to produce some of the astins found in the host plants in culture. Two different variants

Table 5.1: Synoptic table about the nearest neighbors of *P. asterica*.

species	life style	substrate	distinguishable characters	reference
Pelliciarosea asterica	endophyte	in *A. tataricus*	no ascomata determined	own data
Cryptodiscus gloeocapsa	lichen	on bryophytes and algal mats on recently distributed soil on shaded road-cuttings on mineralized, acid soil associated with mine activity in past	no distinct periphysoids thallus crustose hyaline margin	Baloch et al. (2009)
Cryptodiscus microstomus (Stictis microstoma)		on wood of *Juniperus communis*, *Pinus sylvestris*, *Populus tremula* and *Salix caprea*		
Schizoxylon albescens	saprotroph or lichen	on dead, decorticated twigs/branches of *Populus tremula* on bark of *Populus*	large epithecium, no periphysoids margin without or a few scattered crystals	Wedin et al. (2006)
Stictis brunnescens	saprotroph	on decorticated wood/twigs of *Populus tremula* and *Salix caprea* on *Sorbus aucuparia*	straight, sparsely branched, strongly gelatinized periphysoids margin encrusted in crystals	
Stictis radiata	saprotroph	on wood of *Picea abies*, *Populus tremula*, *Salix caprea* and *Ulmus*	no pigmentation in ascoma no differentiated marginal paraphyses margin encrusted in crystals	

of astin F were detected in the plant *A. tataricus* and the fungus *P. asterica*. Further analysis has to be done to determine the differences between both variants.

The discrepancy between the plant and fungal astin profile was interesting. An explanation for this is that either the fungus produced some astins which could then be converted by the plant or the fungus was producing the other astins only when it is inside the plant.

The first assumption that the plant is using the fungal astins and thereby creating the other astins is feasible. The astins found in fungus and plant mainly differ in their chlorination and hydroxylation pattern. If *P. asterica* produces astin C, the plant *A. tataricus* might change this fungal metabolite by hydroxylation into astin A/B explaining the presence of astins A and B in *A. tataricus*. The mono- and non-chlorinated astins, occurring in plants as minor constituents, could be the attempt of the plant to detoxify and/or degrade the fungal astins when they are concentrated too high. Enzymes for hydroxylation like monooxygenases are well known in plants (see section 2.1.5.2) and not exclusively occurring in fungi. Such secondary metabolites produced by endophytes influence the plant metabolome - either beneficial or harmful. Harmful metabolites are often modified by the host plant to detoxify them or to use them in alternative pathways. Examples are the detoxification of HC-toxin produced by *Cochliobolus carbonum* on maize (Meeley and Walton, 1991; Meeley et al., 1992), fusaric acid transformation by tomato or pea plants (Kluepfel, 1957; Jost, 1965) or the degradation of fomannoxin by *Pinus sylvestris* (Zweimuller et al., 1997). The HC-toxin is produced by *Cochliobolus carbonum* as a pathogenicity factor in the interaction with maize. The HC-reductase from resistant maize plants inactivates the HC-toxin by reduction of the 8-carbonyl group. Otherwise, the HC-toxin would inhibit the histone deacetylase (Meeley and Walton, 1991; Meeley et al., 1992). The second example, fusaric acid, induces wilt in many plants (Yabuta et al., 1937; Gaumann, 1957) and is produced by different *Fusarium* species (Bacon et al., 1996). Fusaric acid-resistant plants of tomato detoxify fusaric acid into the non-toxic product N-methyl fusaric acid amide (Kluepfel, 1957). Pea (Jost, 1965), cabbage (Heitefuss et al., 1960), cotton (Jost, 1965) and tomato transform the toxic fusaric acid into the non-toxic form with different degradation rates. Kluepfel described 1957 a correlation between the degradation rate of different tomato varieties and the resistance towards *Fusarium oxysporum* f.sp. *lycopersici*. Similar to *Fusarium* species, the basidiomycete *Heterobasidion annosum* produces during the infection process of wood the phytotoxin fomannoxin which leads to severe growth inhibition in *Pinus albies*. *Pinus sylvestris* can otherwise detoxify fomannoxin into fomannoxin alcohol and shows therefore not such a strong growth retardation like *Pinus albies* (Zweimuller et al., 1997).

However, it is not only possible that *A. tataricus* modify the fungal astins but also that the fungus, once inside the plant, produces the other astins as well. *A. tataricus* would influence the metabolism of *P. asterica* and induce the synthesis of the other astins found in the plant. Different *Heterobasidion* species, for example, are able to produce the phytotoxin fomannoxin. One of them is *Heterobasidion occidentale* from *Abies*, *Tsuga* and *Pseudotsuga* which shows fomannoxin production in liquid culture (Hansson et al., 2012) but not on solid medium (Hansson et al., 2014). Two other *Heterobasidion* species which infect pine synthesize fomannoxin as well. The differences in fomannoxin production are thought to be derived from a differential gene regulation (Hansson et al., 2014).

The necessary NRPS and flavin-dependent halogenase for the astin biosynthesis would be fungal derived in both assumptions and match much better with the current knowledge that these two enzymes only occur in bacteria and fungi (Finking and Marahiel, 2004; Walsh, 2007; van Pée, 2001). Astin-free *A. tataricus* plants which were infected with *P. asterica* showed after several months detectable amounts of almost all astins found in astin-containing plants. This supports the idea that the fungus is the original producer of the astin backbone. Other aster species might be able to modify the fungal derived astins as well. Therefore, an experiment with other aster species or completely other plants could be performed next to see if these plants are able to hydroxylate the fungal astins. This would support the idea that the additional plant astins are degradation products of the fungal astins.

The phenomenon that plant-derived secondary metabolites are produced (as well) by endophytes is well known, especially for medicinal relevant metabolites (see section 2.2.1) and supports the assumption of fungal astins which are modified either by the plant or by the endophyte, once living inside the plant. Many of the known secondary metabolites found in plant and the respective endophytes are either synthesized by plant, by endophyte or by both. Paclitaxel is a secondary metabolite produced by different plants as well as different endophytic fungi (reviewed in Zhao et al. (2010)). Biosynthetic pathways of the same product are often distinct between the plant and endophyte (Chandra, 2012). The paclitaxel biosynthetic genes evolved separately in *Penicillium aurantiogriseum* and hazel (Yang et al., 2014). However, the biosynthetic enzymes can also be shared between the endophyte and the host plant (see camptothecin in Kusari et al. (2011)).

Isolated endophytes show sometimes a decreasing metabolite production during the *in vitro* cultivation. The longer the endophyte is cultivated the lower the production of the interesting secondary metabolite. *Fusarium solani* was isolated from *Camptotheca*

acuminata and lost more and more the ability to produce camptothecin during subculturing. The camptothecin synthesis was not improved by infection of the host plant followed by re-isolation of *Fusarium solani*. *Fusarium solani* uses a strictosidine synthase which is provided by the host. Therefore, the *in vitro* cultivation led to a declining camptothecin synthesis (Kusari et al., 2011). This phenomenon of a decreasing synthesis in *in vitro* cultures was not observed in *P. asterica*. The astin synthesis did not decline during the cultivation in PDB or MEB which was seen best in the RNA sequencing experiment. The fungal cultures for the qPCR showed an even higher astin production than the cultures for the RNA sequencing although they were set up one year later.

The two investigated *A. tataricus* cultivars showed different astin profiles over the time. The Austrian cultivar contained astins since it was cultivated in the greenhouse and climate chamber. The Dresden cultivar showed first no detectable astins in plants after sowing them in pots or in plants grown in the botanical garden. These plants developed detectable amounts of astins during the cultivation in the greenhouse and climate chamber over the time. The investigation of the astin profile of astin-free plants (cultivar Dresden) from the botanical garden in the greenhouse over the time showed that during and after the winter months the astin production in some of these plants was induced. The pot size did not play an important role for the induction of the astin biosynthesis. Due to the fact that *A. tataricus* is a perennial the leaves were dying in the early winter months and the insects like thrips and flies had no problem to attack the weak plants. Hence, the biotic stress might be a trigger to induce the astin biosynthesis.

P. asterica seems to produce more astins when it is growing in a stressful environment. The growth experiments showed that *P. asterica* produced in ethanol containing cultures more astins even if *P. asterica* was growing slower as in the corresponding water samples. This and the fact that the Dresden cultivar showed only after cultivation for three years a detectable astin production indicates that *P. asterica* might produce astins as stress response. Several fungi respond to abiotic and biotic stress with an increased production of secondary metabolites. Cell suspension cultures of *Taxus chinensis* were treated with an fungal elicitor to induce oxidative stress. This led to an accumulation of paclitaxel in the cells (Yu et al., 2002). *Pestalotiopsis microspora* - an endophyte of rainforest trees like *Torreya taxifolia* or *Taxus brevifolia* - produces different secondary metabolites (e.g. pestalotiopsins A and B) dependent on the environmental conditions of the host plant (Strobel et al., 2004). Endophyte-infected tall fescue plants contain different insecticides produced by their fungal endophytes. The concentration of two of them (peramine and lolitrem B) is influenced by temperature. The production of the toxic alkaloid ergopeptine is dependent on the nutrient status of the tall fescue. High levels

of nitrogen support the production of ergopeptine in tall fescue plants infected with endophytes (reviewed in Latch (1993)). But not only endophytic fungi can increase their production of secondary metabolites, endophytic bacteria do this as well. *Pseudomonas fluorescens* from *Catharanthus roseus* produces the antihypertensive drug ajmalicine which is used against high blood pressure. The production of ajmalicine is increased by *Pseudomonas fluorescens* in drought stressed plants (Jaleel et al., 2007).

Further experiments has to be performed to highlight the influence of biotic and abiotic stressors to the astin production in *A. tataricus* and *P. asterica*.

5.3 Synthesis of astins by *P. asterica*

Different enzymes are necessary to synthesize astins (see section 2.1.5 and Figure 2.2): NRPS as well as flavin-dependent halogenase.

Different approaches were performed to find a flavin-dependent halogenase. The PCR search in *A. tataricus* with primers of known or putative halogenases revealed no candidate, neither did the Southern blot and the screen of the cDNA library. After the isolation of *P. asterica* from the astin producing *A. tataricus* plant, it is clear why no halogenase could be isolated from the plant. As discussed above, *P. asterica* seems to synthesize the astin backbone. Due to the high similarity of the two different cyclic pentapeptides (astins from *A.tataricus* respectively *P. asterica* and cyclochlorotine from *T. islandicus*) it can be assumed that the involved halogenases are similar in structure and sequence.

Despite the correlation in the structure of the two cyclic pentapeptides and in the two conserved motifs, no halogenase candidate gene was found in the fungus *P. asterica* neither with the bacterial halogenase primers nor with the halogenase primers from *T. islandicus*. The genome sequence of *P. asterica* surprisingly did not seem to contain a halogenase gene.

In contrast to that, a NRPS candidate gene (gene.g10100) was found in *P. asterica* which is currently characterized (T. Schafhauser, personal communication).

The three dichlorinated astins A, B and C share the same basic structure except a hydroxylation at the second or fifth amino acid. These hydroxylations make the difference between these three astins. *P. asterica* synthesized only astin C in *in vitro* cultures which is not hydroxylated at the second and fifth amino acid. Morita et al. (1993b) isolated all three dichlorinated astins from *A. tataricus*. The hydroxylation is either done by *P. asterica* or by *A. tataricus*. *P. asterica* was fed with L-threonine which is a precursor

of the hydroxylated second and fifth amino acid to see if *P. asterica* is able to use L-threonine instead of α-aminobutyric acid in the biosynthesis of astin C. *P. asterica* was not able to use L-threonine to produce astins A or B. Therefore, it seems that the hydroxylation at the astins A and B is done after the astin synthesis, either by the plant or by the fungus once inside the plant. Such a modification of fungal secondary metabolites by the plant is seen in the detoxification (see above). The fungus can also modify the synthesized fungal astins to metabolize them or to convert them into more active forms.

5.4 Growth of *P. asterica* in culture

P. asterica grew during the first months after isolation very poorly in culture. Growth experiments shortly after the isolation (like the experiment with different plant extracts in May 2013, see section 4.3.2) showed that *P. asterica* did not grow detectable within one month. After half a year, growth of P. asterica was detectable within one month (see sections 4.3.2 and 4.8.1). The different variability tests (section 4.3.3) showed - in continuation with the prior experiments - an enhancement in the growth of *P. asterica* in summer and autumn 2014. The growth experiment on plates with *P. asterica* during the winter 2015 (seen in section 4.3.4) indicated that *P. asterica* was now well adapted to the *in vitro* conditions and that growth within one month was now measurable.

Plant-associated microorganisms were found in plant fossils and therefore believed to evolve together with the appearance of higher plants (Taylor and Taylor, 2000). This long co-existence of endophytes and host-plants led to a strong adaptation of the endophytes to their plant environment by genetic variation (e.g. the integration of plant DNA into their own genome) and vice versa (Stierle et al., 1993). A consequence of this genetic adaptation is the complex interaction of the biochemical metabolisms between plant and endophyte (Strobel, 2003). The endophyte is therefore adapted on the plant metabolism. If, for example, the fungal endophyte is now isolated from the plant, the fungus needs some time to adapt its metabolism to the new environment. The new environment - in this case the fungal growth media - provide not the optimal growth conditions as in the plant. Temperature, pH, nutrient supply and others vary between the plant and the fungal growth media. This effect on shortly isolated endophytes which grows in culture very slowly is long known. *Acremonium coenophialum* was isolated from tall fescue (Bacon et al., 1977). Due to the slow grow (Clark et al., 1983) Davis and colleagues improved the growth medium for *Acremonium coenophialum* to enable

further investigations on the fescue toxicosis (Davis et al., 1986). Some fungi might hardly adapt to the new environment or grow slowly also in the natural environment. *Undifilum oxytropis*, for example, is a slow growing endophytic fungus isolated from *Oxytropis* spp. locoweed plants (Pryor et al., 2009; Yu et al., 2010b) and causes toxicosis in grazing animals (Braun et al., 2003). The slow growth of endophytes is often seen together with asexual reproduction over the seeds of the host plant (White et al., 1991). Such slow growing endophytes can be missed during the isolation of endophytes from plants because they will be overgrown and repressed by faster growing endophytes like *Aspergillus* (Davis et al., 1986).

5.5 Biofertilization of phosphates and production of exoenzymes by *P. asterica*

The endophytic fungus *P. asterica* was able to mobilize different phosphate sources like hydroxylapatite and iron(III) phosphate. The phosphates made available can be used by *A. tataricus*. *P. asterica* used hydroxylapatite superior to iron(III) phosphate. Due to the rapid mobilization of hydroxylapatite, *P. asterica* grew faster as on the control plate without any phosphate. The solubilization of iron(III) phosphate from the substrate was not as simple as for the hydroxylapatite. Hydroxylapatite is usually the phosphate source which is faster solubilized from the substrate than iron(III) phosphate. *Aspergillus niger* strain An2 solubilized up to 900 mg/l hydroxylapatite within three days, whereas only 215 mg/l of iron(III) phosphate was solubilized within five days (Li et al., 2015). Another *Aspergillus niger* strain FS1 was able to solubilize 71 % of hydroxylapatite but only 36 % of the iron(III) phosphate (de Oliveira Mendes et al., 2013). *Penicillium radicum* showed as well a faster and better solubilization of hydroxylapatite than of the hardly soluble iron(III) phosphate (Whitelaw et al., 1999).

P. asterica had to use more energy to metabolize iron(III) phosphate as to grow without phosphate. Therefore, *P. asterica* grew slower on the iron(III) phosphate source. Organisms which use additional pathways (for example for additional nutrients) grow slower than microorganisms without using such a pathway. The respective microorganisms have to put energy into such a metabolic pathway which is then not available for growth. This phenomenon is known amongst others in the bacterium *E. coli*. Vector carrying bacteria grow slower as cells without an additional vector because they have to replicate the vector which is energy-consuming (Seo and Bailey, 1985). If microorganisms are able to use a pathway which produces additional energy then they grow faster as the

ones which cannot use such a pathway.

Phosphate is essential for plants and only available for plants in low concentrations (Zou et al., 1992). Therefore, plants inhabiting endophytes which make phosphates available for the plant have benefits against other plants. Many different species are known to solubilize phosphate. Mentioned are here the most important genera: *Bacillus*, *Pseudomonas*, *Aspergillus*, *Penicillium* (Whitelaw, 1999; Ben Farhat et al., 2009; Khan et al., 2010; Viruel et al., 2011). *P. asterica* supports most likely *A. tataricus* with additional phosphate and will get in change more polysaccharides and other useful substances.

The proteases which were produced by *P. asterica* degrade animal proteins like casein (in skim milk) or gelatin. Proteases are used among others to prevent a phytopathogen attack. *Stenotrophomonas maltophilia* uses proteases to protect sugar beet from *Pythium ultimum* (Dunne et al., 1997). Many phytopathogenic fungi use proteases during the infection of plants like *Verticillium dahliae* (Dobinson et al., 1997), *Sclerotia sclerotium* (Billon-Grand et al., 2002) or *Fusarium eumartii* (Olivieri et al., 2002). *Fusarium eumartii* uses an extracellular serine protease to degrade pathogenesis related proteins produced by the plant as part of the systemic acquired resistance (Olivieri et al., 2002). Thus, proteases can be used for different purpose. The exact function of the proteases found in *P. asterica* needs to be analyzed in further experiments.

5.6 Antibiosis by *P. asterica* against other fungi

P. asterica inhibited the growth of several fungi (see section 4.4.3). The inhibition of different wood decaying fungi (*Bjerkandera adusta*, *Schizophyllum commune* and others) can prevent *A. tataricus* from damage. These fungi are able to degrade cellulose (brown rot) and lignin (white rot) and can act also on living plant parts (e.g. *Phellinus pini* in living conifers, Blanchette (1980)). Wood decaying fungi attack the heartwood of trees by direct penetration (*Armillaria* spp.) or through lesions and wounds (*Chondrostereum purpureum*, *Stereum gausapatum*) (Pearce, 1996)). *P. asterica* inhibits these fungi possible to prevent degrading of ligneous plant tissue (e.g. inflorescence axis). The substances produced by *P. asterica* in the living plant organs would therefore prevent the spreading of wood decaying fungi in *A. tataricus*.

Antifungal activity against wood-decaying fungi by other fungi is also known from other organisms. *Trichoderma* sp., for example, produces volatile organic compounds which show fungicidal and fungistatic effects against wood decaying fungi (Bruce et al., 1984). Not only endophytes but also plants produce specific substances to inhibit the decay of

cellulose or lignin by wood decaying fungi. Cinnamon (*Cinnamomum osmophloeum*) produces different oils (especially cinnamaldehyde) which inhibit the growth of *Coriolus versicolor* and *Laetiporus sulphureus* (Wang et al., 2005). Stilbenes and polyphenols inhibit wood-decaying fungi in *Eucalyptus sideroxylon* (Hart and Hillis, 1974). *Quercus alba* uses ellagitannins to prevent damage through wood decaying fungi (Hart and Hillis, 1972).

However, not only wood decaying fungi are inhibited by *P. asterica*. Phytopathogens like *Fusarium culmorum* or *Macrophomina phaseolina* were as well inhibited by *P. asterica*. The antimycotic effect of phytopathogens which would degrade *A. tataricus* is seen by many different endophytic fungi. The antimycotic activity against phytopathogens prevents the living environment of the endophyte. *Collophora aceris* from Douglas maple produces collophorin which affects the growth of phytopathogens like *Pythium ultimum*, *Phytophthora cinnamomi* or *Rhizoctonia solani* (Xie et al., 2013). Cryptocandin is an antimycotic from *Cryptosporiopsis* cf. *quercina*, an endophyte of hardwood species in Europe (Strobel et al., 1999). Endophytes from *Artemisia annua* influence differentially phytopathogenic fungi of crops (Liu et al., 2001).

Beside wood decaying and phytopathogenic fungi, there are endophytes which were also inhibited by *P. asterica*. Other possible endophytes vie with *P. asterica* for their habitat, therefore *P. asterica* tried to prevent the colonization of *A. tataricus* by other endophytes (seen in the inhibition of *Acremonium alternatum*, *Chaetomium globosum*, *Metarhizium anisopliae* and *Piriformospora indica*). Endophytes are known to prevent the infection of the host plant by other endophytes. *Acremonium* sp. inhibits the colonization by mycorrhizal fungi (Chu-Chou et al., 1992) and endophytic bacteria prevent the early colonization of rice by *Azospirillum brasilense* (Bacilio-Jiménez et al., 2001).

P. asterica inhibited different fungi depending on the growth substrate. The interaction assay on MEA showed different results than on PDA (see section 4.4.3). *P. asterica* grew better and faster on MEA whereas the growth on PDA was slower and more compact. Hence, *P. asterica* seems to produce different compounds if its growing on different media. Due to different metabolite spectra on MEA and PDA, *P. asterica* inhibited specific fungi differently. *Trichoderma* sp. produces different compounds as well which act more or less as antimycotic agents (Wheatley et al., 1997). *Trichoderma* sp. produced volatiles on malt extract agar and minimal medium. The volatiles from the minimal medium did not have any effect on the wood decaying fungi, whereas the volatiles from the malt extract agar inhibited the tested fungi.

If *P. asterica* influenced other fungi, then other fungi influenced *P. asterica* for the

same reasons (seen for example with *Gloeophyllum sepiarium*, *Trichoderma* sp. or *Fusarium culmorum*). Microorganisms compete with other microorganisms for habitat, nutrition and reproduction. Therefore, antibiotic compounds not only known from endophytes are widely known and used in the pharmaceutical industry like penicillin or griseoflavin (reviewed in Bennett (1998)). *P. asterica* is a member of a big community of microorganisms, especially endophytes, which fight for their exclusive survive within their host plant and support the plant by defending against different attacks.

5.7 *P. asterica* moves from roots into rhizomes as well as seeds

Astins were not equally distributed in the plant organs similar to the distribution of *P. asterica*. The astin levels and the fungus did not coincide in the different organs of the two *A. tataricus* cultivars (Figure 5.2). The highest concentration of astins could be found in roots, whereas the highest concentration of fungal DNA was found in the above-ground parts and rhizomes. The Dresden cultivar of *A. tataricus* showed the highest concentration of fungal DNA in the rhizomes, whereas the leaves and the inflorescence showed a moderate accumulation of fungal DNA. All three organs showed a moderate astin level. The Austrian cultivar showed the highest concentration of fungal DNA in the leaves and in the inflorescence, while the rhizomes contained only small amounts of *P. asterica*. The astin profile of these three plant organs of the Austrian cultivar is comparable to that of the Dresden cultivar. The difference between both cultivars is that the Dresden cultivar showed much higher astin concentrations in the roots than the Austrian cultivar.

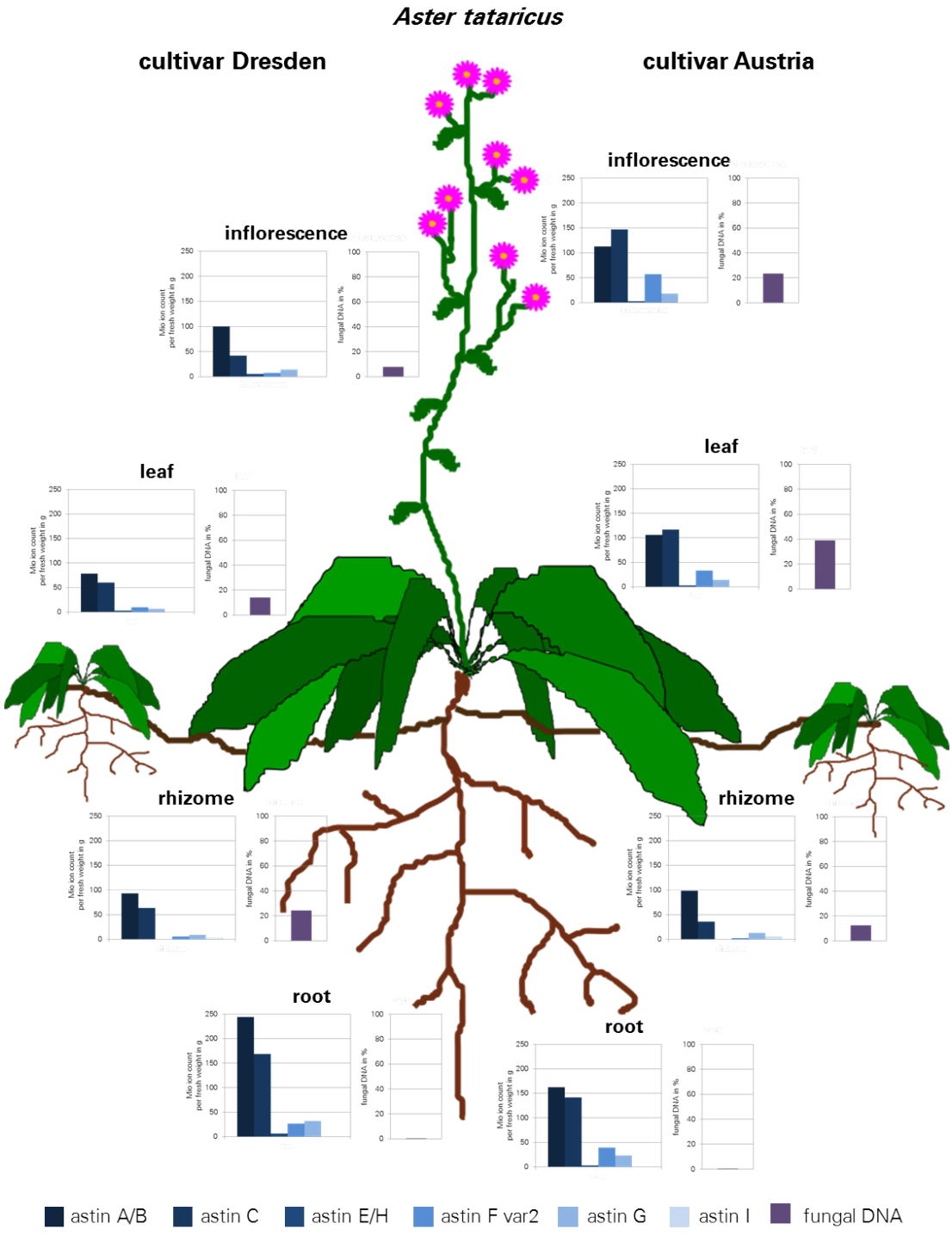

Figure 5.2: Distribution of astins and fungal DNA in the plant organs of both cultivars of *A. tataricus*. Both *A. tataricus* cultivars showed similar patterns in the distribution of astins and fungal DNA in the whole plant. However, the astin level and the fungal DNA did not coincide. The roots showed the highest concentration of astins but the lowest content of fungal DNA. For more details see text.

P. asterica was moving into the leaves and inflorescence possibly to infect the seeds of *A. tataricus* and to spread thereby over the seeds. Seed-borne endophytes, which were transmitted vertically by the seed coats (Redman et al., 2002), are known from other plants like *Dichantelium lanuginosum*. The methylotrophic bacterium *Curtobacterium plantarum* is a seed-borne endophyte in soybean and corn (Dunleavy, 1989). Diazotrophic bacteria in sugar cane, rice, wheat, sorghum and other crops spread from generation to generation as well by the seeds of the host plant (James and Olivares, 1998). However, endophytes are known not only to use the host for reproduction but also to produce sexual spores. The grass endophytes *Epichloë* sp. is transmitted not only vertically via seeds (asexual form known as *Neotyphodium* sp.) but also horizontally with sexual spores through infected host tissue (sexual form known as *Epichloë*) (Freeman, 1904; Sampson, 1933). Both forms appear in the *Poaceae* as a continuum from mutualism (*Neotyphodium*) to antagonism (*Epichloë*) (Ahlholm et al., 2002; Schardl et al., 2004)). Another example for this life form is *Fusarium moniliforme* in maize. *Fusarium moniliforme* is transmitted horizontally through insects and soil debris and vertically by infecting the seeds (reviewed in Bacon et al. (2001)).

It is not clear if *P. asterica* - once the leaves and inflorescence wither during the late autumn - withdraw into the roots of *A. tataricus* surviving during the winter in the soil and/or if *P. asterica* is delivered into the soil during the decay of the plant material and survives in the soil. Usually, when plant parts die the endophytic fungus emerges rapidly and sporulates on the dying tissue (Weber et al., 2004). But no such structure could be observed on the decaying leaves of *A. tataricus* - neither on the Austrian nor on the Dresden cultivar. Thus, *P. asterica* might be transmitted vertically by rhizomes and possibly by seeds of *A. tataricus*. *A. tataricus* is spreading mainly over its rhizomes, therefore it is useful for *P. asterica* to use the same way.

It was shown that *P. asterica* could infect the *A. tataricus* cultivar Dresden over the roots. However, it is not known if this also happens *in vivo*. The fungus used for the infection of the *A. tataricus* plants was long cultivated *in vitro* in shaking culture and was therefore adapted to an environment outside the plant. The fungus living inside the plant is only adapted to the plant environment and was growing very, very slowly in culture (what was detected at the beginning of the cultivation on usual fungal media). Hence, it is not clear if *P. asterica* can infect *A. tataricus* in the natural environment over the roots. Other fungi are known to infect their host plants over the roots. The root endophyte *Piriformospora indica* from orchid plants develops appressoria after root contact. The endophytic fungus colonizes the cortex cells inter- and intracellularly (Varma et al., 1999). After infection of plant roots with *Acremonium alternatum*, the fungus can

also be detected in the leaves of these plants (Hodges and Campbell, 1998; Doan et al., 2010; Jäschke et al., 2010).

Latch et al. (1984) detected hyphae of *Acremonium* endophytes only in stem and leaf tissue, no mycelia was microscopically visible in roots of infected plants. *Acremonium lolii* was found during the vegetative growth mainly in the leaf sheath of perennial ryegrass as well as in the crown and pseudostem. During the reproductive growth, *Acremonium lolii* was detected predominantly in the crown (Musgrave and Flechter, 1984). The endophyte was withdrawn into the rhizomes and was also found in the crown during the dormancy of the plant (reviewed in Breen (1994)). *P. asterica* showed a similar distribution of fungal DNA (see section 4.5.1) as described for the mycelia of *Acremonium lolii*.

The discrepancy in astin concentration and detection of fungal DNA indicates that *P. asterica* moves from the roots into the above-ground parts of *A. tataricus*. The fungal astins might be produced in the above-ground parts as well as the rhizomes and then transported somehow back into the roots. This would also explain the higher astin concentration in the roots of the Dresden cultivar. If the fungus is most present in the rhizomes (cultivar Dresden) then the transport way of the astins is not as long as if they would be transported from the leaves into the roots (cultivar Austria). To elucidate a possible transport way of astins in *A. tataricus*, further experiments are needed.

The question arises if astins can be transported in *A. tataricus* and which way they use. Astins are soluble in water which was used for the extraction from fresh plant tissue (see section 3.7). Moreover, *P. asterica* secreted many of the fungal astins into the liquid culture. Due to the water solubility it is possible to transport astins in the phloem from source to sink. It is known from arbuscular mycorrhiza that secondary metabolites of plants like catapol is transported into the fungal partner during a fungivore attack to protect the mycelium (Duhamel et al., 2013).

Once the fungus is moving up into the leaves and - if existing - the inflorescence, astins and maybe other metabolites are transported back into the roots. What the astins do in the roots remains up to know unclear. A possible explanation is an antimicrobial activity against root pathogens and competing organisms. Podophyllotoxin as example has among others antiviral and antibacterial effects (Eyberger et al., 2006). The tropical tree *Theobroma cacao* was infected with different endophytes and showed reduced damage caused by *Phytophthora* sp. (Arnold et al., 2003). *Acremonium* and other endophytes protect turf grasses against different insect species (Breen, 1994).

Further work has to be done on this issue to illuminate the questions after the life cycle

of *P. asterica* and the use of astins for *A. tataricus* and *P. asterica*.

5.8 RNA sequencing

The addition of plant leaf extract from *A. tataricus* led in former cultivation to an increase in the astin production (see sections 4.3.1 and 4.3.2). Therefore, *P. asterica* was set up with the leaf extracts of the two different *A. tataricus* cultivars to find in the up-regulated genes of these cultures possible astin biosynthesis candidate genes. The 51 days old culture and the MEB culture were chosen to see what happens when *P. asterica* is cultivated in another growth medium and when *P. asterica* is getting older in culture.

An increase in astin production would correlate with an up-regulation of the astin biosynthesis genes. The genome sequencing of *P. asterica* revealed one NRPS candidate gene (gene.g10100) which might be involved in the astin biosynthesis. However, the genome of *P. asterica* was screened for a flavin-dependent halogenase candidate gene but none was found.

Surprisingly, the addition of plant leaf extract or the change of the growth medium from PDB to MEB did not change the expression of many genes. Only a few genes were differentially regulated in these cultures which belonged in the most cases to the primary metabolism. Transcription/translation, amino acid biosynthesis or replication were just examples for the processes in which the differentially regulated genes were involved. In contrast to that, the 51 days old culture showed much more differentially expressed genes in which most of them were down-regulated. Again, the regulated genes in the 51 days old culture belonged in most cases to the primary metabolism like protein biosynthesis, cell cycle, transport or stress response. A large bulk of the differentially expressed genes remained hypothetical. It is possible that genes involved in the astin biosynthesis were hidden in these hypothetical proteins.

The data of the RNA sequencing had to be verified due to the fact that only one replicate per condition was sequenced. The analyzes of five different genes by qPCR showed that not all data of the RNA sequencing could be confirmed by qPCR. One explanation might be the time-lag between the harvest of the RNA sequencing and the qPCR samples. *P. asterica* was better adjusted to the culture conditions in the qPCR samples than one year before the cultures of the RNA sequencing.

RNA sequencing and qPCR are different methods to determine the gene expression, here, in different cultures of *P. asterica*. The RNA sequencing revealed genes which were up-regulated, down-regulated or not regulated. Only five genes were analyzed

by qPCR in all five cultures. 65 % (13 out of 20 culture/gene combinations) of these analyzed genes in all cultures could be confirmed by qPCR. Only 35 % (7 out of 20 culture/gene combinations) of the RNA sequencing data of the respective genes could not be confirmed by qPCR (Table 5.2).

Table 5.2: Correlation of fold change between RNA sequencing and qPCR.

direction of change	RNA sequencing	confirmed by qPCR	not confirmed by qPCR
not regulated	14	10	2 (up-regulated) 2 (down-regulated)
up-regulated	2	1	1 (not regulated)
down-regulated	4	2	1 (up-regulated) 1(not regulated)

Dallas et al. (2005) investigated the correlation between microarray and qPCR data of 48 human genes. They found a strong correlation between the microarray data and the following qPCR: 67 to 69 % of the analyzed genes could be confirmed by qPCR. The direction of the differential gene expression - if the genes were up- or down-regulated - were predicted very accurately with both methods (Dallas et al., 2005). Morey and colleagues analyzed 2006 also the correlation between microarray and qPCR data of different mouse and human tissue. The direction of gene expression change was the same for 72.9 % of the samples (202 out of 277). 78.7 % of the samples which did not have the same direction of change showed only minor changes (< 1.4 fold) in the gene expression level in both methods (Morey et al., 2006). These data show comparable results for the correlation between microarray and qPCR data. Information about the correlation between RNA sequencing and qPCR are not available so far.

RNA sequencing and qPCR use different methods for the normalization of their data. ReadXplorer (Hilker et al., 2014) uses the DEseq package (Anders and Huber, 2010) which normalize the expression data using the binomial distribution (Anders and Huber, 2010). The qPCR in contrast uses different reference genes to quantify the expression level to a certain set of reference genes. In this experiment, only one reference gene which showed no regulation during the RNA sequencing was used due to the fact that no other typical fungal reference genes were found in the genome of *P. asterica*. The qPCR with the cDNA of the different cultures should be repeated to confirm the first results as soon as other typical fungal reference genes are identified in *P. asterica.*

Concluding this, RNA sequencing data has to be verified by a complementary method like qPCR. Data of both methods have to be properly filtered and analyzed, keep in mind that RNA sequencing and qPCR use different methods for normalization of the data.

6 Summary and outlook

The ostropalean fungus *P. asterica* is an endophyte from *A. tataricus*. *P. asterica* is able to produce some of the astins found in *A. tataricus*. These astins are believed to be the backbone of the other plant-derived astins. There are two possibilities: first, *A. tataricus* uses the fungal astins and modify them or second, *P. asterica* is only producing the other astins once it is inside the plant. NRPS and flavin-dependent halogenase are necessary enzymes for the astin biosynthesis. An NRPS candidate gene was found in *P. asterica*, but up to now no halogenase candidate gene. *P. asterica* is present more in the above-ground organs but the highest astin concentrations are found in the roots. Therefore, astins seems to be transported from source to sink.

Beside the astin production *P. asterica* supports *A. tataricus* also with other "services": *P. asterica* utilize different phosphate source and inhibits the growth of phytopathogenic and wood decaying fungi. *P. asterica* inhibits the growth of other competing endophytes as well as to protect its shelter.

Further work has to be done to understand the interaction between *P. asterica* and *A. tataricus*. Two major challenges arise from the results: at the one hand the understanding of the endophytic life style including how *A. tataricus* is supported by *P. asterica* and at the other hand the elucidation of the astin biosynthesis as well as the benefit of astins for *P. asterica* and *A. tataricus*. Until now, a plant of *A. tataricus* does not exist which contains no endophyte. Therefore, it is difficult to investigate the benefits of the astin production for *A. tataricus*.

The stabilization of other substrate like sulfates or nitrogen or the use of exoenzymes gives insights into the support of *A. tataricus*. The cellulase assay has to be repeated to get a clear evidence if *P. asterica* is producing extracellular cellulases. Lipases and hemicellulases are also interesting exoenzymes used by fungi to penetrate plant tissue. The detection of *P. asterica* in different plant organs should be repeated with at least two replicates of each plant cultivar to confirm the first results. Additional *A. tataricus* plants from other independent sources will be analyzed. To locate *P. asterica* inside *A. tataricus*, the fungus can be labeled with GFP to detect *P. asterica* with the help of a fluorescence microscope.

The search for a halogenase gene candidate and as well of other biosynthetic genes like monooxygenases should be continued to find the other genes of the astin biosynthesis. Some factors seems to induce the astin biosynthesis *in planta*, therefore, enhancers and inhibitors may play a role in the different astin distributions in the various cultivars. These enhancers can then be used to induce the astin biosynthesis in *P. asterica* cultures for future production strategies of the astins.

List of Figures

List of Tables

Bibliography

Aerts, J. M. F. G., Boot, R. G., and Renkema, G. H. 1996. Chitotriosidase: A human macrophage chitinase that is a marker for Gaucher disease manifestation. In Muzzarelli, R., editor, *Chitin enzymology*, pages 3–10. Atec Edizioni-Grottammare, 2 edition.

Agrawal, T. and Kotasthane, A. S. 2012. Chitinolytic assay of indigenous *Trichoderma* isolates collected from different geographical locations of Chhattisgarh in Central India. *SpringerPlus*, 1(73):1–10.

Ahlholm, J. U., Helander, M., Lehtimaki, S., Wali, P., and Saikkonen, K. 2002. Vertically transmitted fungal endophytes: Different responses of host-parasite systems to environmental conditions. *Oikos*, 99(1):173–183.

Anders, S. and Huber, W. 2010. Differential expression analysis for sequence count data. *Genome Biology*, 11(10):R106.

Apweiler, R., Bairoch, A., Wu, C. H., Barker, W. C., Boeckmann, B., Ferro, S., Gasteiger, E., Huang, H., Lopez, R., Magrane, M., Martin, M. J., Natale, D. A., O'Donnovan, C., Redaschi, N., and Yeh, L. L. 2004. UniProt: The universal protein knowledgebase. *Nucleic Acids Research*, 32(1):D115–D119.

Archer, D. and Peberdy, J. 1997. The molecular biology of secreted enzyme production by fungi. *Critical Reviews in Biotechnology*, 17(4):273–306.

Arima, K., Imanaka, H., Kousaka, M., Fukuta, A., and Tamura, G. 1964. Pyrrolnitrin, a new antibiotic substance, produced by *Pseudomonas*. *Agricultural and Biological Chemistry*, 28(8):575–576.

Arnold, A. E., Mejía, L. C., Kyllo, D., Rojas, E. I., Maynard, Z., Robbins, N., and Herre, E. A. 2003. Fungal endophytes limit pathogen damage in a tropical tree. *Proceedings of the National Academy of Sciences of the United States of America*, 100(26):15649–15654.

Bacilio-Jiménez, M., Aguilar-Flores, S., del Valle, M., Pérez, A., Zepeda, A., and Zenteno, E. 2001. Endophytic bacteria in rice seeds inhibit early colonization of roots by *Azospirillum brasilense*. *Soil Biology and Biochemistry*, 33(2):167–172.

Bacon, C., Porter, J., Norred, W., and Leslie, J. 1996. Production of fusaric acid by *Fusarium* species. *Applied and Environmental Microbiology*, 62(11):4039–4043.

Bacon, C. W., Porter, J. K., Robbins, J. D., and Luttrell, E. S. 1977. *Epichloë typhina* from toxic tall fescue grasses. *Applied and Environmental Microbiology*, 34(5):576–581.

Bacon, C. W., Yates, I. E., Hinton, D. M., and Meredith, F. 2001. Biological control of *Fusarium moniliforme* in maize. *Environmental Health Perspectives*, 109 Suppl:325–332.

Baloch, E., Gilenstam, G., and Wedin, M. 2009. Phylogeny and classification of *Cryptodiscus*, with a taxonomic synopsis of the Swedish species. *Fungal Diversity*, 38:61.

Baloch, E., Lücking, R., Lumbsch, H., and Wedin, M. 2010. Major clades and phylogenetic relationships between lichenized and non-lichenized lineages in Ostropales (Ascomycota: Lecanoromycetes). *Taxon*, pages 1483–1494.

Bartsch, M., Gobbato, E., Bednarek, P., Debey, S., Schultze, J. L., Bautor, J., and Parker, J. E. 2006. Salicylic acid-independent ENHANCED DISEASE SUSCEPTIBILITY1 signaling in Arabidopsis immunity and cell death is regulated by the monooxygenase FMO1 and the Nudix hydrolase NUDT7. *The Plant Cell*, 18(4):1038–1051.

Bashan, Y. 1998. Inoculants of plant growth-promoting bacteria for use in agriculture. *Biotechnology Advances*, 16(4):729–770.

Ben Farhat, M., Farhat, A., Bejar, W., Kammoun, R., Bouchaala, K., Fourati, A., Antoun, H., Bejar, S., and Chouayekh, H. 2009. Characterization of the mineral phosphate solubilizing activity of *Serratia marcescens* CTM 50650 isolated from the phosphate mine of Gafsa. *Archives of microbiology*, 191(11):815–824.

Bennett, J. 1998. Mycotechnology: The role of fungi in biotechnology. *Journal of Biotechnology*, 66(2-3):101–107.

Billon-Grand, G., Poussereau, N., and Fevre, M. 2002. The extracellular proteases secreted *in vitro* and in planta by the phytopathogenic fungus *Sclerotinia sclerotiorum*. *Journal of Phytopathology*, 150(8-9):507–511.

Blanchette, R. A. 1980. Wood decomposition by *Phellinus (Fomes) pini*: A scanning electron microscopy study. *Canadian Journal of Botany*, 58(13):1496–1503.

Braun, K., Romero, J., Liddell, C., and Creamer, R. 2003. Production of swainsonine by fungal endophytes of locoweed. *Mycological Research*, 107(8):980–988.

Breen, J. P. 1994. *Acremonium* endophyte interactions with enhanced plant resistance to insects. *Annual Review of Entomology*, 39(1):401–423.

Brockmann, H., Haschad, M., Maier, K., and Pohl, F. 1939. Hypericin, the photodynamically active pigment from *Hypericum perforatum*. *Naturwissenschaften*, 32:550.

Bruce, A., Austin, W., and King, B. 1984. Control of growth of *Lentinus lepideus*

by volatiles from *Trichoderma*. *Transactions of the British Mycological Society*, 82(3):423–428.

Buzina, W. and Lang-Loidolt, D. 2001. Development of molecular methods for identification of *Schizophyllum commune* from clinical samples. *Journal of Clinical Microbiology*, 39(7):2391–2396.

Caboche, S., Pupin, M., Leclère, V., Fontaine, A., Jacques, P., and Kucherov, G. 2008. NORINE: A database of nonribosomal peptides. *Nucleic Acids Research*, 36:D326–D331.

Chandra, S. 2012. Endophytic fungi: Novel sources of anticancer lead molecules. *Applied Microbiology and Biotechnology*, 95(1):47–59.

Chau, M. and Croteau, R. 2004. Molecular cloning and characterization of a cytochrome P450 taxoid 2alpha-hydroxylase involved in Taxol biosynthesis. *Archives of Biochemistry and Biophysics*, 427(1):48–57.

Chau, M., Jennewein, S., Walker, K., and Croteau, R. 2004. Taxol biosynthesis: Molecular cloning and characterization of a cytochrome P450 taxoid 7 beta-hydroxylase. *Chemistry & Biology*, 11(5):663–672.

Cheng, Y., Dai, X., and Zhao, Y. 2006. Auxin biosynthesis by the YUCCA flavin monooxygenases controls the formation of floral organs and vascular tissues in Arabidopsis. *Genes & Development*, 20(13):1790–1799.

Chu-Chou, M., Guo, B., An, Z.-Q., Hendrix, J., Ferriss, R., Siegel, M., Dougherty, C., and Burrus, P. 1992. Suppression of mycorrhizal fungi in fescue by the *Acremonium coenophialum* endophyte. *Soil Biology and Biochemistry*, 24(7):633–637.

Clark, E., White, J., and Patterson, R. 1983. Improved histochemical techniques for the detection of *Acremonium coenophialum* in tall fescue and methods of *in vitro* culture of the fungus. *Journal of Microbiological Methods*, 1(3):149–155.

Cozzolino, R., Palladino, P., Rossi, F., Calì, G., Benedetti, E., and Laccetti, P. 2005. Antineoplastic cyclic astin analogues kill tumour cells via caspase-mediated induction of apoptosis. *Carcinogenesis*, 26(4):733–739.

Czerepanov, S. K. 1995. *Vascular plants of Russia and adjacent states (the Former USSR)*. Cambridge University Press.

Dallas, P. B., Gottardo, N. G., Firth, M. J., Beesley, A. H., Hoffmann, K., Terry, P. A., Freitas, J. R., Boag, J. M., Cummings, A. J., and Kees, U. R. 2005. Gene expression levels assessed by oligonucleotide microarray analysis and quantitative real-time RT-PCR - How well do they correlate? *BMC Genomics*, 6(1):59.

Davis, N. D., Clark, E. M., Schrey, K. A., and Diener, U. L. 1986. *In vitro* growth of *Acremonium coenophialum*, an endophyte of toxic tall fescue grass. *Applied and Environmental Microbiology*, 52(4):888–891.

de Oliveira Mendes, G., Moreira de Freitas, A. L., Liparini Pereira, O., Ribeiro da Silva, I., Bojkov Vassilev, N., and Dutra Costa, M. 2013. Mechanisms of phosphate solubilization by fungal isolates when exposed to different P sources. *Annals of Microbiology*, 64(1):239–249.

De St. Groth, S., Webster, R., and Datyner, A. 1963. Two new staining procedures for quantitative estimation of proteins on electrophoretic strips. *Biochimica et Biophysica Acta*, 71:377–391.

Denison, S. H. 2000. pH regulation of gene expression in fungi. *Fungal Genetics and Biology*, 29(2):61–71.

Doan, T., Jäschke, D., and Ludwig-Müller, J. 2010. An endophytic fungus induces tolerance against the clubroot pathogen *Plasmodiophora brassicae* in *Arabidopsis thaliana* and *Brassica rapa* roots. *Acta Horticulturae (ISHS)*, 867:173–180.

Dobinson, K. F., Lecomte, N., and Lazarovits, G. 1997. Production of an extracellular trypsin-like protease by the fungal plant pathogen *Verticillium dahliae*. *Canadian Journal of Microbiology*, 43(3):227–233.

Dolle, C. 2011. Untersuchung der Expression der Tocopherol-Biosynthese-Enzyme in Helianthus annuus-Sorten sowie Arabidopsis thaliana mittel RT-PCR.

Dong, C., Flecks, S., Unversucht, S., Haupt, C., van Pée, K.-H., and Naismith, J. H. 2005. Tryptophan 7-halogenase (PrnA) structure suggests a mechanism for regioselective chlorination. *Science*, 309(5744):2216–2219.

Duhamel, M., Pel, R., Ooms, A., Bücking, H., Jansa, J., Ellers, J., van Straalen, N. M., Wouda, T., Vandenkoornhuyse, P., and Kiers, E. T. 2013. Do fungivores trigger the transfer of protective metabolites from host plants to arbuscular mycorrhizal hyphae? *Ecology*, 94(9):2019–2029.

Dunleavy, J. M. 1989. *Curtobacterium plantarum* sp. nov. is ubiquitous in plant leaves and is seed transmitted in soybean and corn. *International Journal of Systematic Bacteriology*, 39(3):240–249.

Dunne, C., Crowley, J. J., Moenne-Loccoz, Y., Dowling, D. N., Bruijn, S., and O'Gara, F. 1997. Biological control of *Pythium ultimum* by *Stenotrophomonas maltophilia* W81 is mediated by an extracellular proteolytic activity. *Microbiology*, 143(12):3921–3931.

Dvorak, M. T. 2006. *Real-time PCR*. Taylor & Francis Group, Abingdon, UK.

Edgar, R. C. 2004. MUSCLE: Multiple sequence alignment with high accuracy and high throughput. *Nucleic Acids Research*, 32(5):1792–1797.

Eneyskaya, E. V., Kulminskaya, A. A., Savel'ev, A. N., Savel'eva, N. V., Shabalin, K. A., and Neustroev, K. N. 1999. Acid protease from *Trichoderma reesei*: Limited proteolysis of fungal carbohydrases. *Applied Microbiology and Biotechnology*, 52(2):226–231.

Eriksson, K., Blanchette, R., and Ander, P. 1990. *Microbial and enzymatic degradation of wood and wood components.* Springer.

Escott, G. M., Walters, C. E., Ingham, E., and Adams, D. J. 1996. Expression of chitinase activity during monocyte differentiation. In Muzzarelli, R., editor, *Chitin enzymology*, pages 11–20. Grottammase: European Chitin Society, 2 edition.

Eyberger, A. L., Dondapati, R., and Porter, J. R. 2006. Endophyte fungal isolates from *Podophyllum peltatum* produce podophyllotoxin. *Journal of Natural Products*, 69(8):1121–1124.

Felsenstein, J. 1985. Confidence limits on phylogenies: An approach using the bootstrap. *Evolution*, 39(4):783–791.

Finking, R. and Marahiel, M. A. 2004. Biosynthesis of nonribosomal peptides. *Annual Review of Microbiology*, 58:453–488.

Flann, C. 2009. Global Compositae Checklist.

Freeman, E. 1904. *Symbiosis in the genus Lolium*.

Fridlender, M., Inbar, J., and Chet, I. 1993. Biological control of soilborne plant pathogens by a beta-1,3 glucanase-producing *Pseudomonas cepacia*. *Soil Biology and Biochemistry*, 25(9):1211–1221.

Gaiero, J. R., McCall, C. A., Thompson, K. A., Day, N. J., Best, A. S., and Dunfield, K. E. 2013. Inside the root microbiome: Bacterial root endophytes and plant growth promotion. *American Journal of Botany*, 100(9):1738–1750.

Gaumann, E. 1957. Fusaric acid as a wilt toxin. *Phytopathology*, 47:342–357.

Gibson, U. E., Heid, C. A., and Williams, P. M. 1996. A novel method for real time quantitative RT-PCR. *Genome Research*, 6(10):995–1001.

Gooday, G. W. 1995. Diversity of roles for chitinases in nature. In Zakaria, M., Wan Muda, W., and Abdullah, M., editors, *Chitin and chitosan*, pages 191–202. Malaysia Penerbig University Kebangsaan.

Grube, M., Baloch, E., and Lumbsch, H. T. 2004. The phylogeny of Porinaceae (Ostropomycetidae) suggests a neotenic origin of perithecia in Lecanoromycetes. *Mycological Research*, 108(Pt 10):1111–1118.

Grube, M. and Hawksworth, D. L. 2007. Trouble with lichen: The re-evaluation and re-interpretation of thallus form and fruit body types in the molecular era. *Mycological Research*, 111(9):1116–1132.

Gruber, S., Vaaje-Kolstad, G., Matarese, F., López-Mondéjar, R., Kubicek, C. P., and Seidl-Seiboth, V. 2011. Analysis of subgroup C of fungal chitinases containing chitin-binding and LysM modules in the mycoparasite *Trichoderma atroviride*. *Glycobiology*, 21(1):122–133.

Gubanov, I. A. 1996. *Conspectus of the flora of outer Mongolia (vascular plants)*. Moscow.

Guo, B., Li, H., and Zhang, L. 1998a. Isolation of an fungus producting vinbrastine. *Journal of Yunnan University (Natural Sciences Edition)*, 20(3):214–215.

Guo, B., Li, H., and Zhang, L. 1998b. Isolation of the fungus producing vinblastine. *Journal of Yunnan University (Natural Sciences Edition)*, 20:214–215.

Hall, B. G. 2013. Building phylogenetic trees from molecular data with MEGA. *Molecular Biology and Evolution*, 30(5):1229–1235.

Hansen, B. G., Kliebenstein, D. J., and Halkier, B. A. 2007. Identification of a flavin-monooxygenase as the S-oxygenating enzyme in aliphatic glucosinolate biosynthesis in Arabidopsis. *The Plant Journal*, 50(5):902–910.

Hansson, D., Menkis, A., Olson, K., Stenlid, J., Broberg, A., and Karlsson, M. 2012. Biosynthesis of fomannoxin in the root rotting pathogen *Heterobasidion occidentale*. *Phytochemistry*, 84:31–39.

Hansson, D., Wubshet, S., Olson, A., Karlsson, M., Staerk, D., and Broberg, A. 2014. Secondary metabolite comparison of the species within the *Heterobasidion annosum* s.l. complex. *Phytochemistry*, 108:243–251.

Harman, G., Hayes, C., and Lorito, M. 1993. Chitinolytic enzymes of *Trichoderma harzianum*: purification of chitobiosidase and endochitinase. *Phytopathology*, 83(3):313–318.

Hart, J. and Hillis, W. 1972. Inhibition of wood-rotting fungi by ellagitannins in the heartwood of *Quercus alba*. *Phytopathology*, 62:620–626.

Hart, J. and Hillis, W. 1974. Inhibition of wood-rotting fungi by stilbenes and other polyphenols in *Eucalyptus sideroxylon*. *Phytopathology*, 64(7):939–948.

Hartl, L., Zach, S., and Seidl-Seiboth, V. 2012. Fungal chitinases: Diversity, mechanistic properties and biotechnological potential. *Applied Microbiology and Biotechnology*, 93(2):533–543.

Heitefuss, R., Stahmann, M. A., and Walker, J. C. 1960. Production of pectolytic enzymes and fusaric acid by *Fusarium oxysporum* f. *conglutinans* in relation to cabbage yellows. *Phytopathology*, 50(5):367–370.

Henssen, A. 1976. Studies in the developmental morphology of lichenized Ascomycetes. In Brown, D. H., Hawksworth, D. L., and Bailey, E. H., editors, *Lichenology: Progress and Problems; Proceedings of an International Symposium*, pages 107–138. Academic Press Inc., London.

Henssen, A. 1995. *Sagiolechia atlantica*, eine neue Flechte von den Atlantischen Inseln (Ascomycotina, Ostropales). *Bibliotheca Lichenologica*, 58:123–136.

Henssen, A. and Lücking, R. 2002. Morphology, anatomy, and ontogeny in the Asterothyriaceae (Ascomycota: Ostropales), a misunderstood group of lichenized fungi. *Annales Botanici Fennici*, 39:273–299.

Hider, R. C. and Kong, X. 2010. Chemistry and biology of siderophores. *Natural Product Reports*, 27(5):637–657.

Hilker, R., Stadermann, K. B., Doppmeier, D., Kalinowski, J., Stoye, J., Straube, J., Winnebald, J., and Goesmann, A. 2014. ReadXplorer - visualization and analysis of mapped sequences. *Bioinformatics (Oxford, England)*, 30(16):2247–2254.

Hoagland, D. and Arnon, D. 1950. The water-culture method for growing plants without soil. *Circular. California Agricultural Experiment Station*, 347:1 – 32.

Hodges, C. F. and Campbell, D. A. 1998. Growth response of *Agrostis palustris* to adventitious root infection by *Acremonium rutilum* and *Acremonium alternatum*. *Journal of Phytopathology*, 146(8-9):437–443.

Holmes, A., Govan, J., and Goldstein, R. 1998. Agricultural use of *Burkholderia (Pseudomonas) cepacia*: A threat to human health? *Emerging Infectious Diseases*, 4(2):221–227.

Homma, Y., Sato, Z., Hirayama, F., Konno, K., Shirahama, H., and Suzui, T. 1989. Production of antibiotics by *Pseudomonas cepacia* as an agent for biological control of soilborne plant pathogens. *Soil Biology and Biochemistry*, 21(5):723–728.

Huijbers, M. M., Montersino, S., Westphal, A. H., Tischler, D., and van Berkel, W. J. 2014. Flavin dependent monooxygenases. *Archives of Biochemistry and Biophysics*, 544:2–17.

Hull, A. K., Vij, R., and Celenza, J. L. 2000. Arabidopsis cytochrome P450s that catalyze the first step of tryptophan-dependent indole-3-acetic acid biosynthesis. *Proceedings of the National Academy of Sciences of the United States of America*, 97(5):2379–2384.

Hummel, K. M., Inselman, A. L., Ramos, E. R., Gathman, A. C., and Lilly, W. W. 1998. Extracellular protease production by submerged cultures of Schizophyllum commune. *Mycologia*, 90(5):883.

Hurek, T., Handley, L. L., Reinhold-Hurek, B., and Piché, Y. 2002. *Azoarcus* grass endophytes contribute fixed nitrogen to the plant in an unculturable state. *Molecular Plant-Microbe Interactions*, 15(3):233–242.

Itokawa, H., Morita, H., Nagashima, S., and Takeya, K. 1994. Cyclic peptides from higher plants. Part 8. Three novel cyclic pentapeptides, astins F, G and H from Aster tataricus. *Heterocycles*, 38(10):2247–2252.

Itokawa, H., Takeya, K., Hitotsuyanagi, Y., and Morita, H. 2000. Antitumor compounds isolated from higher plants. *Studies in Natural Products Chemistry*, 24:269–350.

Jaleel, C. A., Manivannan, P., Sankar, B., Kishorekumar, A., Gopi, R., Somasundaram, R., and Panneerselvam, R. 2007. *Pseudomonas fluorescens* enhances biomass yield and ajmalicine production in *Catharanthus roseus* under water deficit stress. *Colloids and Surfaces B: Biointerfaces*, 60(1):7–11.

James, E. K. and Olivares, F. L. 1998. Infection and colonization of sugar cane and other graminaceous plants by endophytic diazotrophs. *Critical Reviews in Plant Science*, 17(1):77–119.

Jäschke, D., Dugassa-Gobena, D., Karlovsky, P., Vidal, S., and Ludwig-Müller, J. 2010. Suppression of clubroot (*Plasmodiophora brassicae*) development in *Arabidopsis thaliana* by the endophytic fungus *Acremonium alternatum*. *Plant Pathology*, 59(1):100–111.

Jost, J.-P. 1965. Contribution à l'etude de la résistance toxicologique des végétaux a l'acide fusarique. *Journal of Phytopathology*, 54(4):338–378.

Kasana, R. C., Salwan, R., Dhar, H., Dutt, S., and Gulati, A. 2008. A rapid and easy method for the detection of microbial cellulases on agar plates using gram's iodine. *Current microbiology*, 57(5):503–507.

Kaurichev, I., Ivanova, T., and Nozdrunova, Y. 1963. Low molecular organic acid content of water-soluble organic matter in soils. *Soil Sciences and Plant Analysis*, 22:223–229.

Kearse, M., Moir, R., Wilson, A., Stones-Havas, S., Cheung, M., Sturrock, S., Buxton, S., Cooper, A., Markowitz, S., Duran, C., Thierer, T., Ashton, B., Meintjes, P., and Drummond, A. 2012. Geneious Basic: An integrated and extendable desktop software platform for the organization and analysis of sequence data. *Bioinformatics*, 28(12):1647–1649.

Keller, S., Wage, T., Hohaus, K., Hölzer, M., Eichhorn, E., and van Pée, K. H. 2000. Purification and partial characterization of tryptophan 7-halogenase (PrnA) from *Pseudomonas fluorescens*. *Angewandte Chemie (International ed. in English)*, 39(13):2300–2302.

Khan, A., Shinwari, Z., Kim, Y., and Waqas, M. 2012. Role of endophyte *Chaetomium globosum* lk4 in growth of *Capsicum annuum* by producion of gibberellins and indole acetic acid. *Pakistan Journal of Botany*, 44(5):1601–1607.

Khan, M. S., Zaidi, A., Ahemad, M., Oves, M., and Wani, P. A. 2010. Plant growth promotion by phosphate solubilizing fungi - current perspective. *Archives of Agronomy and Soil Science*, 56(1):73–98.

Killian, M., Steiner, U., Krebs, B., Junge, H., Schmiedeknecht, G., and Hain, R. 2000. FZB24 *Bacillus subtilis* - mode of action of a microbial agent enhancing plant vitality. *Pflanzenschutz-Nachrichten Bayer*, 1:72–93.

Kimura, M. 1980. A simple method for estimating evolutionary rates of base substitutions through comparative studies of nucleotide sequences. *Journal of Molecular Evolution*, 16(2):111–120.

Kluepfel, D. 1957. Über die Biosynthese und die Umwandlung von Fusarinsäure in Tomatenpflanzen. *Phytopathology*, 29:349–379.

Koch, M., Vorwerk, S., Masur, C., Sharifi-Sirchi, G., Olivieri, N., and Schlaich, N. L. 2006. A role for a flavin-containing mono-oxygenase in resistance against microbial pathogens in Arabidopsis. *The Plant Journal: For Cell and Molecular Biology*, 47(4):629–639.

Koressaar, T. and Remm, M. 2007. Enhancements and modifications of primer design program Primer3. *Bioinformatics*, 23(10):1289–91.

Kunike, G. 1925. Nachweis und Verbreitung organischer Skeletsubstanzen bei Tieren. *Zeitschrift für Vergleichende Physiologie*, 2(3):233–253.

Kusari, S., Lamshöft, M., Zühlke, S., and Spiteller, M. 2008. An endophytic fungus from *Hypericum perforatum* that produces hypericin. *Journal of Natural Products*, 71(2):159–162.

Kusari, S., Zühlke, S., and Spiteller, M. 2011. Effect of artificial reconstitution of the interaction between the plant *Camptotheca acuminata* and the fungal endophyte *Fusarium solani* on camptothecin biosynthesis. *Journal of Natural Products*, 74(4):764–775.

Latch, G. C. 1993. Physiological interactions of endophytic fungi and their hosts. Biotic stress tolerance imparted to grasses by endophytes. *Agriculture, Ecosystems & Environment*, 44(1-4):143–156.

Latch, G. C. M., Christensen, M. J., and Samuels, G. J. 1984. Five endophytes of *Lolium* and *Festuca* in New Zealand. *Mycotaxon*, 20:535–550.

Le, S. Q. and Gascuel, O. 2008. An improved general amino acid replacement matrix. *Molecular Biology and Evolution*, 25(7):1307–1320.

Lederberg, J. 1992. Cellulases. In *Enzyclopedia of Microbiology*. Academic Press Inc.

Leger, R. J. S., Joshi, L., and Roberts, D. W. 1997. Adaptation of proteases and carbohydrases of saprophytic, phytopathogenic and entomopathogenic fungi to the requirements of their ecological niches. *Microbiology*, 143(6):1983–1992.

Leisinger, T. and Margraff, R. 1979. Secondary metabolites of the fluorescent pseudomonads. *Microbiological Reviews*, 43(3):422.

Li, J., Hansen, B. G., Ober, J. A., Kliebenstein, D. J., and Halkier, B. A. 2008. Subclade of flavin-monooxygenases involved in aliphatic glucosinolate biosynthesis. *Plant Physiology*, 148(3):1721–1733.

Li, X., Luo, L., Yang, J., Li, B., and Yuan, H. 2015. Mechanisms for solubilization of various insoluble phosphates and activation of immobilized phosphates in different soils by an efficient and salinity-tolerant *Aspergillus niger* strain An2. *Applied Biochemistry and Biotechnology*, 175(5):2755–2768.

Liu, C. H., Zou, W. X., Lu, H., and Tan, R. X. 2001. Antifungal activity of *Artemisia annua* endophyte cultures against phytopathogenic fungi. *Journal of Biotechnology*, 88(3):277–282.

Liu, X., Cao, P., Zhang, C., Xu, X., and Zhang, M. 2012. Screening and analyzing potential hepatotoxic compounds in the ethanol extract of Asteris Radix by HPLC/DAD/ESI-MS(n) technique. *Journal of Pharmaceutical and Biomedical Analysis*, 67-68:51–62.

Livak, K. and Schmittgen, T. 2001. Analysis of relative gene expression data using real-time quantitative PCR and the 2(- delta delta C(t)) method. *Methods*, 25(4):402–408.

Longoni, P., Rodolfi, M., Pantaleoni, L., Doria, E., Concia, L., Picco, A. M., and Cella, R. 2012. Functional analysis of the degradation of cellulosic substrates by a *Chaetomium globosum* endophytic isolate. *Applied and Environmental Microbiology*, 78(10):3693–3705.

Lutzoni, F., Kauff, F., Cox, C. J., McLaughlin, D., Celio, G., Dentinger, B., Padamsee, M., Hibbett, D., James, T. Y., Baloch, E., Grube, M., Reeb, V., Hofstetter, V., Schoch, C., Arnold, A. E., Miadlikowska, J., Spatafora, J., Johnson, D., Hambleton, S., Crockett, M., Shoemaker, R., Sung, G.-H., Lücking, R., Lumbsch, T., O'Donnell, K., Binder, M.,

Diederich, P., Ertz, D., Gueidan, C., Hansen, K., Harris, R. C., Hosaka, K., Lim, Y.-W., Matheny, B., Nishida, H., Pfister, D., Rogers, J., Rossman, A., Schmitt, I., Sipman, H., Stone, J., Sugiyama, J., Yahr, R., and Vilgalys, R. 2004. Assembling the fungal tree of life: Progress, classification, and evolution of subcellular traits. *American Journal of Botany*, 91(10):1446–80.

Madden, T. 2002. The BLAST Sequence Analysis Tool. In McEntyre, J. and Ostell, J., editors, *The NCBI Handbook (Internet)*, chapter 16, pages 1–15. National Center for Biotechnology Information (US), Bethesda (MD).

Mann, H. and Whitney, D. 1947. On a test of whether one of two random variables is stochastically larger than the other. *The Annals of Mathematical Statistics*, pages 50–60.

Meeley, R. B., Johal, G. S., Briggs, S. P., and Walton, J. D. 1992. A biochemical phenotype for a disease resistance gene of maize. *The Plant Cell*, 4(1):71–77.

Meeley, R. B. and Walton, J. D. 1991. Enzymatic detoxification of HC-toxin, the host-selective cyclic peptide from *Cochliobolus carbonum*. *Plant Physiology*, 97(3):1080–1086.

Milbredt, D. 2010. *Molekulargenetische und biochemische Untersuchungen zur Biosynthese von Thienodolin in Streptomyces albogriseolus*. Dissertation, TU Dresden.

Mishina, T. E. and Zeier, J. 2006. The Arabidopsis flavin-dependent monooxygenase FMO1 is an essential component of biologically induced systemic acquired resistance. *Plant Physiology*, 141(4):1666–1675.

Mitchell, A., Chang, H.-Y., Daugherty, L., Fraser, M., Hunter, S., Lopez, R., McAnulla, C., McMenamin, C., Nuka, G., Pesseat, S., Sangrador-Vegas, A., Scheremetjew, M., Rato, C., Yong, S.-Y., Bateman, A., Punta, M., Attwood, T. K., Sigrist, C. J. A., Redaschi, N., Rivoire, C., Xenarios, I., Kahn, D., Guyot, D., Bork, P., Letunic, I., Gough, J., Oates, M., Haft, D., Huang, H., Natale, D. A., Wu, C. H., Orengo, C., Sillitoe, I., Mi, H., Thomas, P. D., and Finn, R. D. 2014. The InterPro protein families database: The classification resource after 15 years. *Nucleic Acids Research*, 43(Database issue):D213–D221.

Mizutani, K., Hirasawa, Y., Sugita-Konishi, Y., Mochizuki, N., and Morita, H. 2008. Structural and conformational analysis of hydroxycyclochlorotine and cyclochlorotine, chlorinated cyclic peptides from Penicillium islandicum. *Journal of Natural Products*, 71(7):1297–1300.

Möller, E. M., Bahnweg, G., Sandermann, H., and Geiger, H. H. 1992. A simple and efficient protocol for isolation of high molecular weight DNA from filamentous fungi, fruit bodies and infected plant tissues. *Nucleic Acids Research*, 20(22):6115–6116.

Moreth, U. and Schmidt, O. 2000. Identification of indoor rot fungi by taxon-specific priming polymerase chain reaction. *Holzforschung*, 54:1–8.

Morey, J. S., Ryan, J. C., and Van Dolah, F. M. 2006. Microarray validation: Factors influencing correlation between oligonucleotide microarrays and real-time PCR. *Biological Procedures Online*, 8:175–193.

Morita, H., Nagashima, S., Shirota, O., Takeya, K., and Itokawa, H. 1993a. Two novel monochlorinated cyclic pentapeptides, astins D and E from *Aster tataricus*. *Chemistry Letters*, 22(11):1877–1880.

Morita, H., Nagashima, S., Takeya, K., and Itokawa, H. 1993b. Astins A and B, antitumor cyclic pentapeptides from *Aster tataricus*. *Chemical & Pharmaceutical Bulletin*, 41(5):992–993.

Morita, H., Nagashima, S., Takeya, K., and Itokawa, H. 1994. A novel cyclic pentapeptide with beta-hydroxy-gamma-chloroproline from *Aster tataricus*. *Chemistry Letters*, 23(11):2009–2010.

Morita, H., Nagashima, S., Takeya, K., and Itokawa, H. 1995a. Structure of a new peptide, astin J, from *Aster tataricus*. *Chemical & Pharmaceutical Bulletin*, 43(2):271–273.

Morita, H., Nagashima, S., Takeya, K., Itokawa, H., and Iitaka, Y. 1995b. Structures and conformation of antitumour cyclic pentapeptides, astins A, B and C, from *Aster tataricus*. *Tetrahedron*, 51(4):1121–1132.

Morita, H., Nagashima, S., Uchiumi, Y., Kuroki, O., Takeya, K., and Itokawa, H. 1996. Cyclic peptides from higher plants. XXVIII. Antitumor activity and hepatic microsomal biotransformation of cyclic pentapeptides, astins, from *Aster tataricus*. *Chemical & Pharmaceutical Bulletin*, 44(5):1026–1032.

Mullis, K., Faloona, F., and Scharf, S. 1986. Specific enzymatic amplification of DNA *in vitro*: The polymerase chain reaction. *Cold Spring Harbor Symposia on Quantitative Biology*, 51:263–273.

Mullis, K. B. and Faloona, F. A. 1986. Specific synthesis of DNA *in vitro* via a polymerase-catalyzed chain reaction. *Methods in Enzymology*, 155:335–350.

Munsell, A. H. 1905. *A color notation*. G. H. Ellis, Boston.

Murashige, T. and Skoog, F. 1962. A revised medium for rapid growth and bio assays with tobacco tissue cultures. *Physiologia Plantarum*, 15(3):473–497.

Musgrave, D. R. and Flechter, L. F. 1984. The development and applications of ELISA. Detection of *Lolium* endophyte in ryegrass staggers research. *Animal Production*, 44:185–187.

Nahrstedt, A. and Butterweck, V. 1997. Biologically active and other chemical constituents of the herb of *Hypericum perforatum* L. *Pharmacopsychiatry*, 30:129–134.

Naumann, C., Hartmann, T., and Ober, D. 2002. Evolutionary recruitment of a flavin-dependent monooxygenase for the detoxification of host plant-acquired pyrrolizidine alkaloids in the alkaloid-defended arctiid moth *Tyria jacobaeae*. *Proceedings of the National Academy of Sciences of the United States of America*, 99(9):6085–6090.

Nei, M. and Kumar, S. 2000. *Molecular evolution and phylogenetics*. Oxford University Press.

Neilands, J., Winkelmann, G., and der Helm, D. V. 1987. *Iron transport in microbes, plants and animals*. VCH Press, Weinheim.

Neilands, J. B. 1995. Siderophores: Structure and function of microbial iron transport compounds. *Journal of Biological Chemistry*, 270(45):26723–26726.

Olivieri, F., Zanetti, M. E., Oliva, C. R., Covarrubias, A. A., and Casalongué, C. A. 2002. Characterization of an extracellular serine protease of *Fusarium eumartii* and its action on pathogenesis related proteins. *European Journal of Plant Pathology*, 108(1):63–72.

Ordentlich, A., Elad, Y., and Chet, I. 1988. The role of chitinase of *Serratia marcescens* in the biocontrol of *Sclerotium rolfsii*. *Phytopathology*, 78(1):84–88.

Palumbo, J. D., Yuen, G. Y., Jochum, C. C., Tatum, K., and Kobayashi, D. Y. 2005. Mutagenesis of beta-1,3-glucanase genes in *Lysobacter enzymogenes* strain C3 results in reduced biological control activity toward *Bipolaris* leaf spot of tall fescue and *Pythium* damping-off of sugar beet. *Phytopathology*, 95(6):701–707.

Paoletti, M., Clavé, C., and Bégueret, J. 1998. Characterization of a gene from the filamentous fungus *Podospora anserina* encoding an aspartyl protease induced upon carbon starvation. *Gene*, 210(1):45–52.

Pearce, R. B. 1996. Antimicrobial defences in the wood of living trees. *New Phytologist*, 132(2):203–233.

Pfaffl, M. 2004. Real-time RT-PCR: Neue Ansätze zur exakten mRNA Quantifizierung. *BIOspektrum*, 1(04):92–95.

Pfaffl, M. W. and Hageleit, M. 2001. Validities of mRNA quantification using recombinant RNA and recombinant DNA external calibration curves in real-time RT-PCR. *Biotechnology Letters*, 23(4):275–282.

Pryor, B. M., Creamer, R., Shoemaker, R. A., McLain-Romero, J., and Hambleton, S. 2009. *Undifilum*, a new genus for endophytic *Embellisia oxytropis* and parasitic *Helminthosporium bornmuelleri* on legumes. *Botany*, 87(2):178–194.

Puri, S., Verma, V., and Amna, T. 2005. An endophytic fungus from *Nothapodytes foetida* that produces camptothecin. *Journal of Natural Products*, 68(12):1717–1719.

Qin, J.-C., Zhang, Y.-M., Gao, J.-M., Bai, M.-S., Yang, S.-X., Laatsch, H., and Zhang, A.-L. 2009. Bioactive metabolites produced by *Chaetomium globosum*, an endophytic fungus isolated from *Ginkgo biloba*. *Bioorganic & Medicinal Chemistry Letters*, 19(6):1572–1574.

Quan, C. S., Zheng, W., Liu, Q., Ohta, Y., and Fan, S. D. 2006. Isolation and characterization of a novel *Burkholderia cepacia* with strong antifungal activity against *Rhizoctonia solani*. *Applied Microbiology and Biotechnology*, 72(6):1276–84.

Radulovic, N., Stankov-Jovanovic, V., Stojanovic, G., Smelcerovic, A., Spiteller, M., and Asakawa, Y. 2007. Screening of *in vitro* antimicrobial and antioxidant activity of nine *Hypericum species* from the Balkans. *Food Chemistry*, 103(1):15–21.

Rasmussen, R. 2001. Rapid cycle real-time PCR. In Meuer, S., Wittwer, C., and Nakagawara, K.-I., editors, *Rapid cycle real-time PCR: Methods and application*, pages 21–34. Springer Press Heidelberg, Berlin, Heidelberg.

Redman, R. S., Sheehan, K. B., Stout, R. G., Rodriguez, R. J., and Henson, J. M. 2002. Thermotolerance generated by plant/fungal symbiosis. *Science*, 298(5598):1581.

Richardson, A. E., Barea, J.-M., McNeill, A. M., and Prigent-Combaret, C. 2009. Acquisition of phosphorus and nitrogen in the rhizosphere and plant growth promotion by microorganisms. *Plant and Soil*, 321(1-2):305–339.

Rodríguez, H. and Fraga, R. 1999. Phosphate solubilizing bacteria and their role in plant growth promotion. *Biotechnology Advances*, 17(4-5):319–339.

Rossi, F., Zanotti, G., Saviano, M., Iacovino, R., Palladino, P., Saviano, G., Amodeo, P., Tancredi, T., Laccetti, P., Corbier, C., and Benedetti, E. 2004. New antitumour cyclic astin analogues: Synthesis, conformation and bioactivity. *Journal of Peptide Science*, 10(2):92–102.

Rupp, O., Becker, J., Brinkrolf, K., Timmermann, C., Borth, N., Pühler, A., Noll, T., and Goesmann, A. 2014. Construction of a public CHO cell line transcript database using versatile bioinformatics analysis pipelines. *PloS One*, 9(1):e85568.

Saito, M., Enomoto, M., Tatsuno, T., and Uraguchi, K. 1971. Yellowed rice toxins: Luteoskyrin and related compounds, chlorine-containing compounds and citrinin. *Microbial Toxins*, 6:299–380.

Sampson, K. 1933. The systemic infection of grasses by *Epichloe typhina* (pers.) tul. *Transactions of the British Mycological Society*, 18:30–IN3.

Samson, R., Yilmaz, N., Houbraken, J., Spierenburg, H., Seifert, K., Peterson, S., Varga, J., and Frisvad, J. C. 2011. Phylogeny and nomenclature of the genus *Talaromyces* and taxa accommodated in *Penicillium* subgenus *Biverticillium*. *Studies in Mycology*, 70:159–183.

Saviano, G., Benedetti, E., Cozzolino, R., De Capua, A., Laccetti, P., Palladino, P., Zanotti, G., Amodeo, P., Tancredi, T., and Rossi, F. 2004. Influence of conformational flexibility on biological activity in cyclic astin analogues. *Biopolymers - Peptide Science Section*, 76(6):477–484.

Sawai, S., Uchiyama, H., Mizuno, S., Aoki, T., Akashi, T., Ayabe, S.-I., and Takahashi, T. 2011. Molecular characterization of an oxidosqualene cyclase that yields shionone, a unique tetracyclic triterpene ketone of *Aster tataricus*. *FEBS letters*, 585(7):1031–1036.

Schardl, C. L., Leuchtmann, A., and Spiering, M. J. 2004. Symbioses of grasses with seedborne fungal endophytes. *Annual Review of Plant Biology*, 55:315–40.

Schilling, A. G., Müller, E. M., and Geiger, H. H. 1996. Polymerase chain reaction-based assays for species-specific detection of *Fusarium culmorum*, *F. graminearum* and *F. avenaceum*. *Phytopathology*, 86(5):515–522.

Schmitt, I., Prado, R. D., Grube, M., and Lumbsch, H. T. 2009. Repeated evolution of closed fruiting bodies is linked to ascoma development in the largest group of lichenized fungi (Lecanoromycetes, Ascomycota). *Molecular Phylogenetics and Evolution*, 52(1):34–44.

Schomburg, I., Chang, A., Ebeling, C., Gremse, M., Heldt, C., Huhn, G., and Schomburg, D. 2004. BRENDA, the enzyme database: Updates and major new developments. *Nucleic Acids Research*, 32:D431–D433.

Schulze, P. 1924. Der Nachweis und die Verbreitung des Chitins mit einem Anhang über das komplizierte Verdauungssystem der Ophryoscoleciden. *Zeitschrift für Morphologie und Ökologie der Tiere*, 2(2-3):643–666.

Schwyn, B. and Neilands, J. B. 1987. Universal chemical assay for the detection and determination of siderophores. *Analytical Biochemistry*, 160(1):47–56.

Seo, J. H. and Bailey, J. E. 1985. Effects of recombinant plasmid content on growth properties and cloned gene product formation in *Escherichia coli*. *Biotechnology and Bioengineering*, 27(12):1668–1674.

Shao, Y., Ho, C. T., Chin, C. K., Poobrasert, O., Yang, S. W., and Cordell, G. a. 1997a. Asterlingulatosides C and D, cytotoxic triterpenoid saponins from *Aster lingulatus*. *Journal of Natural Products*, 60(7):743–746.

Shao, Y., Ho, C.-T., Chin, C.-K., Rosen, R. T., Hu, B., and Qin, G.-W. 1997b. Triterpenoid saponins from *Aster auriculatus*. *Phytochemistry*, 44(2):337–340.

Shen, Y., Luo, Q., Xu, H., Gong, F., Zhou, X., Sun, Y., Wu, X., Liu, W., Zeng, G., Tan, N., and Xu, Q. 2011. Mitochondria-dependent apoptosis of activated T lymphocytes induced by astin C, a plant cyclopeptide, for preventing murine experimental colitis. *Biochemical Pharmacology*, 82(3):260–268.

Sherwood, M. 1977a. The ostropalean fungi. *Mycotaxon*, 5:1–277.

Sherwood, M. 1977b. The ostropalean fungi II: *Schizoxylon*, with notes on *Stictis*, *Acarosporina*, *Coccopeziza* and *Carestiella*. *Mycotaxon*, 6:215–260.

Shirota, O., Morita, H., Takeya, K., Itokawa, H., and Iitaka, Y. 1997. Cytotoxic triterpene from *Aster tataricus*. *Natural Medicines*, 51(2):170–172.

Sijam, K. and Dikin, A. 2005. Biochemical and physiological characterization of *Burkholderia cepacia* as biological control agent. *International Journal of Agriculture and Biology*, 7(3):385–388.

Small, C. and Bidochka, M. 2005. Up-regulation of Pr1, a subtilisin-like protease, during conidiation in the insect pathogen *Metarhizium anisopliae*. *Mycological Research*, 109(03):307–313.

Southern, E. M. 1975. Detection of specific sequences among DNA fragments separated by gel electrophoresis. *Journal of Molecular Biology*, 98(3):503–517.

Stein, T. 2005. *Bacillus subtilis* antibiotics: Structures, syntheses and specific functions. *Molecular Microbiology*, 56(4):845–857.

Stevenson, F. 1967. Organic acids in soil. In McLaren, A. and Peterson, G., editors, *Soil Biochemistry*, pages 119–146. Marcel Dekker, New York, vol 1 edition.

Stierle, A., Strobel, G., and Stierle, D. 1993. Taxol and taxane production by *Taxomyces andreanae*, an endophytic fungus of Pacific yew. *Science*, 260(5105):214–216.

Strieker, M., Tanović, A., and Marahiel, M. A. 2010. Nonribosomal peptide synthetases: Structures and dynamics. *Current Opinion in Structural Biology*, 20(2):234–240.

Strobel, G., Daisy, B., Castillo, U., and Harper, J. 2004. Natural products from endophytic microorganisms. *Journal of Natural Products*, 67(2):257–268.

Strobel, G. A. 2003. Endophytes as sources of bioactive products. *Microbes and Infection*, 5:535–544.

Strobel, G. A., Miller, R. V., Martinez-Miller, C., Condron, M. M., Teplow, D. B., and Hess, W. M. 1999. Cryptocandin, a potent antimycotic from the endophytic fungus *Cryptosporiopsis* cf. *quercina*. *Microbiology*, 145(8):1919–1926.

Sundara, R. and Sinha, M. 1963. Organisms phosphate solubilizers in soil. *Indian Journal of Agricultural Sciences*, 33:272–278.

Sunitha, V., Devi, D., and Srinivas, C. 2013. Extracellular enzymatic activity of endophytic fungal strains isolated from medicinal plants. *World Journal of Agricultural Sciences*, 9(1):01–09.

Susca, A., Stea, G., Mulè, G., and Perrone, G. 2007. Polymerase chain reaction (PCR) identification of *Aspergillus niger* and *Aspergillus tubingensis* based on the calmodulin gene. *Food Additives and Contaminants*, 24(10):1154–1160.

Tammaro, F. and Xepapadakis, G. 1986. Plants used in phytotherapy, cosmetics and dyeing in the Pramanda district (Epirus, North-West Greece). *Journal of Ethnopharmacology*, 16(2-3):167–174.

Tamura, K., Stecher, G., Peterson, D., Filipski, A., and Kumar, S. 2013. MEGA6: Molecular Evolutionary Genetics Analysis version 6.0. *MBE*, 30(12):2725–2729.

Tatsuno, T., Tsukioka, M., Sakai, Y., Suzuki, Y., and Asami, Y. 1955. Study of the toxic principle in yellow rice. *Pharmaceutical Bulletin*, 3(6):476–477.

Taylor, T. and Taylor, E. 2000. The rhynie chert ecosystem: A model for understanding fungal interactions. In Bacon, C. W. and White, J. F., editors, *Microbial Endophytes*, pages 31–47. Marcel Dekker Inc., New York.

Terao, K., Ito, E., and Tatsuno, T. 1984. Liver injuries induced by cyclochlorotine isolated from *Penicillium islandicum*. *Archives of Toxicology*, 55(1):39–46.

Thielking, H. and Schmidt, M. 2000. Cellulose ethers. In *Ullmann's Encyclopedia of Industrial Chemistry*. Wiley-VCH Verlag GmbH & Co. KG, Weinheim, Germany.

Tibbett, M., Sanders, F. E., Cairney, J. W. G., and Leake, J. R. 1999. Temperature regulation of extracellular proteases in ectomycorrhizal fungi (*Hebeloma* spp.) grown in axenic culture. *Mycological Research*, 103(06):707–714.

Untergasser, A., Cutcutache, I., Koressaar, T., Ye, J., Faircloth, B. C., Remm, M., and Rozen, S. G. 2012. Primer3 - new capabilities and interfaces. *Nucleic Acids Research*, 40(15):e115.

Urlacher, V. B. and Girhard, M. 2012. Cytochrome P450 monooxygenases: An update on perspectives for synthetic application. *Trends in Biotechnology*, 30(1):26–36.

van Pée, K.-H. 2001. Microbial biosynthesis of halometabolites. *Archives of Microbiology*, 175(4):250–258.

van Pée, K.-H. and Patallo, E. P. 2006. Flavin-dependent halogenases involved

in secondary metabolism in bacteria. *Applied Microbiology and Biotechnology*, 70(6):631–641.

van Pée, K.-H. and Zehner, S. 2003. Enzymology and molecular genetics of biological halogenation. In *Natural production of organohalogen compounds*, pages 171–199. Springer.

Varma, A., Verma, S., Sahay, N., Bütehorn, B., and Franken, P. 1999. *Piriformospora indica*, a cultivable plant-growth-promoting root endophyte. *Applied and Environmental Microbiology*, 65(6):2741–2744.

Vilgalys, R. and Hester, M. 1990. Rapid genetic identification and mapping of enzymatically amplified ribosomal DNA from several *Cryptococcus* species. *Journal of Bacteriology*, 172(8):4238–4246.

Viruel, E., Lucca, M. E., and Siñeriz, F. 2011. Plant growth promotion traits of phosphobacteria isolated from Puna, Argentina. *Archives of Microbiology*, 193(7):489–496.

Wall, M. E., Wani, M. C., Cook, C. E., Palmer, K. H., McPhail, A. T., and Sim, G. A. 1966. Plant antitumor agents. I. The isolation and structure of camptothecin, a novel alkaloidal leukemia and tumor inhibitor from *Camptotheca acuminata*. *Journal of the American Chemical Society*, 88(16):3888–3890.

Walsh, C. T. 2007. The chemical versatility of natural-product assembly lines. *Accounts of Chemical Research*, 41(1):4–10.

Wang, B. and Qiu, Y. L. 2006. Phylogenetic distribution and evolution of mycorrhizas in land plants. *Mycorrhiza*, 16:299–363.

Wang, D., Yang, S., Tang, F., and Zhu, H. 2012. Symbiosis specificity in the legume: Rhizobial mutualism. *Cellular Microbiology*, 14(3):334–342.

Wang, L., Li, M.-D., Cao, P.-P., Zhang, C.-F., Huang, F., Xu, X.-H., Liu, B.-L., and Zhang, M. 2014. Astin B, a cyclic pentapeptide from *Aster tataricus*, induces apoptosis and autophagy in human hepatic L-02 cells. *Chemico-Biological Interactions*, 223(September):1–9.

Wang, S.-Y., Chen, P.-F., and Chang, S.-T. 2005. Antifungal activities of essential oils and their constituents from indigenous cinnamon (*Cinnamomum osmophloeum*) leaves against wood decay fungi. *Bioresource Technology*, 96(7):813–818.

Wani, M. C., Taylor, H. L., Wall, M. E., Coggon, P., and McPhail, A. T. 1971. Plant antitumor agents. VI. The isolation and structure of taxol, a novel antileukemic and antitumor agent from *Taxus brevifolia*. *Journal of the American Chemical Society*, 93(9):2325–2327.

Weber, R. W. S., Stenger, E., Meffert, A., and Hahn, M. 2004. Brefeldin a production by *Phoma medicaginis* in dead pre-colonized plant tissue: A strategy for habitat conquest? *Mycological Research*, 108(6):662–671.

Wedin, M., Döring, H., and Gilenstam, G. 2004. Saprotrophy and lichenization as options for the same fungal species on different substrata: Environmental plasticity and fungal lifestyles in the *Stictis-Conotrema* complex. *New Phytologist*, 164(3):459–465.

Wedin, M., Döring, H., and Gilenstam, G. 2006. *Stictis* s. lat. (Ostropales, Ascomycota) in northern Scandinavia, with a key and notes on morphological variation in relation to lifestyle. *Mycological Research*, 110(7):773–789.

Wheatley, R., Hackett, C., Bruce, A., and Kundzewicz, A. 1997. Effect of substrate composition on production of volatile organic compounds from Trichoderma spp. Inhibitory to wood decay fungi. *International Biodeterioration & Biodegradation*, 39(2-3):199–205.

White, J. F., Breen, J. P., and Morgan-Jones, G. 1991. Substrate utilization in selected *Acremonium*, *Atkinsonella* and *Balansia* species. *Mycologia*, 83(5):601.

White, T. J., Bruns, S., Lee, S., and Taylor, J. 1990. Amplification and direct sequencing of fungal ribosomal RNA genes for phylogenetics. In *PCR Protocols: A Guide to Methods and Applications*, pages 315–322.

Whitelaw, M. 1999. Growth promotion of plants inoculated with phosphate-solubilizing fungi. *Advances in Agronomy*, 69:99–151.

Whitelaw, M., Harden, T., and Helyar, K. 1999. Phosphate solubilisation in solution culture by the soil fungus *Penicillium radicum*. *Soil Biology and Biochemistry*, 31(5):655–665.

Willick, G. E., Morosoli, R., Seligy, V. L., Yaguchi, M., and Desrochers, M. 1984. Extracellular proteins secreted by the basidiomycete *Schizophyllum commune* in response to carbon source. *Journal of Bacteriology*, 159(1):294.

Wilson, D. 1995. Endophyte - the evolution of a term and clarification of its use and definition. *Oikos*, 73(2):274–276.

Wittwer, C., Ririe, K., and Andrew, R. 1997. The LightCycler: A microvolume multisample fluorimeter with rapid temperature control. *BioTechniques*, 22(1):176–181.

Wood, T. and Bhat, K. 1988. Methods for measuring cellulase activities. *Methods in Enzymology*, 160:87–112.

Wösten, H., Bohlmann, R., Eckerskorn, C., Lottspeich, F., Bölker, M., and Kahmann, R. 1996. A novel class of small amphipathic peptides affect aerial hyphal growth and surface hydrophobicity in *Ustilago maydis*. *The EMBO Journal*, 15(16):4274.

Xie, J., Strobel, G. A., Mends, M. T., Hilmer, J., Nigg, J., and Geary, B. 2013. *Collophora aceris*, a novel antimycotic producing endophyte associated with Douglas maple. *Microbial Ecology*, 66(4):784–795.

Xu, H.-M., Zeng, G.-Z., Zhou, W.-B., He, W.-J., and Tan, N.-H. 2013. Astins K-P, six new chlorinated cyclopentapeptides from *Aster tataricus*. *Tetrahedron*, 69(37):7964–7969.

Yabuta, T., Kambe, K., and Hayashi, T. 1937. Biochemistry of the bakanaefungus. I. Fusarinic acid, a new product of the bakanae fungus. *Journal of the Agricultural Chemical Society of Japan*, 10:1059–1068.

Yamaura, M., Satoh, K., Yamazaki, T., Ogawa, H., and Makimura, K. 2013. Specific detection of *Bjerkandera adusta* by polymerase chain reaction and its incidence in fungus-associated chronic cough. *Mycopathologia*, 176(5-6):337–43.

Yang, Y., Zhao, H., Barrero, R. A., Zhang, B., Sun, G., Wilson, I. W., Xie, F., Walker, K. D., Parks, J. W., Bruce, R., Guo, G., Chen, L., Zhang, Y., Huang, X., Tang, Q., Liu, H., Bellgard, M. I., Qiu, D., Lai, J., and Hoffman, A. 2014. Genome sequencing and analysis of the paclitaxel-producing endophytic fungus *Penicillium aurantiogriseum* NRRL 62431. *BMC Genomics*, 15:69.

Ye, J., Coulouris, G., Zaretskaya, I., Cutcutache, I., Rozen, S., and Madden, T. L. 2012. Primer-BLAST: A tool to design target-specific primers for polymerase chain reaction. *BMC Bioinformatics*, 13:134.

Yeh, E., Blasiak, L. C., Koglin, A., Drennan, C. L., and Walsh, C. T. 2007. Chlorination by a long-lived intermediate in the mechanism of flavin-dependent halogenases. *Biochemistry*, 46(5):1284–1292.

Yeh, E., Cole, L. J., Barr, E. W., Bollinger, J. M., Ballou, D. P., and Walsh, C. T. 2006. Flavin redox chemistry precedes substrate chlorination during the reaction of the flavin-dependent halogenase RebH. *Biochemistry*, 45(25):7904–7912.

Yu, H., Zhang, L., Li, L., Zheng, C., Guo, L., Li, W., Sun, P., and Qin, L. 2010a. Recent developments and future prospects of antimicrobial metabolites produced by endophytes. *Microbiological Research*, 165(6):437–449.

Yu, L., Lan, W., Qin, W., Jin, W., and Xu, H. 2002. Oxidative stress and taxol production induced by fungal elicitor in cell suspension cultures of *Taxus chinensis*. *Biologia Plantarum*, 45(3):459–461.

Yu, Y., Zhao, Q., Wang, J., Wang, J., Wang, Y., Song, Y., Geng, G., and Li, Q. 2010b. Swainsonine-producing fungal endophytes from major locoweed species in China. *Toxicon*, 56(3):330–8.

Zaichikova, S. G., Grinkevich, N. I., and Barabanov, E. I. 1985. Healing properties and determination of the upper parameters of toxicity of *Hypericum* herb. *Farmatsiya*, 34:62–64.

Zhao, J., Zhou, L., Wang, J., and Shan, T. 2010. Endophytic fungi for producing bioactive compounds originally from their host plants. *Current Research, Technology and Education Topics in Applied Microbiology and Microbial Biotechnology*, pages 567–576.

Zhao, Y., Christensen, S. K., Fankhauser, C., Cashman, J. R., Cohen, J. D., Weigel, D., and Chory, J. 2001. A role for flavin monooxygenase-like enzymes in auxin biosynthesis. *Science*, 291(5502):306–309.

Zou, X., Binkley, D., and Doxtader, K. G. 1992. A new method for estimating gross phosphorous mineralization and immobilization rates in soil. *Plant and Soil*, 147:243–250.

Zubek, S. and Blaszkowski, J. 2009. Medicinal plants as hosts of arbuscular mycorrhizal fungi and dark septate endophytes. *Phytochemistry Reviews*, 8(3):571–580.

Zweimuller, M., Antus, S., Kovacs, T., and Sonnenbichler, J. 1997. Biotransformation of the fungal toxin fomannoxin by conifer cell cultures. *Biological Chemistry*, 378(3):915–921.

Acknowledgment

First of all, I thank my boss Prof. Dr. Jutta Ludwig-Müller for the great opportunity to work on this exiting and interesting topic. She gave me some nice tips and supported me especially during the first two years where I did not have so many results and where the work did not go on so easy. Thank you for reviewing my dissertation, the "well dosed" comments and the following examination.

Thanks goes to my colleagues Sabine Jülke, Sabine Marschollek, Silvia Heinze, Joachim Püschel, Haniyeh Koochak and Mohammad Dehghan for working with them and some interesting idea during the weekly seminar. I thank my colleagues Annemarie Lippert, Susann Auer, Antje Walter, Madeleine Neumann, Kristin Halbauer, Sabine Rößler and Sarah Hense beside the nice working conditions for inspiring and jokey lunch breaks as well as their assistance in the laboratory. Thank you Anja Radziszewska and Daniela Hartmann for doing preliminary tests and some data analysis.

Special thanks goes to Thomas Schafhauser (Department of Microbiology and Biotechnology, University of Tübingen, Germany) for the astin analysis, to Daniel Wibberg (CeBiTec at the University of Bielefeld, Germany) for the genome and RNA sequencing and to Liane Flor (Institute of Biochemistry, TU Dresden, Germany) for the (motivating) discussions and the assistance in the laboratory, especially with the Southern and colony blot.

I thank Prof. Dr. Karl-Heinz van Pée for let me working on the Southern and colony blot in his laboratory and for the examination of my dissertation. I had inspiring discussions with the other members of the MESIAB project (listed below) during the project meetings. They never let me leave a meeting without having new ideas and tasks. Thank you all for this.

Prof. Dr. Karl-Heinz van Pée, Liane Flor	Chair of Biochemistry, TU Dresden, Germany
Prof. Dr. Wolfgang Wohlleben, Dr. Tilman Weber, Thomas Schafhauser	Department of Microbiology and Biotechnology, University of Tübingen, Germany
Prof. Dr. Willem J. H. van Berkel, Mieke M. E. Huijbers	Laboratory of Biochemistry, University of Wageningen, The Netherlands
Prof. Dr. Philippe Jacques, Thibault Caradec	Laboratoire ProBioGEM, Polytech'Lille, France
Prof. Dr. Kaarina Sivonen, Dr. David Fewer	Division of Microbiology, University of Helsinki, Finland

Last but not least I thank my whole family who never let me alone and supported me when I needed it most. Thank you.

This work was part of the project "Multi-enzyme systems involved in astin biosynthesis and their use in heterologous astin production (MESIAB)" and was funded by the European Union (EFRE) and the Free State of Saxony (SAB). The Graduiertenakademie of the TU Dresden funded the last four month with a studentship for the completion phase.

Declaration of authorship

I declare that I wrote independently the dissertation with the following topic

"Characterization of a new endophytic astin producer, *Pelliciarosea asterica*, from *Aster tataricus*"

and that I used only the indicated references, resources and citations. Today, I handed in this thesis to the examination board of the Faculty of Science of the TU Dresden.

Dresden, 29 May 2015

Hiermit erkläre ich, dass ich die von mir am heutigen Tage dem Prüfungsausschuss der Fakultät Mathematik und Naturwissenschaften eingereichte Dissertation zum Thema

"Characterization of a new endophytic astin producer, *Pelliciarosea asterica*, from *Aster tataricus*"

vollkommen selbstständig verfasst und keine anderen als die angegebenen Quellen und Hilfsmittel benutzt sowie Zitate kenntlich gemacht habe.

Dresden, 29. Mai 2015